MODULATION OF IMMUNE FUNCTION AND PROMOTION OF RESTORATIVE GENE EXPRESSION BY AF4 IN A MOUSE MODEL OF EXPERIMENTAL AUTOIMMUNE ENCEPHALOMYELITIS

by

Jordan R.Warford

Submitted in partial fulfilment of the requirements
for the degree of Master of Science

at

Dalhousie University
Halifax, Nova Scotia
December 2012

DALHOUSIE UNIVERSITY

DEPARTMENT OF PHARMACOLOGY

The undersigned hereby certify that they have read and recommend to the Faculty of Graduate Studies for acceptance a thesis entitled "MODULATION OF IMMUNE FUNCTION AND RESTORATIVE GENE EXPRESSION BY AF4 IN A MOUSE MODEL OF EXPERIMENTAL AUTOIMMUNE ENCEPHALOMYELITIS" by Jordan R. Warford in partial fulfilment of the requirements for the degree of Master of Science.

Dated: December 4th, 2012

Supervisor: _____

Readers: _____

_____

_____

DALHOUSIE UNIVERSITY

DATE: December 4th, 2012

AUTHOR: Jordan R Warford

TITLE: MODULATION OF IMMUNE FUNCTION AND RESTORATIVE GENE EXPRESSION BY AF4 IN A MOUSE MODEL OF EXPERIMENTAL AUTOIMMUNE ENCEPHALOMYELITIS

DEPARTMENT OR SCHOOL: Department of Pharmacology

DEGREE: MSc CONVOCATION: May YEAR: 2013

_____

Signature of Author

Dedicated to the women who raised me and the woman who chose to stand beside me.

TABLE OF CONTENTS

LIST OF TABLES

LIST OF FIGURES

ABSTRACT

The anti-inflammatory and restorative effects of the flavonoid-enriched fraction AF4 were examined in a mouse model of experimental autoimmune encephalomyelitis (EAE). Relative to EAE mice that received vehicle (water, 10 ml/kg/day), oral administration of AF4 (25 mg/kg/day) beginning 24 hours after the onset of clinical signs reduced disease progression that was accompanied by diminished pro-inflammatory cytokine gene expression (cerebellum and spinal cord) and protein concentrations in the plasma. LPS-induced release of TNF-α from the whole blood of EAE mice that received AF4 was reduced at peak disease severity (day 18) but not once central inflammation had declined (day 31) indicative of unique immune modulator properties. Lastly, the expression of myelin-associated genes (PGC-1α, SCD1, and MBP) suggestive of remyelination was enhanced in the spinal cord of EAE mice that received AF4. These findings suggest that AF4 reduces EAE severity by selectively inhibiting autoimmunity and enhancing the expression of genes necessary for remyelination.

LIST OF ABBREVIATIONS AND SYMBOLS USED

AF4	Apple Fraction 4
ANOVA	Analysis of variance
BBB	Blood brain barrier
cAMP	Cyclic adenosine monophosphase
CFA	Complete Freund's adjuvant
CNS	Central nervous system
CREB	cAMP response element binding protein
CS	Clinical score
CSF	Cerebrospinal fluid
CXCL2	Chemokine (C-X-C motif) ligand 2
DAB	Diaminobenzidine
DMD	Disease modifying drug
EAE	Experimental autoimmune encephalomyelitis
ELISA	Enzyme-linked immunosorbent assay
g	Gram
i.p	Intraperitoneal injection
Iba-1	Ionized calcium binding adaptor molecule 1
IFN	Interferon
IL-1β	Interleukin-1beta
IL-6	Interleukin-6
JAK/STAT	Janus kinase and signal transducer and activator of transcription
LXR	Liver X receptor

LPS	Lipopolysaccharide
MAG	Myelin associated glycoprotein
MAPK	Mitogen-activated protein kinases
MBP	Myelin basic protein
mg	Milligram
MIG	Monokine induced by interferon-gamma
ml	Milliltre
mM	Millimolar
MOG	Myelin oligodendrocyte glycoprotein
MPP+	1-methyl-4-phenylpyridinium
mRNA	Messenger ribonucleic acid
MS	Multiple sclerosis
MYD88	Myeloid differentiation primary response gene 88
NADPH	Nicotinamide adenine dinucleotide phosphate
NF-kB	Nuclear factor kappa-light-chain-enhancer of activated B cells
ng	Nanogram
OPC	Oligodendrocyte precursor cell
p.o.	Per os
PAMP	Pathogen-assocaited molecular patterns
PBS	Phosphate buffered saline
PBS-PI	Phosphate buffered saline with phosphatase and protease inhibitors
PBS-TX	Phosphate buffered saline with Triton X
PDE	Phosphodiesterase

PDE4	Phosphodiesterase 4
PFA	Paraformaldehyde
PGC-1α	Proliferator-activated receptor gamma co-activator 1-alpha
PKA	Protein kinase A
PLP	Proteolipid protein
PPMS	Primary progressive multiple sclerosis
PRMS	Progressive relapsing multiple sclerosis
PTX	Pertussis toxin
qRT-PCR	Quantitative real-time polymerase chain reaction
RNA	Ribonucleic acid
ROS	Reactive oxygen species
RRMS	Relapsing-remitting multiple sclerosis
s.c.	Subcutaneous injection
SCD1	Steroyl-CoA desaturase-1
SEM	Standard error of the mean
SPMS	Secondary progressive multiple sclerosis
TCR	T cell receptor
TLR	Toll-like receptors
TLR4	Toll-like receptor 4
TNF-α	Tumor necrosis factor alpha
U	Unit
VEGF-A	Vascular endothelial growth factor-A
VEH	Vehicle

VLA4	Very late antigen 4
µl	Microlitre
µm	Micrometer
%	Percent
°C	Degrees Celsius

ACKNOWLEDGEMENTS

If it takes a village to raise a child, then it takes a city to raise a scientist. I have had the privilege of being surrounded by a strong and compassionate wife, supportive and loving family, a charismatic supervisor, and colleagues whom I view as family. First I would like to thank Dr. George Robertson for giving me the opportunity to work in his lab. George - whether it was a trip to Alberta, or road trip to PEI, we have been on a journey together. You have instilled in me a passion for science, shown me the beauty of a concise paragraph, and have worked hard to give me opportunities to publish at an early stage in my career. For this I will be forever grateful. I would also like to thank Kay Murphy and Elizabeth Belland - two women who have taught me the art of science. Kay, you are an inspirational person in my life. The encouragement and love you have extended to my family and I will never be forgotten, I could not have accomplished this without you. Elizabeth - Without you I would not have developed the skills necessary to pursue a PhD. Thank you for being tough, thank you for your patience, and thank you for taking the time to pass along some of your remarkable talent.

Quinn Jones is the only person who can say that he was the first to see every piece of data I have produced for this thesis. Quinn, you are so selfless and caring. Your brilliance and passion has inspired many of the theories presented in this document, and you have taught me so much over the years. I would also like to thank Dr. Eileen Denovan-Wright for her mentorship. Eileen - Words cannot express how grateful I am to you. I suspect you will never fully understand your contributions to my self-confidence as an individual and a scientist. You believed in me, and that belief has propelled me through the rough patches.

Lastly, but certainly most important, I would like to thank God, my family and my friends. Sarah - you have stood beside me and loved me through every step of my academic career. I realize how demanding this life is, and I'm grateful to be with a woman who demonstrates such grace and strength. Mom - what can I say? You are my rock. Nan - Without you I would not be here. Auntie Linda - your prayers have kept me strong. Jean Liu - you are my science pal, and always will be. Thank you for sharing my love of science and being such a kind friend. To rest of the "old" 15E lab - it was a fun ride.

CHAPTER 1: INTRODUCTION[1]

Multiple sclerosis (MS) is a neurodegenerative disorder characterized by autoimmune-mediated destruction of the myelin sheath surrounding neuronal axons in the central nervous system (CNS; Charcot, 1868). The pathological hallmarks of MS include demyelination, gliosis, perivascular cuffing and ultimately axonal and neuronal loss (Trapp *et al.*, 1998; Frohman *et al.*, 2006; Ludwin, 2006; Stadelmann *et al.*, 2011). Focal areas of inflammatory-mediated demyelination produce the primary symptoms of MS, which include difficulty walking (paraparesis), poor coordination of voluntary muscle movement (ataxia), fatigue, tremor, abnormal skin sensations (paresthesia), loss of sight (optic neuritis), cognitive deficits, and bladder dysfunction (Compston & Coles, 2008). While the etiology of MS is unknown, it is thought that both genetic and environmental factors contribute. Four major disease subtypes have been recognized: relapsing-remitting MS (RRMS), secondary progressive MS (SPMS), primary progressive MS (PPMS), and progressive relapsing MS (PRMS). Approximately 85% of the estimated 55 000 – 75 000 Canadians diagnosed with MS initially present with RRMS and roughly 50% of these patients will develop SPMS within 10 years of their diagnosis (Beck *et al.*, 2005).

There are seven Health Canada approved disease modifying drugs (DMDs) that include several immune modulators (interferon beta-1a, interferon beta-1b, glatiramer acetate), a humanized monoclonal antibody against the adhesion molecule α4-integrin (natalizumab), and a sphingosine 1-phosphate receptor modulator (fingolimod). DMDs

---

[1] Portions of this chapter appear in the following publication: Jones, Q.R.D, Warford, J., Rupasinghe, H.P.V., Robertson, G.S. (2012) Target-based selection of flavonoids for neurodegenerative disorders. Trends in Pharmacological Sciences. 11: 602-610. Reprinted with permission from Elsevier.

have been designed to prevent relapses resulting from inflammation and therefore show the highest efficacy in RRMS patients (Saidha *et al.*, 2012). Unfortunately, there are no effective treatments for SPMS, PPMS, and PRMS (Franklin *et al.*, 2012). Mitoxantrone, a type II topoisomerase inhibitor, has been shown to slow the progression of SPMS while also serving as a useful second line therapy for otherwise treatment-resistant RRMS (Hartung *et al.*, 2002). Given the general immune suppression produced by DMDs and their associated side effects, a nutraceutical approach using potent anti-inflammatory flavonoids that demonstrate excellent safety profiles may be a viable alternative to traditional DMD therapy.

The first goal of the present study was to determine whether treatment with an apple-derived flavonoid fraction (AF4) reduced clinical severity in a mouse model of MS known as experimental autoimmune encephalomyelitis (EAE). EAE is induced in mice by immunization with a 20 amino acid portion of myelin oligodendrocyte glycoprotein (MOG_{35-55}) emulsified in complete Freund's adjuvant (CFA) and injected along with pertussis toxin (PTX; Baxter, 2007). The development of clinical disease signs reminiscent of MS symptoms, such as paralysis and walking deficits, begins with the sensitization of myelin-specific T lymphocytes that mediate destruction of the myelin sheath surrounding axons of the CNS. This is the fundamental pathophysiological process responsible for the development of paralysis in MS and EAE. The production of a diverse range of cytokines and chemokines by peripheral blood immune cells, as well as microglia and astrocytes in the CNS, serves as the foundation for inflammatory responses that drive the pathological processes leading to demyelination and neurodegeneration

(Charo & Ransohoff, 2006). Therefore, the second goal of this study was to assess the ability of AF4 to attenuate these inflammatory responses following the induction of EAE.

Another important consideration is the restorative response to demyelinated plaques. Remyelination is necessary for recovery of sensorimotor function in both EAE and MS, and occurs during the initial stages of the clinical disease course (Franklin & ffrench-Constant, 2008). However, remyelination eventually fails in MS resulting in disease progression, typically marking the shift from RRMS to SPMS. Treatments capable of promoting remyelination may halt disease progression and promote recovery following a relapse. Consequently, the third and final goal of this study was to assess the ability of AF4 to promote the induction of genes necessary for remyelination in a mouse model of EAE.

1.1 Pathophysiology of MS

The molecular mimicry hypothesis of MS: Initiation of the autoimmune response

Despite our limited understanding of the etiology of MS, it is widely accepted that the activation of myelin-reactive CD4+ T cells is a critical event in the pathogenesis of this autoimmune disorder. As T cells mature, T cell receptors (TCRs) are generated in an assortment of peptide combinations that enhance their ability to recognize foreign antigens (Stoeckle & Tolosa, 2010). TCRs with specificity for endogenous tissue, such as myelin, are commonly created and considered a normal component of the T cell repertoire. The presence of myelin-specific T cells alone in circulation is therefore considered insufficient to provoke an autoimmune response since both MS patients and healthy neurological controls have a similar number of circulating myelin-specific T cells (Scholz *et al.*, 1998; Frohman *et al.*, 2006).

Several lines of evidence suggest that the inflammatory response leading to MS is initiated in the periphery by a viral or bacterial infection that stimulates myelin-specific T cells (Libbey *et al.*, 2007; Markovic-Plese, 2009). The strongest evidence supporting the involvement of foreign pathogens in the initiation of MS is the elevation of antibodies against viral proteins in the cerebral spinal fluid (CSF) and serum of MS patients that cross-react with myelin components such as myelin basic protein (MBP; Ascherio et al., 2001). This suggests that viruses or bacteria may activate myelin-reactive T cells by producing cross-reactive proteins. This occurs when peptides from these pathogens mimic myelin epitopes and bind to TCRs with sufficient affinity to activate them (Markovic-Plese *et al.*, 2004). However, cross-reactivity is a frequent immunological phenomenon insufficient for autoimmunity (Selin *et al.*, 2004; Libbey *et al.*, 2007). It has been hypothesized that the mobilization of the innate immune system by invading pathogens provides the necessary conditions to trigger T cell-mediated autoimmunity in MS (Markovic-Plese, 2009). Activation of myelin-reactive T cells by the innate immune system is initiated by circulating monocytes that release pro-inflammatory cytokines such as tumor necrosis factor alpha (TNF-α), interleukin-1beta (IL-1β), and interleukin-6 (IL-6; Stadelmann *et al.*, 2011).

Following activation in peripheral circulation, myelin-reactive CD4+ T cells differentiate, producing cell linages that secrete pro-inflammatory cytokines critical for the development of autoimmunity (T_h1 and T_h17; Markovic-Plese, 2009). Myelin-reactive T cells also express integrins, such as very late antigen 4 (VLA4), that bind to adhesion molecules on the surface of endothelial cells, allowing them to cross the blood brain barrier (BBB) by diapedesis, penetrating the parenchyma to form perivascular cuffs

(Steinman & Zamvil, 2005). The production of pro-inflammatory mediators from cells of the innate immune system further damages the BBB, enhancing cellular infiltration. Within the CNS, myelin-reactive CD4+ T_{h1} cells recognize myelin antigens that results in a feed-forward cycle which promotes chronic inflammation (Minagar & Alexander, 2003; Korn, 2008).

The inflammatory milieu in the CNS is also perpetuated by monocytes that differentiate into macrophages as they enter the brain. In addition to presenting antigens to memory T cells, infiltrating macrophages and resident activated microglia shift towards a pro-inflammatory phenotype in the presence of CD4+ T_{h1} cells, producing TNF-α, IL-1β, and IL-6 (Imitola *et al.*, 2005). Furthermore, activated microglia are the primary source of central nicotinamide adenine dinucleotide phosphate (NADPH) oxidase activity in the CNS that generates reactive oxygen species (ROS; Gao et al., 2012). The excessive production of ROS and pro-inflammatory cytokines (TNF-α, IL-1β, and IL-6) results in destruction of the myelin sheath.

The innate immune response part I: Toll-like receptors

The innate immune response determines the outcome of adaptive immunity, with many of these pro-inflammatory cytokines (TNF-α, IL-1β, and IL-6), serving as effectors for the adaptive immune response mediated by T cells (Fernández *et al.*, 2010). Circulating monocytes, mast cells, and tissue macrophages were originally thought to be blind to the specific nature of infectious pathogens. However, it is now understood that these cells can recognize certain types of pathogens by their molecular "pattern." A family of transmembrane proteins called Toll-like receptors (TLRs), comprised of 10

members (TLR1-10), recognizes these different pathogen-associated molecular patterns (PAMPs) triggering activation of the innate response (Takeda & Akira, 2005). Studies that have subjected mice which lack different types of TLRs to EAE indicate that TLR4 receptor activation is necessary for autoimmunity (Marta *et al.*, 2009; Reynolds *et al.*, 2012)

TLR4 receptors, expressed on microglia, macrophages, and monocytes act through two distinct mechanisms: Myeloid differentiation primary response gene 88 (MYD88) dependent and independent pathways (Duprez *et al.*, 2009). The MYD88 dependent pathway is responsible for promoting the expression of pro-inflammatory cytokines such as TNF-α, IL-1β, and IL-6 by activating the transcription factor known as nuclear factor kappa-light-chain-enhancer of activated B cells (NF-kB; Fernández et al., 2010). The MYD88 independent pathway activates the TLR adaptor molecule 1 (TRIF), inducing the transcription of type I interferons (IFNs; Duprez *et al.*, 2009). Type I IFNs are responsible for the induction of genes that play a central role in host resistance to viral infections. Type I IFNs also activate key components of both the innate and adaptive immune systems, resulting in the production of pro-inflammatory cytokines involved in activation of myelin-reactive T cells and antigen presentation via dendritic cells (Takeda & Akira, 2005).

The best characterized role of TLR4 is in the recognition of lipopolysaccharide (LPS), a membrane component of Gram-negative bacteria (Alcázar *et al.*, 2000). Incubation of whole blood with LPS promotes the expression and release of pro-inflammatory cytokines such as TNF-α, IL-1β, and IL-6 from monocytes (Dedrick & Conlon, 1995). In view of the importance of TLR4 receptor activation to innate immune

mechanisms in EAE and MS, this *ex vivo* blood assay will be used to determine the status of TLR4 signaling in peripheral blood immune cells from EAE mice.

The innate immune response part II: TNF-α, IL-1β, and IL-6

Cytokines are critical components of the innate inflammatory response, and are implicated in oligodendrocyte cell death, axonal degeneration, and neuronal cell death, all of which are key features of MS pathology responsible for disease progression (Imitola *et al.*, 2005; Centonze *et al.*, 2010). CSF and serum from MS patients contain high concentrations of pro-inflammatory cytokines that have been shown to induce axonal damage and neuronal apoptosis *in vitro* (Alcázar *et al.*, 2000). Treatments that reduce the production of pro-inflammatory cytokines may therefore promote the survival of oligodendrocytes and axons.

TNF-α is a powerful pro-inflammatory cytokine that regulates cellular differentiation and apoptosis (Fernández *et al.*, 2010). It is expressed by activated mononuclear phagocytic cells, macrophages, T cells, microglia, and astrocytes (Imitola *et al.*, 2005). TNF-α is often associated with a pro-inflammatory T_h1 phenotype in the EAE model, inducing the expression of adhesion molecules, chemokines, and other pro-inflammatory cytokines (Weinberg & Montler, 2005). Systemic injection of human recombinant TNF-α exacerbates EAE that is associated with increased cellular infiltration in the spinal cord and parenchyma (Kuroda & Shimamoto, 1991). By contrast, administration of a TNF-α neutralizing antibody ameliorated EAE, markedly reducing the extent of demyelination and perivascular infiltration. Moreover, mice engineered to overexpress TNF-α show spontaneous clinical signs resembling EAE without immunization, including activation of CD4+ T cells, astrogliosis, and demyelination

(Probert *et al.*, 1995). In the same study, the authors show that the EAE-like phenotype of these transgenic mice is rescued when neutralizing antibodies for TNF-α are administered. However, treatment of MS patients with TNF-α neutralizing antibodies exacerbates rather than improves disease severity (Magnano *et al.*, 2004).

TNF-α receptor null mice show a significant delay in remyelination and a reduction in proliferating oligodendrocytes in a cuprizone model of demyelination (Arnett *et al.*, 2001). While this study does not discount the injurious role of TNF-α in the innate immune response of MS, it leaves room to speculate that this pro-inflammatory cytokine may serve different roles at later stages of the disease. Therefore, while a reduction of TNF-α levels may be beneficial, the complete suppression of this cytokine may inhibit recovery.

IL-1β is a member of the IL-1 cytokine family and is secreted by the cleavage of its precursor, pro- IL-1β by caspase-1 or interleukin-1 converting enzyme (ICE; Simi et al., 2007). IL-1β is increased in the CSF of MS patients with clinically active disease compared to quiescent patients or neurological controls (Hauser *et al.*, 1990). Furthermore, IL-1β null mice display an attenuated EAE phenotype implicating this pro-inflammatory cytokine in the initiation of autoimmunity (Matsuki *et al.*, 2006). The secretion of IL-1β by innate immune cells increased the expression of adhesion molecules by the BBB that faciliatated the entry of T cells into the CNS (Shrikant *et al.*, 1994). Astrocytes were also stimulated by IL-1β to produce vascular endothelial growth factor-A (VEGF-A), a protein that further increases the permeability of the BBB, subsequently enhancing immune infiltration and CNS damage (Shrikant *et al.*, 1994).

IL-6 is produced by mononuclear phagocytes, T cells, microglia, astrocytes, and vascular endothelial cells (Imitola *et al.*, 2005). Recognition of IL-6 by its receptor activates the JAK/STAT and MAPK signaling pathways, inducing the synthesis of acute phase inflammatory proteins (Heinrich *et al.*, 2003). MS patients express more IL-6 receptors on the surface of CD4+ T cells in peripheral whole blood releative to healthy neurological controls, implicating IL-6 in the initiation of autoimmunity by promoting T cell activation (Bongioanni *et al.*, 2000). IL-6 null mice are completely resistant to EAE and display no clinical signs; however, administration of recombinant human IL-6 during the preclinical phase of EAE (from days 1 -15), reinstates the normal disease course (Okuda *et al.*, 1999). IL-6 deficiency is thought to protect against EAE by preventing the activation of autoreactive T cells and by preventing the display of adhesion molecules by vascular endothelial cells that promote diapedesis (Heinrich *et al.*, 2003).

Although it is clear that the elevated production of pro-inflammatory cytokines contribute to both the initiation and progression of EAE and MS, these findings also suggest that such cytokines are required for recovery. It is thought that they may promote recovery by orchestrating the removal of extracellular debris that would otherwise interfere with remyelination. There is also evidence that cytokines such as TNF-α are essential for remyelination (Arnett *et al.*, 2001). Immunomodulators that blunt the early wave of pro-inflammatory activity responsible for CNS injury but permit normal immune function to resume once neuroinflammation has subsided would therefore be ideal therapeutic candidates for the treatment of MS.

1.2 Molecular and cellular orchestration of remyelination

Remyelination is mediated by a complex series of events that reinstate saltatory conduction in the CNS following autoimmune-mediated demyelination and has been the subject of intense study in the search for targeted therapeutics that may promote brain repair (Franklin & ffrench-Constant, 2008). Following a demyelinating episode, oligodendrocyte precursor cells (OPCs) proliferate and then differentiate into myelin-producing oligodendrocytes that restore the myelin sheath (Keough & Yong, 2012). Repeated waves of demyelination and remyelination may occur throughout the MS disease course, with some patients showing significant remyelination decades after diagnosis (Patani *et al.*, 2007). In a seminal study by Patrikios *et al.* (2006), 51 autopsies were performed on patients with different clinical courses and disease durations. The authors reported that only 20% of the cohort showed significant global remyelination (60-69%). Remyelination was often incomplete and therefore insufficient to fully restore myelin function (Patani *et al.*, 2007). Since failed remyelination is considered responsible for disease progression, there is intense interest in the development of drugs that promote remyelination. Mechanisms that are thought to promote remyelination include the generation of OPCs, energy supply, sufficient cholesterol production, and the myelin peptides required for the restoration of the myelin sheath.

OPCs and inflammation

The production of mature oligodendrocytes are required for the generation of myelin *de novo* (Taveggia *et al.*, 2010). This is evidenced by the increased number of oligodendrocytes in areas of active remyelination (Prayoonwiwat & Rodriguez, 1993). Furthermore, the depletion of established oligodendrocytes does not halt remyelination,

indicative of OPC recruitment and the subsequent differentiation of OPCs into oligodendrocytes (Sim et al., 2002). Inflammation resulting from the innate immune system has been shown to improve OPC recruitment; however, the viability of these cells and their ability to differentiate are greatly diminished resulting in impaired remyelination (Robbins *et al.*, 1987; Wang *et al.*, 2011). This is due, in part, to the production of pro-inflammatory cytokines such as chemokine (C-X-C motif) ligand 2 (CXCL2) that inhibit oligodendrocyte myelination (Tsai *et al.*, 2002). Therefore, low expression of inflammatory mediators is ideal to help attract OPCs to the lesion without propagating an injurious environment that promotes their death.

Energy

The production of myelin by oligodendrocytes requires a tremendous amount of energy that is supplied by the mitochondria. As a consequence, mutations in genes that regulate mitochondrial function are invariably associated with dysmyelinating and demyelinating disorders such as Huntington's disease or Charcot-Marie-Tooth disease (Kijima *et al.*, 2005; Xiang *et al.*, 2011). Mitochondrial deficits are also strongly associated with chronic white matter lesions, in both early and late stages of the disease (Lu *et al.*, 2000; Mahad *et al.*, 2008). Inhibition of mitochondrial complex I activity in OPCs prevents maturation into functional oligodendrocytes at very low concentrations that does not impair viability (Schoenfeld *et al.*, 2010). Hence, mitochondrial biogenesis and health are essential for myelination. Mitochondrial biogenesis is driven by peroxisome proliferator-activated receptor gamma co-activator 1-alpha (PGC-1α) enabling remyelination to be monitored by measurement of PGC-1α mRNA levels (St-Pierre *et al.*, 2006).

Cholesterol

Unlike glucose and other nutrients that are transported into the brain, cholesterol biosynthesis occurs *de novo* as required and depends upon functional oligodendrocytes (Saher *et al.*, 2011; Jurevics & Morell, 1995). Cholesterol sysnthesis is the rate-limiting step in myelin formation (Saher *et al.*, 2011). Mice that lack squalene synthase, the first committed enzyme in the biosynthesis of myelin, display hypomyelination during development (Saher *et al.*, 2005). Catalyzing the rate limiting steps of cholesterol biosynthesis by promoting the expression of genes such as steroyl-CoA desaturase-1 (SCD1), essential for cholesterol biosynthesis (Hodson & Fielding, 2012), may therefore improve the efficiency and rate of remyelination.

Myelin

Myelin is a multilayered membrane, comprised of an assortment of myelin peptide building blocks such as proteolipid protein (PLP), myelin associated glycoprotein (MAG), myelin oligodendrocyte glycoprotein (MOG), and MBP (Fulton *et al.*, 2010). Each protein has a unique relationship to oligodendrocyte trophic support. Knocking out PLP or MAG genes does not prohibit the oligodendrocyte from producing myelin; however, the structural quality of the myelin produced is degraded (Griffiths *et al.*, 1998; Pan *et al.*, 2005). Therefore, proper expression of myelin genes is required to produce fully functional myelin.

Targeting cell survival pathways to protect the CNS and promote recovery

Pathways for OPC differentiation have been well characterized; however, for remyelination to occur it is essential that newly differentiated OPCs survive in a hostile

environment (Keough & Yong, 2012). This may be achieved by targeting pathways that promote cell survival signaling mediated by the activation of the transcriptional regulating factor CREB (cyclic adenosine monophosphate (cAMP) response element binding protein; Wen *et al.*, 2010). Adenylyl cyclase is activated by a range of signaling molecules through stimulatory G protein-coupled receptors, resulting in increased levels of intracellular cAMP that promote cAMP dependent protein kinase A (PKA) activity resulting in the phosphorylation of CREB. Upon translocating to the nucleus, phosphorylated CREB reduces inflammation by inhibiting NFkB mediated pro-inflammatory gene expression (Wen et al., 2010). CREB also activates the expression of PGC-1α resulting in mitochondrial biogenesis and the expression of genes required for cholesterol synthesis such as SCD1 (Lemberger *et al.*, 2008; St-Pierre *et al.*, 2006). The expression of constitutively active CREB in dorsal root ganglion neurons is sufficient to promote regeneration after transection indicating an important restorative role for CREB (Gao *et al.*, 2004). Treatments that enhance CREB signaling may therefore protect the brain from injury and improve outcome by enhancing transcriptional events necessary for recovery.

A recent study reported that patients with MS show increased mRNA levels in peripheral blood lymphocytes for several phosphodiesterase (PDE) subfamilies that mediate the degradation of cAMP (Mizrachi *et al.*, 2010; Bollen & Prickaerts, 2012). Small molecule inhibitors of PDE4 reduce the disease severity of EAE mice by raising cAMP levels in activated immune cells that suppress the production of pro-inflammatory mediators such as TNF-α, IL-1β and Il-6 (Moore *et al.*, 2006). PDE inhibitors also enhance cAMP mediated signaling within the CNS that promotes the survival of

vulnerable oligodendrocytes and neurons as well as increasing the proliferation of OPCs necessary for remyelination.

1.3 Experimental autoimmune encephalomyelitis (EAE)

EAE is a T cell mediated model of autoimmunity characterized by neuroinflammation, demyelination and paralysis that mimics certain features of MS (Denic *et al.*, 2011). The EAE model has played an important role in the pre-clinical development of three Health Canada approved therapies for MS: Tysabri® (Natalizumab), Copaxone® (Glatiramer Acetate) and Novantrone® (Mitoxantrone; Baxter, 2007). EAE can be induced in a number of species ranging from non-human primates to rodents by immunization with myelin antigens such as PLP, MBP or MOG. Mouse models of EAE include acute, chronic, and relapsing-remitting disease courses (McCarthy *et al.*, 2012). C57Bl/6 mice immunized with MOG_{35-55} develop a chronic disease course with marginal recovery.

Induction phase of EAE

The induction phase of the disease involves the priming of myelin epitope-specific CD4+ T cells following immunization with myelin antigens emulsified in complete Freund's adjuvant (CFA) in the presence of pertussis toxin (PTX; Denic *et al.*, 2010). CFA is an ancillary adjuvant injected in conjunction with myelin antigens to promote antibody production, consisting of mineral oil (the sole component of incomplete Freund's adjuvant) and heat killed extracts from *mycobacterium tuberculosis*. Administration of PTX following immunization permeabilizes the BBB, permitting myelin reactive T cells to infiltrate the CNS (Munoz et al., 1984). During the induction

phase, mice remain asymptomatic with no observable motor deficits until days 7-11. The induction phase culminates with the first clinical manifestation of the disease, when antigen presentation and clonal expansion of myelin-specific T cells occur (Mix *et al*., 2010).

Effector phase of EAE

During the effector phase, the migration of myelin-specific CD4+ T cells into the CNS is mediated by cell adhesion molecules on the surface of cerebral vascular endothelial cells and facilitated by disruption of the BBB. EAE lesions are characterized by “perivascular cuffing", which is an accumulation of leukocytes in the perivascular space (Denic *et al.*, 2011). Lesions are predominantly composed of CD4+ T lymphocytes and macrophages associated with demyelination (Mix *et al.*, 2010). Throughout the effector phase clinical signs will become apparent mice will lose weight followed by ascending hind limb paralysis, initially presenting with a flaccid tail.

Chronic EAE and demyelination

Demyelination in the EAE model is not a synchronized event, occurring in a variable fashion over time and space. Acute and relapsing-remitting mouse models show little demyelination, making them unsuitable for assessing the effects of treatments that promote remyelination. By contrast, the MOG_{35-55} C57Bl/6 mouse model consistently displays demyelination throughout the effector phase (Jones *et al.*, 2008). Peak inflammation occurs two days following maximal clinical severity, occurring from days 16-18 in MOG_{35-55} induced EAE. Maximum demyelination is first observed several days after peak inflammation. Neuropathology in EAE mice is primarily restricted to the spinal

cord and cerebellum (Jones *et al.*, 2008; Mix *et al.*, 2010).

1.4 Flavonoids

Structure

Flavonoids are plant-derived polyphenolic compounds found in wine, fruits, vegetables, and teas that display potent anti-oxidant activities (Youdim *et al.*, 2004). The basic chemical structure of flavonoids is comprised of an aromatic A-ring connected to a heterocyclic C-ring joined by three carbons that bond to make a closed pyran ring structure, which connects to an aromatic B ring (Figure 1A). Flavonoids are divided into different subclasses based on the number and position of hydroxyl functional groups on the B-ring, and the degree of unsaturation of the bond between the C2 and C3 carbons in the heterocyclic C-ring. The six major subclasses of dietary flavonoids include flavonols, flavones, isoflavones, flavanones, catechins, and anthocyanidins (Figure 1B).

The ability of flavonoids to scavenge free radicals is based, in part, on their ability to add a hydrogen atom to stabilize free radical species. This is made possible by the presence of hydroxyl groups on the B ring and a carbonyl group at the C4 position on the C-ring (Arora *et al.*, 1998). In addition to exhibiting anti-oxidant properties, structural modifications of the B ring result in compounds that inhibit, to varying degrees, enzymes that phosphorylate (kinases) and dephosphorylate (phosphatases) proteins critical to signal transduction pathways involved in the regulation of oxidative stress, inflammation and cell survival (Arora *et al.*, 1998; Peluso, 2006; Chirumbolo, 2010).

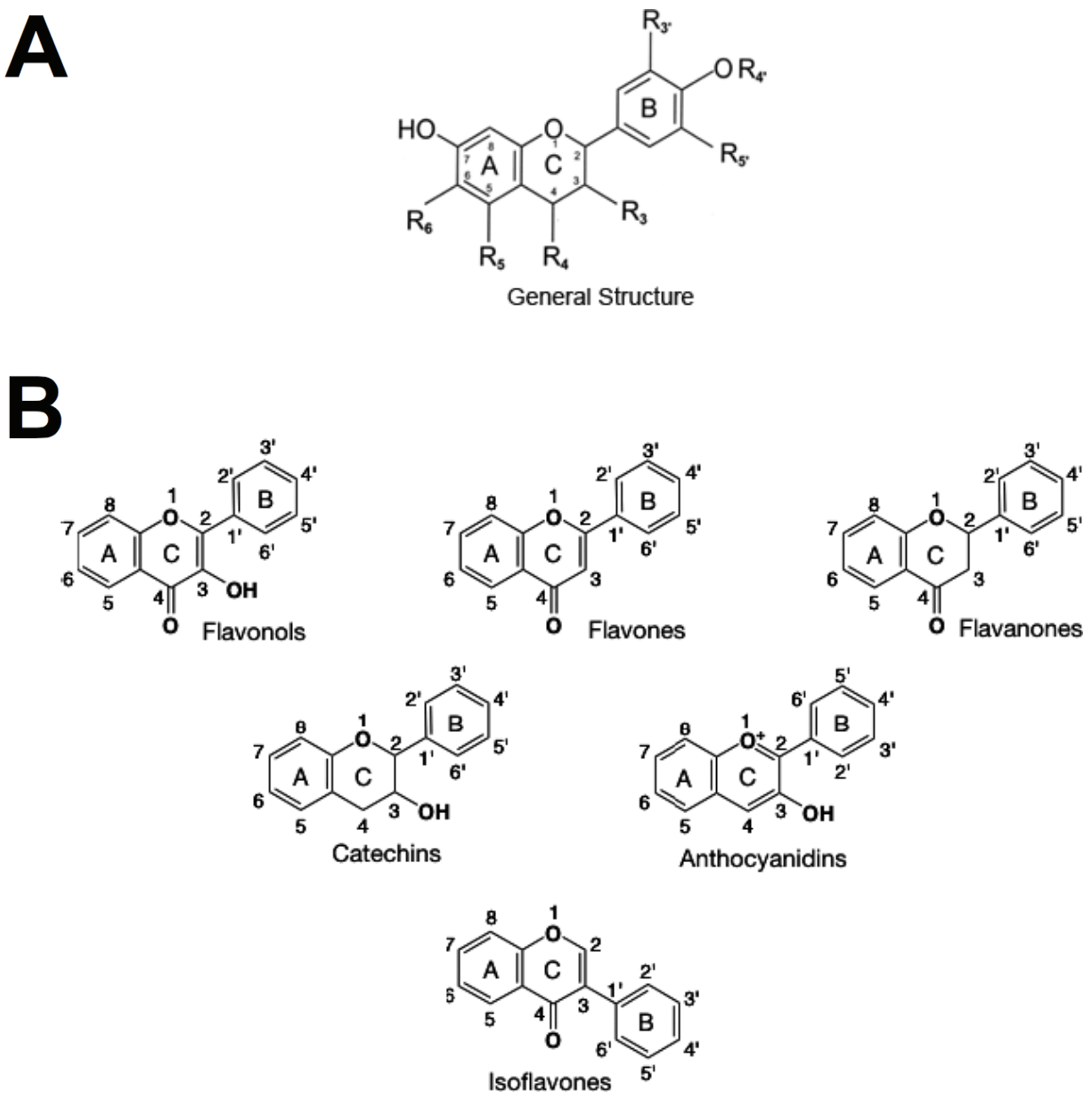

Figure 1: Structures of flavonoids. **(A)** The general structure is compromised of three six-membered rings: an aromatic A-ring fused to a heterocyclic C-ring that is attached through a single carbon-carbon bond to an aromatic B-ring. **(B)** Structures of the six main flavonoid subclasses. There are six main classes of flavonoids, including the flavanones, flavonols, flavones, flavonols, anthocyanidins, and isoflavonoids. These subclasses of flavonoids differ mainly in the addition of functional groups and changes in the degree of unsaturation in the C ring. Adapted from Peluso (2006).

Flavonoids are extensively metabolized following oral administration

Flavonoids must be viewed from the perspective of their absorption, distribution, metabolism and elimination (Kroon et al., 2004). Quercetin, the primary constituent of AF4, has been extensively studied, as it represents one of the most abundant flavonoids in foods where it is present in the form of glycosides (Hertog *et al.*, 1995). Following ingestion of quercetin by humans, even at high doses (1.5 g/day), very little of the total dose (<1%) reaches the circulation in the unaltered aglycone form (quercetin) achieving only nanomolar (5 ng/ml-15 nM) plasma concentrations (Ader *et al.*, 2000; Wang & Morris, 2005; Williamson & Manach, 2005). This is because quercetin is extensively transformed by phase II enzymes in the gut and liver to conjugated metabolites that reach plasma concentrations of 300 ng/ml (~900 nM) or 150x the concentration of the unaltered aglycone (Wang & Morris, 2005; Williamson & Manach, 2005). By comparison, quercetin glycosides found in dietary sources are better absorbed generating plasma concentrations of quercetin and its metabolites several times higher than achieved after ingestion of the aglycone (Makino et al., 2009; Reinboth *et al*., 2010). This is because of sodium-dependent glucose transporters that facilitate transport of quercetin glycoside across the epithelial barrier in the small intestine (Hollman *et al.*, 1995).

Within epithelial cells of the small intestine, quercetin glycosides are immediately cleaved by the enzyme β-glucosidase yielding the aglycone that is then transformed by phase II enzymes into sulfonated (quercetin-3'-*O*-sulfate), methylated (3'-*O*-methylquercetin) and glucuronidated (quercetin-3'-*O*-glucuronide; quercetin-4'-*O*-glucuronide; quercetin-3-*O*-glucuronide) metabolites (Day *et al.*, 1998, 2000; Murota & Terao, 2003). In blood and organs such as kidney, liver and brain the predominant forms of quercetin are quercetin-3'-*O*-sulfate, 3'-*O*-methylquercetin and 3'-*O*-methylquercetin-

3-*O*-glucuronide that constitute over 90% of the metabolites with an intact flavonol structure (Day *et al.*, 2000; Mullen *et al.*, 2006; Terao *et al.*, 2011). In general, these metabolites display anti-inflammatory and anti-oxidant properties distinct from quercetin which may contribute to the biological effects of this flavonoid (Mullen *et al.*, 2006; Terao *et al.*, 2011).

The near absence of quercetin aglycone in blood and brain following ingestion is difficult to reconcile with the large number of studies indicating that the aglycone mediates the anti-oxidant, neuroprotective and anti-inflammation effects of this flavonoid (Jones *et al.*, 2012). One explanation for this paradox is that metabolic transformation of quercetin generates metabolites with unique pharmacological properties. However, another explanation may be that quercetin is regenerated from glucuronidated metabolites by the action of β-glucuronidase in the appropriate target tissues. β-glucuronidase activity is elevated in inflammatory immune cells and inflamed endothelial cells of the BBB (Shimoi & Nakayama, 2005). Hence, the induction of β-glucuronidase in these cells may promote a mechanism for regeneration of quercetin from glucuronidated metabolites in the EAE model (Perez-Vizcaino *et al.*, 2012).

Anti-oxidative properties of flavonoids

Flavonoids have been shown to specifically preserve and enhance mitochondrial function in a variety of ways. Quercetin and epigallocatechin-3-gallate preferentially accumulate in mitochondria (Schroeder *et al.*, 2009; Fiorani *et al.*, 2010), resulting in μM concentrations sufficient to directly scavenge ROS without inhibiting mitochondrial respiration (Lagoa et al., 2011). Quercetin has also been shown to reverse the inhibition of complex I activity by rotenone and MPP+ (Van Kampen *et al.*, 2003; Carrasco-Pozo *et*

al., 2011). This activity is derived from the ability of flavonoids to serve as coenzyme Q-mimetics. Thus, bypassing Complex I inhibition by these mitochondrial toxins (Jones *et al.*, 2012). Flavonoids can also reduce oxidative stress by chelating iron, thus reducing the generation of ROS by the Fenton reaction (Scapagnini *et al.*, 2011). Lastly, by inhibiting PDE4 and raising intracellular cAMP concentrations, flavonoids promote the transcription of PGC-1α resulting in mitochondrial biogenesis (Jones *et al*., 2012).

PDE inhibition by flavonoids

As previously discussed, cell signaling events activated by cAMP are terminated by the action of PDEs, of which over 50 have been characterized to date (Bollen & Prickaerts, 2012). These enzymes are blocked to varying degrees by several major flavonoid subtypes represented by quercetin (flavonols), luteolin (flavones), catechin (flavan-3-ols), hesperetin (flavanones), genistein (isoflavones) and cyanidin (anthocyanidins; Ko *et al.*, 2004). Moreover, these activities are preserved in sulphonated, methylated, and glucuronidated metabolites for quercetin suggesting that PDE inhibition may be relevant to the mechanism of action of dietary flavonoids and hold particular application for the treatment of MS (Suri *et al.*, 2010). Unlike the quercetin aglycone, circulating levels of these quercetin metabolites observed in feeding studies reach concentrations necessary to inhibit PDE (IC_{50}=10-30 μM; Ko *et al.*, 2004). Therefore, the ability of flavonoids such as quercetin to potently inhibit PDE activities that oppose the production of pro-inflammatory cytokines and enhance the survival of oligodendrocytes and neurons suggests that flavonoids may be useful for the treatment of MS.

1.5 Apples as an abundant source of biologically active flavonoids

Next to oranges, apples are the second highest source of anti-oxidants and phenolics in the North American diet. The structural classes of phenolics represented in apples include flavonols (quercetin glycosides), flavan-3-ols (epicatechin, catechin), anthocyanins (cyanidin-3-O-galactoside), hydrochalcones (phloridzin) and phenolic acids (chlorogenic acid, cafeic acid). Apple skin contains approximately 46% of the total phenolics in apples, and specific flavonoids such as quercetin glycosides and cyanidin-3-*O*-galactoside are not found in the flesh of apples (Huber & Rupasinghe, 2009). Extensive experimentation has demonstrated that flavonols (quercetin glycosides), flavan-3-ols (epicatechin, catechin), anthocyanins (cyanidin glycosides), hydrochalcones (phloridzin) and phenolic acids (chlorogenic acid) abundant in apple skin exhibit anti-oxidant, anti-inflammatory, and neuroprotective properties in both *in vitro* and *in vivo* models that recapitulate the unfavorable conditions responsible for inflammatory brain injury (Simonyi et al., 2005; Gutierrez-Merino et al., 2011; Wang et al., 2011; Kim et al., 2012). Apple peel that is discarded as a waste by-product from apple processing therefore represents a considerable untapped source for biologically active phenolics.

1.6 Apple Fraction 4 (AF4)

Apple skins of the apple cultivar, Northern Spy, were collected from a commercial pie manufacturer, Apple Valley Foods Inc., Kentville, NS, Canada. The phenolic profile of the AF4 fraction measured by LC-MS/MS is provided in Table 1. The primary phenolic compounds in AF4 were flavonols, phenolic acids, flavan-3-ols, anthocyanins, and dihydrochalcones. The majority (72%) of these monomeric phenolics were quercetin glycosides. As previously discussed, these phenolics have anti-

inflammatory and pro-survival effects in the CNS, suggestive of the capacity to ameliorate the progression of MS. It is proposed that the additive and synergistic effects of the phenolics that comprise AF4 are responsible for the potent activity of this extract, as it preserves the natural combinations of the compounds (Liu, 2003). This may partially explain why diet supplementation with flavonoid-rich fruits and vegetables reduces the risk of neurodegenerative disorders. Clinical studies involving the dietary administration of an individual antioxidant have not been found to consistently offer preventive effects, partially explaining why modified dietary supplementation in MS is not effective (Sun *et al.*, 2002; Liu, 2003). This further suggests that synergism between individual phenolics is necessary to achieve therapeutically relevant anti-inflammatory, neuroprotective, and restorative effects in patients with MS.

Table 1: Concentration of polyphenolic compounds of AF4 determined by LC-MS/MS. The total concentration of phenolic content present in AF4 was determined to be 12132.7 μg/ml. The major polyphenolic compounds detected in AF4 belong to subclasses of flavonols, anthocyanins, dihydrochalcones, flavan-3-ols, phenolic acids, and flavanols and were similar to those reported by other investigations. The most abundant phenolics in AF4 were quercetin-3-*O*-galactoside, quercetin-3-*O*-rutinoside, quercetin-3-*O*-glucoside, quercetin-3-*O*-rhamnoside, chlorogenic acid, and (-)-epicatechin.

Phenolic compounds		Concentration[a] (μg/ml)
Flavonol	Quercetin (Q)	9.9 ± 0.3
	Q-3-*O*-paltoside	63.8 ± 2.4
	Q-3-*O*- rutinoside	1535.7 ± 46.2
	Q-3-*O*-galactoside	2914.9 ± 72.8
	Q-3-*O*-glucoside	1474.8 ± 58.9
	Q-3-*O*-rhamnoside	2771.6 ± 77.5
	Total Flavonols	8770.7
Anthocyanins	Cyanidin-3-*O*-galactoside	559.4 ± 16.7
Dihydrochalcones	Phloridzin	386.8 ± 13.6
Phenolic acids	Chlorogenic acid	1221.1 ± 31.2
	Cafeic acid	43.6 ± 2.0
	Total phenolic acids	1264.7
Flavan-3-ols	Catechin	106.8 ± 3.7
	Epicatechin	1044.3 ± 36.8
	Total Flavan-3-ol	1151.1
	Total phenolics	12132.7

[a]mean ± standard deviation of the mean for three determinations

1.7 Rationale and hypotheses

Flavonoids are plant-derived polyphenolic compounds found in wine, fruits, vegetables, and teas that display anti-inflammatory, anti-oxidative, and neuroprotective properties in animal models of neurodegenerative disorders, including stroke and MS. These properties combined with the well-established safety profiles of dietary flavonoids in humans has led to the suggestion that they should be given strong consideration as a novel therapeutic candidates for the treatment of MS. Flavonoids found within AF4, such as quercetin, inhibit PDE4 activity thus raising cAMP levels and initiating the phosphorylation of CREB. Phosphorylated CREB reduces the production of pro-inflammatory cytokines and promotes the expression of genes necessary for remyelination (Lemberger *et al.*, 2008; Wen *et al.*, 2010; St-Pierre *et al.*, 2006).

A major component of AF4, quercetin-3-*O*-glucoside, is thought to reduce clinical disease progression in various models of EAE by anti-inflammatory mechanisms (Hendriks, 2004; Muthian & Bright, 2004a; Zeng *et al.*, 2007; Wu *et al.*, 2012; Yin *et al.*, 2012). Clinical improvements in these studies were accompanied by reductions in central inflammation and demyelination. Taken together, these findings suggest that AF4 may also have the potential to reduce inflammation and promote the restorative events necessary for remyelination.

To test the potential benefit of AF4 in the reduction of autoimmune-mediated neuropathology and clinical severity, the MOG_{35-55} EAE model will be used in mice. The development of paralysis associated with inflammatory lesions and demyelination in the spinal cord have resulted in the widespread use of the EAE model to identify therapeutics useful in the treatment of MS.

Oral administration of either vehicle (10 ml/kg; once daily) or AF4 (25 mg/kg; once daily) will begin 24 hours after the first clinical signs of EAE, and continue until day 18 or 31 following immunization with MOG_{35-55}. EAE mice sacrificed at these time points will provide the necessary tissue to assess the immune modulatory actions of AF4 at peak (day 18) and chronic (day 31) phases of this disease. These studies will test each of the following hypotheses that are based on comparison to EAE mice that receive vehicle:

Hypothesis I: AF4 will reduce neurological and neuropathological signs of EAE

Hypothesis II**:** AF4 will reduce the concentrations of pro-inflammatory cytokines in whole blood.

Hypothesis III**:** AF4 will attenuate LPS-induced release of TNF-α in whole blood.

Hypothesis IV**:** AF4 will decrease the expression of pro-inflammatory cytokines in the spinal cord and cerebellum.

Hypothesis V**:** AF4 will increase the expression of genes associated with remyelination in the spinal cord and cerebellum.

CHAPTER 2: METHODS

2.1 Animal care

All experiments involving the use of animals were approved by the Dalhousie University Committee on Laboratory Animals and done in accordance with guidelines for the Canadian Council on Animal Care. The animal holding rooms were on a 12-hour dark/light cycle and water and food were provided *ad libitum*.

2.2 Induction of EAE

Eighty-seven female 6-8 week-old C57Bl/6 mice (Charles River Canada; St. Constant, QC) were immunized with myelin oligodendrocyte glycoprotein fragment 35-55 (MOG_{35-55}; Sheldon Biotechnology Centre, Montreal, QC) dissolved in sterile phosphate buffered saline (PBS; pH=7.4) and emulsified in a 1:1 ratio with incomplete Freund's adjuvant (IFA; Difco Laboratories, Detroit, MI, USA) containing 10 mg/ml of Mycobacterium tuberculosis H37RA to make complete Freund's adjuvant (CFA; Difco Laboratories, Detroit, MI, USA). Pertussis toxin (PTX; Sigma, St. Louis, MO, USA), an immune adjuvant, was diluted in sterile Type I water and administered intraperitoneally (i.p.; 300 ng/mouse) on day 0, and again on day 2. Forty-eight age, sex, and weight matched C57Bl/6 mice served as antigen controls and received CFA plus PTX but not MOG_{35-55}. On day 0 mice were injected subcutaneously (s.c.) bilaterally at the base of the tail with either the MOG_{35-55} emulsion (300 μg/mouse; EAE group) or CFA alone (200 μl/mouse; CFA+PTX group; Figure 2). A health check was carried out on day 3 and any animal with gait disturbances resulting from the immunization procedure was excluded from the study. The initial presentation of clinical signs occurred between days 7-11, at

which point mice were assigned to one of two EAE groups so that the average clinical scores for these groups were the same. The two CFA+PTX groups were matched for weight. Half of the animals in the EAE and CFA+PTX groups received either vehicle (water; 10 ml/kg, p.o.; once daily; CFA+PTX-VEH, EAE-VEH) or AF4 (25mg/kg, p.o.; once daily; CFA+PTX-AF4, EAE-AF4). The weight and clinical score of each mouse was recorded daily beginning at day 7. Animals were sacrificed on either day 18 or 31. Blood and CNS tissues were harvested from these animals for subsequent analysis (Figure 3)

2.3 Behavioural assessment of clinical scores

The following grading scheme was used to clinically score the animals: 0, no clinical signs; 0.5, hooked tail; 1, hooked tail with splay; 1.5, flaccid tail with splay; 2, minor walking deficits, mild ataxia; 2.5, severe walking deficits, chronic ataxia; 3, dropped pelvis in addition to severe walking deficits; 3.5, unilateral hindlimb paralysis; 4, bilateral hindlimb paralysis; 4.5, forelimb paralysis; 5, moribund (Figure 4). The humane endpoint was defined as weight loss greater than 20% for three consecutive days or a clinical score of 5 for three consecutive days, or both. The designation of "moribund" indicated that the animal displayed severe lateral recumbency deficits in addition to hind limb paralysis and was incapable of independent feeding or hydration. Mice were supplied with DietGel® Recovery (ClearH20; Portland, ME, USA) and handfed Neutri-Cal® (Evsco Pharmaceuticals; Buena, NJ, USA) as a nutrient supplement when they were no longer able to reach food. Lactated Ringer's solution (50 U/daily) was provided when a mouse reached a score ≥2.5 or when their weight fell 10% below baseline. A trained observer unaware of the treatment conditions recorded all clinical scores.

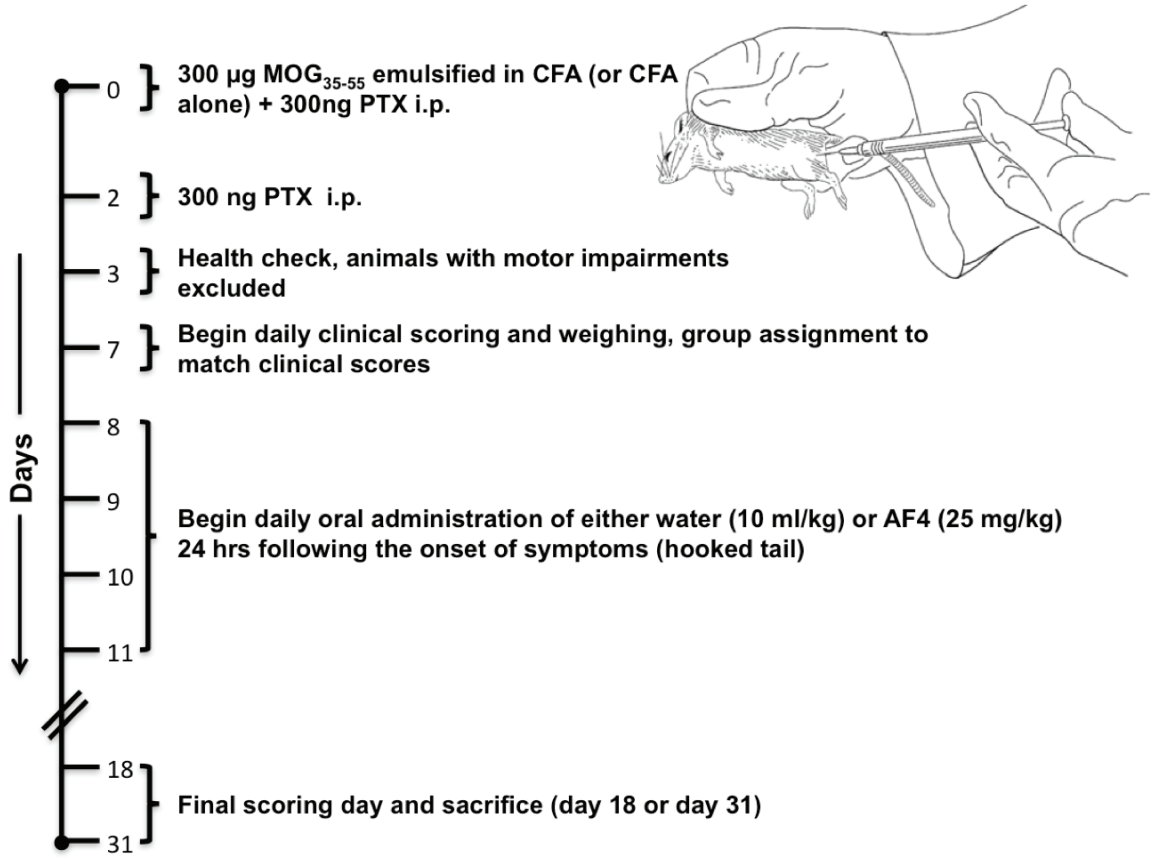

Figure 2: Timeline for CFA, MOG_{35-55} and PTX injections, determinations of bodyweight and clinical score, group assignments and sacrifice. Female adult C57Bl/6 mice (6-8 weeks old) were immunized with MOG_{35-55} emulsified in a 1:1 ratio with CFA containing 0.5 mg/ml of Mycobacterium tuberculosis H37RA (EAE group). Age, sex, and weight matched C57Bl/6 mice served as antigen controls and received CFA and PTX but not MOG_{35-55} (CFA+PTX group). On day 0, MOG_{35-55} (300 µg/mouse) or CFA alone (200 µl/mouse) was injected s.c. bilaterally at the base of the tail. PTX, an immune booster, was diluted in saline and administered i.p. (300 ng/mouse) on day 0, and again on day 2 to both groups. A health check was carried out on day 3 and scoring began on day 7. Initial presentation of clinical signs occurred between days 8-11, at which point mice in both the EAE and CFA+PTX groups were subdivided and assigned to either a treatment group (AF4) or a vehicle group (water). The weights and clinical scores of each individual mouse were recorded daily over either 18 or 31 days, at which point mice were humanely euthanized and tissues were collected.

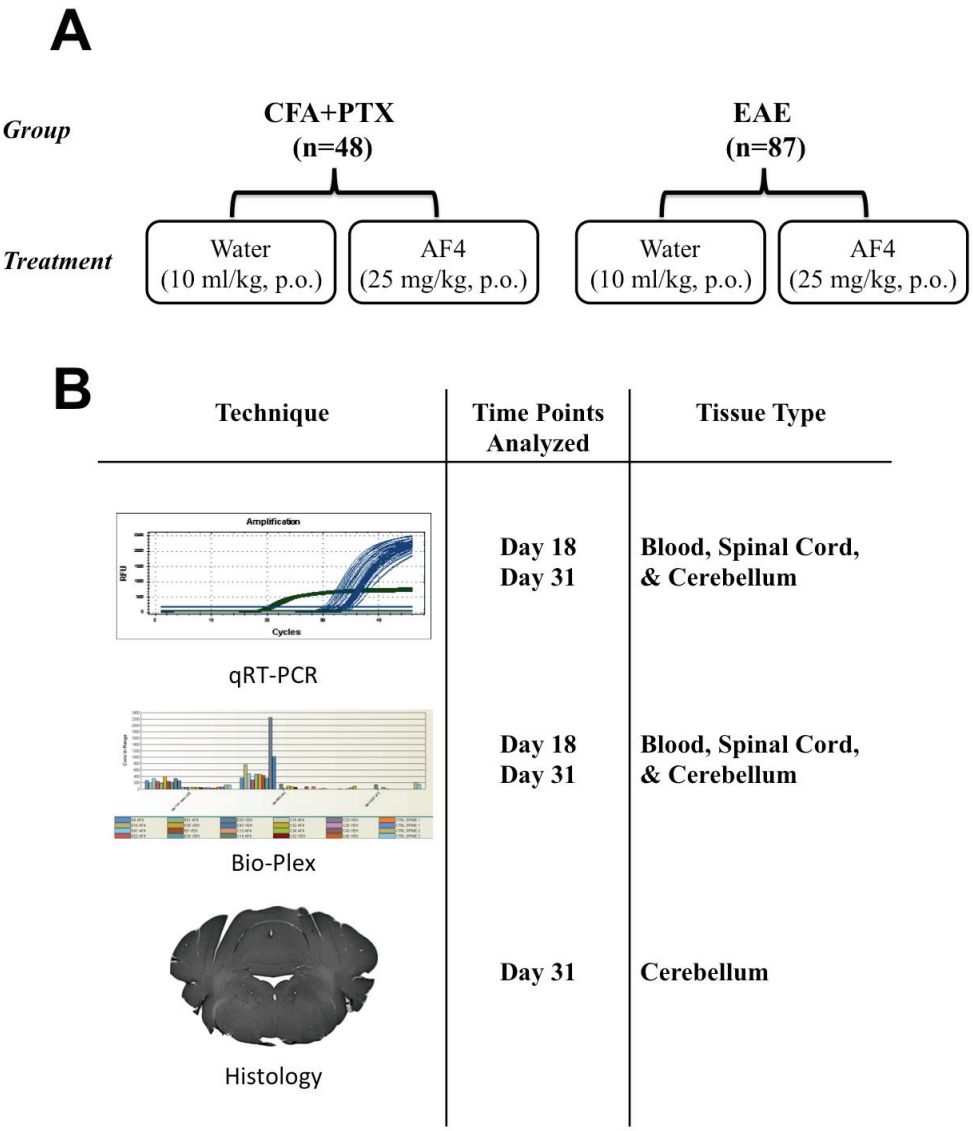

Figure 3: Experimental group assignment, techniques, and associated time points analyzed. **(A)** Female C57Bl/6 mice were injected with CFA+PTX alone (n=47) or immunized with MOG_{35-55} (n=87) and received either vehicle (water; 10 ml/kg/day, p.o.) or AF4 treatment (25 mg/kg/day, p.o). **(B)** Tissue was harvested at either day 18 or 31 and processed for qRT-PCR or Bio-Plex multi-plexed ELISAs. Histology was carried out on cerebellar tissue that was collected and fixed at day 31.

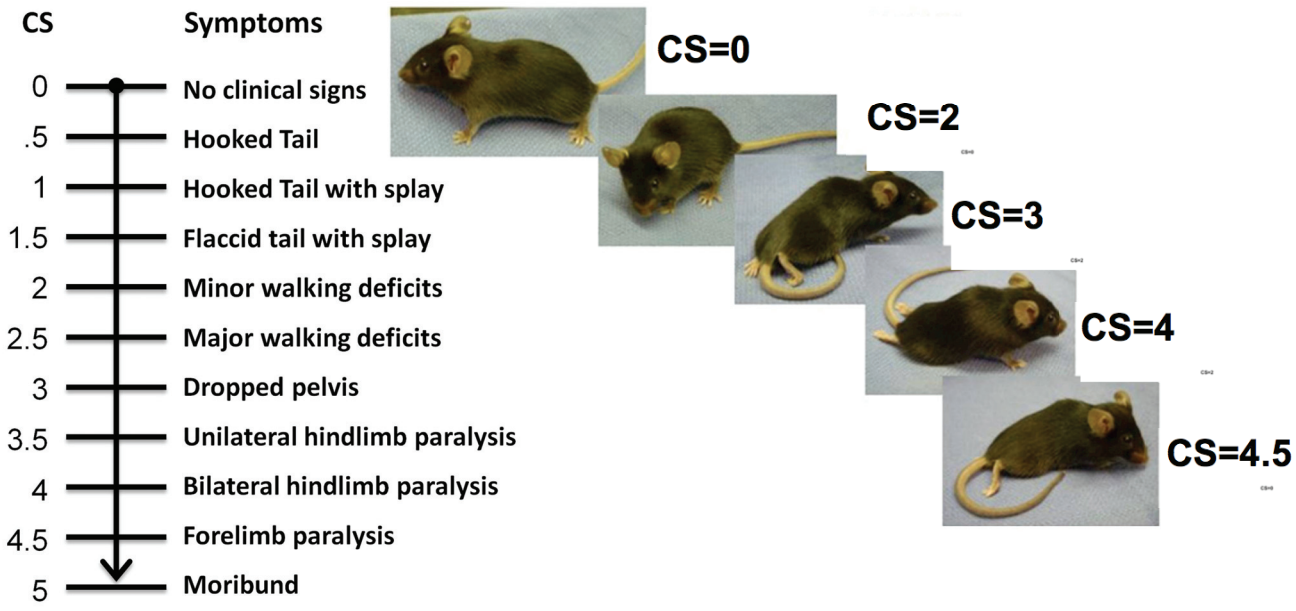

Figure 4: Grading scheme for clinical disease course in EAE. The following grading scheme was used to clinically score the animals (CS): 0, no clinical signs; 0.5, hooked tail; 1, hooked tail with splay; 1.5, flaccid tail with splay; 2, beginning of walking deficits with mild ataxia; 2.5, severe walking deficits with chronic ataxia; 3, dropped pelvis in addition to severe walking deficits; 3.5, unilateral hindlimb paralysis; 4, bilateral hindlimb paralysis; 4.5, forelimb paralysis 5, moribund. A scorer unaware of the treatment conditions recorded all clinical scores. Mouse pictures from Peggy Ho (Stanford University).

2.4 Treatment with AF4 or vehicle

A flavonoid-enriched fraction (AF4) was extracted from the skins of Northern Spy apples (Keddy *et al*., 2012). The AF4 dose for each experiment was standardized based on the total concentration of non-polymeric phenolics in AF4 comprised primarily of quercetin glycosides (approximately 70%) that included quercetin-3-*O*-glucoside, quercetin-3-*O*-galactoside, quercetin-3-*O*-rhamnoside, and quercetin-3-*O*-rutinoside. Epicatcehin, cyanidin-3-*O*-gluco, cholorgenic acid, and phlorizidin accounted in approximately equal proportions accounted for the remaining 30% of the total phenolic content of AF4. Vehicle treated animals received water (10 ml/kg, p.o.) once daily. AF4 was suspended in water and administered by oral gavage (p.o.) once daily at a dose of 25 mg/kg.

2.5 Preparation of brain tissue for histology

On day 31, mice were transcardially perfused with 0.9% saline (10.0 ml) followed by 4% paraformaldehyde (PFA, 10 ml) in 0.1 M phosphate buffer at pH 7.4. Brains were post-fixed by storing in 4% PFA for 48-72 hours at 4 °C. Following post-fixation, the brains were cryoprotected with 30% sucrose in 0.1 M phosphate buffer for 48 hours at 4 °C. Coronal sections 30 μm thick were cut at the level of the cerebellum using a freezing microtome (Microm HM-400; Thermo Fisher Scientific, Walldorf, Deutschland) and stored at 4 °C in a solution of PBS with 0.5% sodium azide.

2.6 Regressive haematotoxylin & eosin staining

Serial brain sections were mounted on Superfrost® glass slides (Fisher Scientific, Nepean, ON) and allowed to dry for 24 hours. Sections were then placed into Wheaton

jars and put under a gentle flow of tap water for ~1 minute and placed in Harris' haematoxylin (Sigma-Aldrich, Oakville, ON) for 5 minutes. The sections were then rinsed in tap water to remove the excess stain. This was followed by rapid immersion in a 1% acid alcohol solution (70 ml of 100% ethanol, 30 ml distilled water, and 1 ml of 1 M HCL) and a rinse under running tap water for 10-15 seconds. The sections were then placed in Scott's tap water solution (1.75 g of sodium bicarbonate, 10 g of magnesium sulfate, and 500 ml of tap water to make a 500 ml solution) for 2 minutes, or until the sections turned blue. Slides underwent repeated cycles of dipping in 1% acid alcohol, followed by plunging into tap water and placement into Scott's tap water solution until the background of the tissue was no longer blue. Sections were then washed for 5 minutes in running tap water and stained in 1% acidified eosin (2 g in 200 ml of a solution of 600 ml 95% ethanol, 4 ml glacial acetic acid) for 5-10 seconds. Sections were quickly checked under a light microscope to insure the correct contrast had been achieved. The sections were then dehydrated through a series of graded ethanol solutions of increasing concentrations (50%, 70%, 95%, and 100%) and cleared with xylene before coverslipping using Cytoseal (Stephens Scientific, Riverdale, NJ, USA).

2.7 Immunohistochemistry using the avidin-biotin complex method

Free-floating brain sections were rinsed three times with PBS containing 0.1 % Triton X (PBS-TX) for 10 minutes at room temperature. Then the tissue was placed in 1 % H_2O_2 in PBS-TX for 30 minutes to quench endogenous peroxidases. The tissue was rinsed three times in PBS-TX, and incubated in the appropriate serum (10% serum, PBS-TX) for 60 minutes. Following incubation in serum, sections were incubated with primary antibody, polyclonal anti-Iba1 antibody raised in rabbit (Wako, Tx, USA), at a dilution of 1:1000 in PBS for one

hour at room temperature for one hour then placed on a shaker at 4°C for 48 hours. The concentration of the primary antibody was determined using an initial titration series aimed at defining the optimal signal-to noise ratio. After incubation with the primary antibody was complete, the tissue was rinsed three times in PBS-TX and incubated in secondary antibody, biotinylated anti-rabbit raised in goat (Vector Laboratories Inc., Burlingame, CA, USA) at a dilution of 1:500 for one hour at room temperature.

Following another series of washes in PBS-TX, sections were incubated with Vectastain® avidin-biotin complex (Vector Laboratories Inc., Burlingame, CA, USA) in PBS-TX at a dilution of 1:1000 for 1 hour to amplify the signal of the secondary antibody. The sections were then washed and placed in a solution of 0.5 mg/ml diaminobenzidine (DAB; Sigma-Aldrich, Oakville, ON) with nickel and H_2O_2 in PBS. The tissue was reacted with the DAB solution for 5-10 minutes until the desired staining density was achieved. Next, the tissue was washed in PBS, mounted on Superfrost® glass slides (Fisher Scientific, Nepean, ON) and allowed to dry overnight. Once dry, the sections were dehydrated in a graded ethanol series of 50%, 70%, 95%, and 100%, cleared in xylene, and coverslipped using Cytoseal (Stephen's Scientific, Riverdale, NJ, USA). To ensure signal specificity, all immunohistochemistry was carried out in parallel with control sections incubated either without primary antibody, or secondary antibody, or ABC signal amplification.

2.8 Image analysis

Representative photomicrographs of sections that displayed Iba-1 immunoreactivity in the cerebellum 5.88 mm posterior to bregma were captured at 50X amplification (10X objective and a 5X lens) using a Zeiss microscope. Images of H&E

stained sections were captured from the cerebellum 5.88 mm posterior to bregma at 50X (10X objective and a 5X lens).

A 5-point cumulative pathology index score was used to describe the extent of inflammation and overall cellular degeneration observed in the cerebellar parenchyma in EAE mice treated with either AF4 or water (Racke *et al.*, 1995; Langer-Gould *et al.*, 2002). A trained observer unaware of the treatment conditions provided a score for the cerebellum of each EAE mouse using Iba-1 and H&E stains, both of which allow for the detection of inflammatory mediated pathology. A collective score reflective of overall inflammation and tissue damage for each animal was recorded (Figure 5).

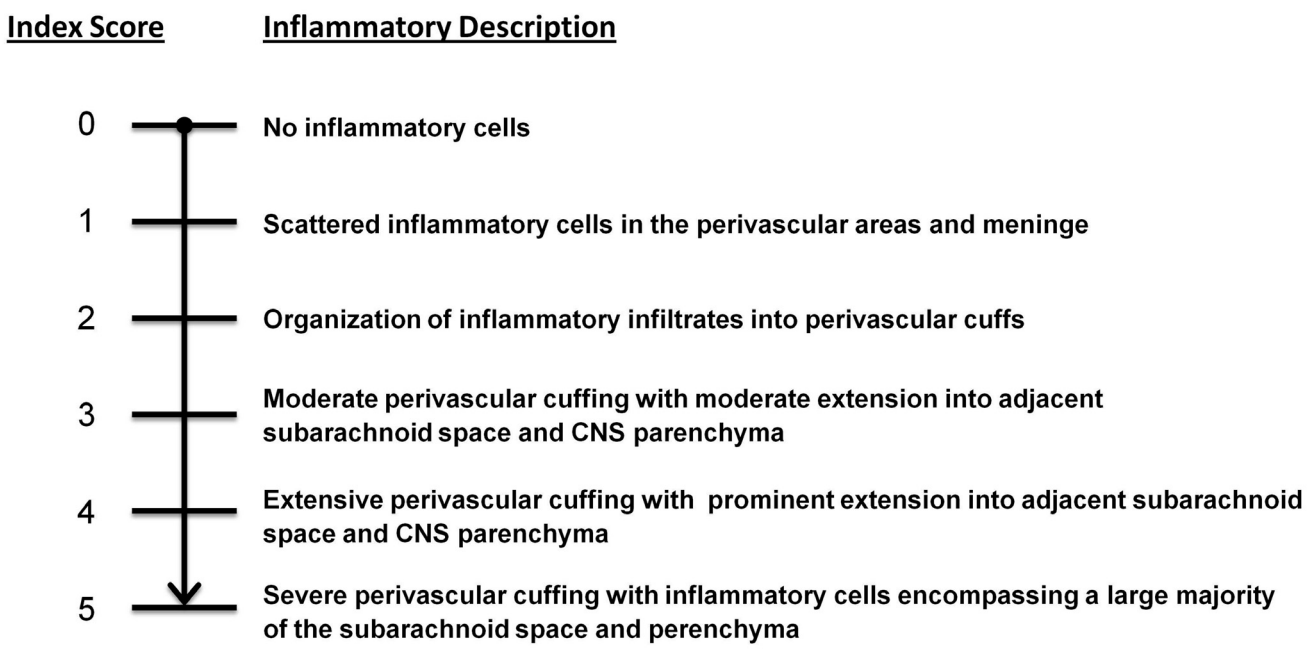

Figure 5: Pathology index scoring for immune cell infiltration. Sections stained for Iba-1 immunoreactivity and H&E staining were analyzed by an observer unaware of the treatment conditions using the following scoring scheme: 0; no inflammatory cells; 1, scattered inflammatory cells in the perivascular areas and meninges; 2, organization of inflammatory infiltrates into perivascular cuffs; 3, moderate perivascular cuffing with moderate extension into adjacent subarachnoid space and parenchyma of the cerebellum; 4, extensive perivascular cuffing with prominent extension into adjacent subarachnoid space and parenchyma of the cerebellum; 5, severe perivascular cuffing with inflammatory cells encompassing a large majority of the subarachnoid and parenchymal areas. This pathology index scale was adapted from Rack *et al.* (1995) and Langer-Gould *et al.* (2002).

2.9 Tissue preparation for RNA extraction

Following euthanasia, the cerebellum and spinal cord from each animal were collected, immediately submerged in RNAlater stabilization reagent (Qiagen, Toronto, ON) and stored at -20 °C.

2.10 RNA extractions and quality control

Total RNA was extracted from cerebellum and spinal cords using an RNeasy Lipid Tissue Mini Kit (Qiagen, Toronto, ON) according to the procedures described by the manufacturer. To measure the concentration, quality and overall purity of isolated total RNA, an Experion bioanalzer equipped with a RNA StdSens Analysis Kit was used (Bio-Rad, Hercules, CA, USA). Briefly, the Experion system uses microfluidic electrophoresis technology coupled with a fluorescent dye that interacts directly with the nucleic acids that are quantified by detection of laser-induced fluorescence. Total RNA (1 µl) from cerebellum and spinal cord were run on an Experion RNA StdSens chip equipped with a dynamic range capable of detecting RNA concentrations from 5-500 ng/µl. Quality of the RNA samples was determined using the RNA quality indicator (RQI). The RQI reports a number between 1 (very degraded RNA) to 10 (intact RNA), and each sample must have obtained a RQI value ≥7 to be considered acceptable for qRT-PCR experiments (Figure 6A). RQI values are determined by comparing the ribosomal peaks of the 28S region, 18S region, and the pre-18S region from the electropherogram of the RNA sample to a series of standardized degraded RNA samples (Figure 6B). Conditional upon passing quality control by Experion electrophoresis, total RNA from each sample was diluted with RNase-free water to a working concentration of 10 ng/µl, aliquoted, and stored at -80 °C.

A

Lane	Sample Name	RNA Area	RNA Concentration (ng/µl)	Ratio [28S/18S]	RQI
L	Ladder	500.22	160		
1	**Spinal Cord** *Sample 1*	2638.93	1044.82	1.2	8.9
2	**Spinal Cord** *Sample 2*	1539.49	609.53	1.03	8.6
3	**Spinal Cord** *Sample 3*	1656.69	655.93	1.33	8.8
4	**Spinal Cord** *Sample 4*	1658.44	656.62	1.23	9.2
5	**Cerebellum** *Sample 1*	3559.47	1715.95	1.17	9.4
6	**Cerebellum** *Sample 2*	3941.53	1900.13	1.2	9.4
7	**Cerebellum** *Sample 3*	6506.63	3136.72	1.07	9.2
8	**Cerebellum** *Sample 4*	7903.84	3810.29	0.68	7.7

B

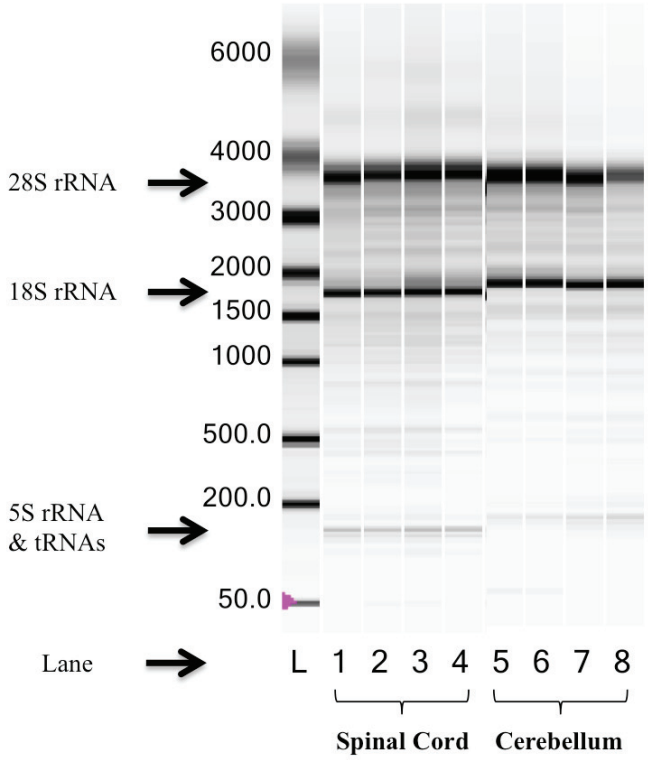

Figure 6: Experion automated electrophoresis RNA quality control system. **(A)** Results table detailing concentration, 28S/18S data, and RNA quality indicator (RQI) **(B)** Virtual gel of representative RNA samples from cerebellum, and spinal cord tissue.

2.11 Quantitative RT-PCR

Quantitative reverse-transcription polymerase chain reaction (qRT-PCR) was performed to measure the relative changes in the levels of mRNAs shown in Table 1. A final concentration of 50 ng of RNA was reverse transcribed to generate first-strand cDNA and amplified using Taqman one-step EZ RT-PCR core reagents (Applied Biosystems; Foster City, CA). Mouse primers and probes were purchased pre-mixed from Applied Biosystems (Table 2). Reverse transcription, PCR amplification and fluorescence detection were performed in duplicate using a CFX 96 Touch™ real-time PCR detection system with CFX manager 2.1 software (Bio-Rad, Hercules, CA, USA), with β-actin as an endogenous control gene. PCR cycling conditions were 50 °C for 2 min, 60°C for 30 min, 95°C for 5 min, followed by 40 cycles of 95°C for 10 s and 60°C for 1 min. Results are expressed as fold changes relative to a tissue-matched calibrator sample extracted from untreated age and sex matched C56Bl/6 mice. Relative changes from the calibrator were calculated using the $2^{-\Delta\Delta Ct}$ method (Livak & Schmittgen, 2001).

Table 2: Primer and probe sets used for qRT-PCR. For each respective sample, a total of 50 ng of total RNA was reverse transcribed to generate first-strand cDNA and amplified using Taqman one-step EZ RT-PCR core reagents (Applied Biosystems; Foster City, CA). Mouse primers and probes were purchased pre-mixed from Applied Biosystems.

Gene name	Assay ID	Reference Sequence	Anchor Nucleotide Location	Amplicon length
TNF-α	Mm00443258_m1	NM_013693.2	341	81
IL-1β	Mm01336189_m1	NM_008361.3	55	63
IL-6	Mm00446190_m1	NM_031168.1	237	78
PGC -1α	Mm01208835_m1	NM_008904.2	1015	68
SCD1	Mm00772290_m1	NM_009127.4	598	60
EPO	Mm01202755_m1	NM_007942.2	490	59
PMCA2	Mm00437640_m1	NM_009723.3	1694	79
β-Actin	Mm00607939_s1	NM_007393.3	1230	115

Gene name	Context Sequence
TNF-α	tc tgtctactga acttcggggt gatcggtccc caaagggatg **a**gaagttccc aaatggcctc cctctcatca gttctatggc cca
IL-1β	catc tgggatcctc tccagccaag cttccttgtg caag**t**gtctg aagcagctat ggcaactgtt cctgaactca act
IL-6	cac atgttctctg ggaaatcgtg gaaatgagaa aagagt**t**gtg caatggcaat tctgattgta tgaacaacga tgatgc
PGC-1α	gagc gaaccttaag tgtggaactc tctggaactg cagg**c**ctaac tcctcccaca actcctcctc ataaagccaa cca
SCD1	actggttccc tcctgcaagc tctacacctg cctcttcg**g**g attttctact acatgaccag cgctctgggc atcacag
EPO	tctacgtag cctcacttca ctgcttcggg tactgggag**c** tcagaaggaa ttgatgtcgc ctccagatac caccccac
PMCA2	gggcaag ctcaccaaac tggctgtgca gataggcaag gcg**g**gcctgg tgatgtcggc catcacagtg atcatcctgg tactctactt
β-Actin	aagcagg agtacgatga gtccggcccc tccatcgtgc accgcaagtg cttctaggcg gactgttact gagctgcgt**t** ttacaccctt tctttgacaa aacctaactt gcgcagaaaa aaaaaaaata agagacaaca ttggcatggc tttgtt

2.12 Multi-plexed ELISA

Protein extracts from cerebellar and spinal cord tissue were homogenized in 500 µl of sterile PBS (pH=7.4) containing a protease inhibitor (Sigma-Aldrich, Oakville, ON) and phosphatase inhibitor (50 mM sodium fluoride and 1 mM sodium orthovanadate; PBS-PI) using a Pro 200 handheld homogenizer (Pro Scientific Inc., Oxford, CT, USA) for one minute on a bed of ice. Homogenates were aliquoted into two 1.5 ml tubes and immediately frozen and stored at -80 ^{o}C.

Multiplexed ELISAs were conducted using the Bio-Plex® suspension array system that utilizes multiplexing technology to detect numerous cytokines in the same sample. The Bio-Plex® suspension array is built around three core technologies. The first is the family of fluorescently dyed monodisperse polystyrene beads (Luminex® xMAP®) conjugated with antibodies against a specific epitope. The second is a flow cytometer equipped with a dual laser detector and necessary optics to measure fluorescence from the surface of monodisperse polystyrene beads specific to a particular epitope. The third is a high-speed digital signal processor to efficiently manage the fluorescent output capable of distinguishing up to 100 different fluorescent-coded beads. The Bio-Plex 200 has a dynamic range capable of detecting 1-32 000 pg/ml of protein.

Bio-Plex Pro™ premixed 9-plex mouse cytokine kits were used (Table 3A) to obtain an overview of the inflammatory status in the cerebellum and spinal cord (Bio-Rad, Hercules, CA, USA). A standard curve was constructed using a series of beads with a known fluorescent spectrum unique to each cytokine and diluted to a final concentration of 500 µg/ml with PBS-PI. Magnetic beads (50 µl) were added to a 96-well plate and washed with 100 µl of assay buffer. This was followed by adding, in duplicate, 50 µl each of standards, samples, or negative controls to the wells. The plate was covered and

incubated in the dark at room temperature on a shaker set at 300 rpm for 30 minutes followed by three washes. Next, detection antibody was added to each well and incubated in the dark at room temperature on a shaker set at 300 rpm for 30 minutes followed by three washes. Lastly, fifty microliters of strepavidin-PE was added to the wells, incubated in the dark for 10 minutes at room temperature. The beads were washed three times and read in a Bio-Plex® 200 luminometer (Bio-Rad, Hercules, CA, USA).

2.13 Assessment of basal and LPS-induced Release of Inflammatory Cytokines in Whole Blood of EAE Mice

Induction of cytokine release in whole blood by LPS was used as an *ex vivo* assay to assess the immune-modulatory effects of AF4 at days 18 and 31 following induction of EAE. Basal concentrations of TNF-α, IL-1β, and IL-6 were assessed at both time points to serve as a negative control for both LPS-induction to assess the cytokine profile of EAE and CFA+PTX treated mice that received either AF4 or vehicle. Two hours following the last oral administration of either 25 mg/kg of AF4 or 10 ml/kg water, whole blood was collected via cardiac puncture in Microtainer® containing no additive specimen tubes (BD Biosciences; Franklin Lakes, NJ, USA) containing 50 µl of 4% tri-sodium citrate dihydrate. Each blood sample was split into two tubes, one containing LPS and one with PBS. LPS (serotype 0111:B4, Sigma-Aldrich; Oakville, ON) derived from *E. coli*, a TLR-4 ligand, was used to induce the release of TNF-α. LPS was freshly prepared at a concentration of 10 mg/ml in 0.1% BSA in PBS and diluted to a final concentration of 100 µg LPS/ml of blood. Both stimulated and non-stimulated blood was incubated for 4 h at 37 ^{o}C in a humidified tissue culture incubator supplemented with 5%

CO_2. Following incubation, 10 µl of PBS-PI was added to whole blood and the tube was inverted several times. Each sample was transferred to a Microtainer® plasma separator tube containing lithium heparin (BD; Franklin Lakes, NJ) and centrifuged at 10 000 × g for 2 min at room temperature. Plasma was collected and immediately stored at -80 ^{o}C.

Using the previously described Bio-Plex® suspension array system (Bio-Rad, Hercules, CA, USA), a 3-plex assay was used to measure protein concentrations of TNF-α, IL-1β, and IL-6 in the plasma of EAE (EAE-VEH, EAE-AF4) mice at days 18 and 31 (Table 3B).

Table 3: Cytokines and chemokines measured utilizing the Bio-Plex® suspension array system. (A) Cytokines and chemokines included in the mouse cytokine 9-plex assays. (B) Cytokines included in the mouse cytokine 3-plex assays.

A

Bio-Plex Pro™ Mouse Cytokine 9-Plex Assay
IL-15
IL-18
basic FGF
LIF
M-CSF
MIG
CXCL2
PDGF-BB
VEGF

B

Bio-Plex Pro™ Mouse Cytokine 3-plex Assay
IL-1β
IL-6
TNF-α

2.14 Statistical Analyses

Student's t-test and Mann Whitney U test were used to calculate differences between groups with normal and non-Gaussian distributions, respectively. Comparison between three or more groups was performed using a one-way ANOVA with Newman-Keuls post-hoc analyses. EAE curves were analyzed using a two-way ANOVA followed by Bonferroni's post-hoc analyses. Area under the curve and the number of days with a clinical score greater than 2.5 were used as additional measures of EAE disease severity as per the recommendations of Baker and Amor (2012). All statistics were computed using GraphPad Prism version 6.0 for Macintosh (GraphPad Software, San Diego, CA). Differences between groups for all tests were considered statistically significant at an alpha level of less than 0.05.

CHAPTER 3: RESULTS

3.1 Effects of oral administration of AF4 on EAE severity

Eighty-seven 6-8 week old (15-20 g) female C57Bl/6 mice were immunized with MOG_{35-55} in a 1:1 ratio with complete Freund's adjuvant (CFA) on day 0 and boosted with pertussis toxin injections (PTX) on days 0 and 2 (EAE group). Forty-eight age, sex, and weight matched C57Bl/6 mice served as antigen controls and received CFA and pertussis toxin but not MOG_{35-55} (CFA+PTX group). Both EAE and CFA+PTX groups were weighed and scored daily for signs of clinical disease beginning at day 7. Mice injected with CFA+PTX alone or immunized with MOG_{35-55} received either vehicle (CFA+PTX-VEH; EAE-VEH) or AF4 treatment (CFA+PTX-AF4; EAE-AF4). Oral administration of vehicle (water, 10 ml/kg/day, p.o.) or AF4 (25 mg/kg/day, p.o.) began 24 hours following the first clinical signs of EAE and continued until either day 18 or day 31, at which point the mice were humanely euthanized followed by the harvesting of blood and CNS tissue for subsequent experimentation.

Mice that received MOG_{35-55} developed clinical signs of EAE from days 7-11 with 100% incidence (Figures 7A and 10A); CFA+PTX mice remained asymptomatic with no clinical signs for the duration of the experiments (data not shown). Two independent EAE experiments were conducted to determine the efficacy of AF4 by day 18, and three additional experiments were carried out to assess the efficacy of AF4 against EAE until day 31.

Oral administration of AF4 did not reduce EAE clinical severity from days 7-18.

Oral administration of AF4 beginning 24 hours after the onset of clinical disease signs failed to reduce EAE severity relative to vehicle treated mice from days 7-18 (Figure 7A). To determine if there were any differences in the duration of maximal clinical scores between EAE-VEH and EAE-AF4 treated mice, the total number of days each animal had a clinical score greater than 2.5 (severe walking deficits with ataxia) was calculated. This metric reflects the total number of days each mouse experienced moderate to severe paralysis. There was no difference between these treatment groups in terms of the number of days each mouse had a clinical score greater than 2.5 from days 7 to 18 (Figure 8). The mean ± SEM area under the curve for clinical scores from days 7-18 was calculated for both treatment groups. The mean area under the curve was not significantly different between EAE-AF4 (8.3 ± 0.6) and EAE-VEH mice (9.1 ± 0.7) from days 7-18 (Figure 9). EAE (EAE-VEH and EAE-AF4) mice weighed significantly less than the CFA+PTX (CFA+PTX-VEH, and CFA+PTX-AF4) groups from days 7-18 (Figure 7B). EAE mice were significantly lower than CFA+PTX mice with respect to body weight from days 7-18. Treatment conditions (vehicle or AF4) within EAE and CFA+PTX groups were not different with respect to body weight from days 7-18.

Oral administration of AF4 reduced EAE clinical severity from days 19-31.

Clinical scores and body weight for EAE mice treated with vehicle or AF4 from the onset of clinical signs are shown in Figure 10. Relative to EAE-VEH mice, oral administration of AF4 reduced clinical severity from days 19-31 (Figure 10A). Body weight did not differ between these groups with both showing a comparable reduction and recovery from days 7-31 (Figure 10B). Relative to EAE-VEH (11.6 ± 1.2), EAE-AF4

mice (4.9 ± 1.0) spent fewer days with a clinical score greater than 2.5 between days 7 and 31 (Figure 11). The mean area under the curve for clinical scores from days 7-18 did not differ between groups. By contrast, the mean area under the curve for clinical scores was decreased in EAE-AF4 mice (12.9 ± 0.7) relative to EAE-VEH treated mice (17.5 ± 1.6) from days 19-31 (Figures 12A and B).

EAE (EAE-VEH and EAE-AF4) mice weighed significantly less than the CFA+PTX (CFA+PTX-VEH, and CFA+PTX-AF4) groups from days 7-31 (Figure 10B). Treatment conditions (vehicle or AF4) within EAE and CFA+PTX groups were not different with respect to body weight from days 7-31.

Figure 7: Oral administration of AF4 did not ameliorate clinical severity relative to vehicle treated EAE mice from days 7-18. Mice injected with CFA+PTX alone or in combination with MOG_{35-55} received either vehicle (CFA+PTX-VEH; EAE-VEH) or AF4 (CFA+PTX-AF4; EAE-AF4). Oral administration of vehicle or AF4 began 24 hours after the first clinical signs of EAE (days 7-11; ***a*)** and continued until day 18, at which point tissue from the mice was harvested. **(A)** EAE-VEH (n=14) and EAE-AF4 (n=13) mice showed no clinical differences at day 18 ($p>0.05$). (**B)** EAE-VEH and EAE-AF4 treated mice weighed significantly less relative to CFA+PTX-VEH and CFA+PTX-AF4 mice from days 7-18 ($p<0.01$). There were no differences between treatment conditions (vehicle or AF4) within both EAE and CFA+PTX groups with respect to body weight from days 7-18 ($p>0.05$). Data are expressed as the mean ± SEM pooled from two independent experiments and were analyzed using a two-way ANOVA followed by Bonferroni post-hoc tests.

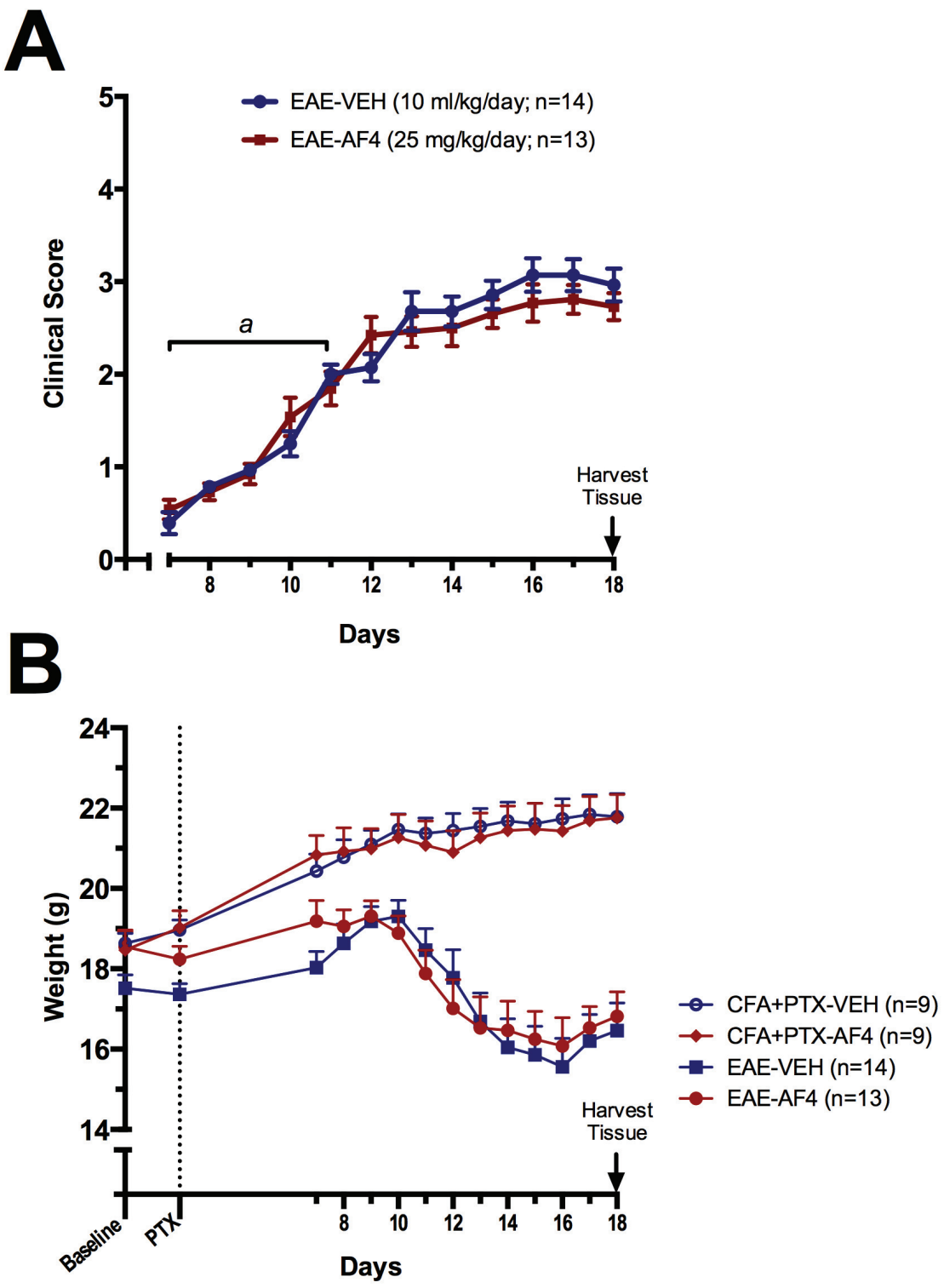
A
EAE-VEH (10 ml/kg/day; n=14)
EAE-AF4 (25 mg/kg/day; n=13)
Clinical Score
a
Harvest Tissue
Days
B
Weight (g)
Harvest Tissue
Baseline
PTX
Days
CFA+PTX-VEH (n=9)
CFA+PTX-AF4 (n=9)
EAE-VEH (n=14)
EAE-AF4 (n=13)

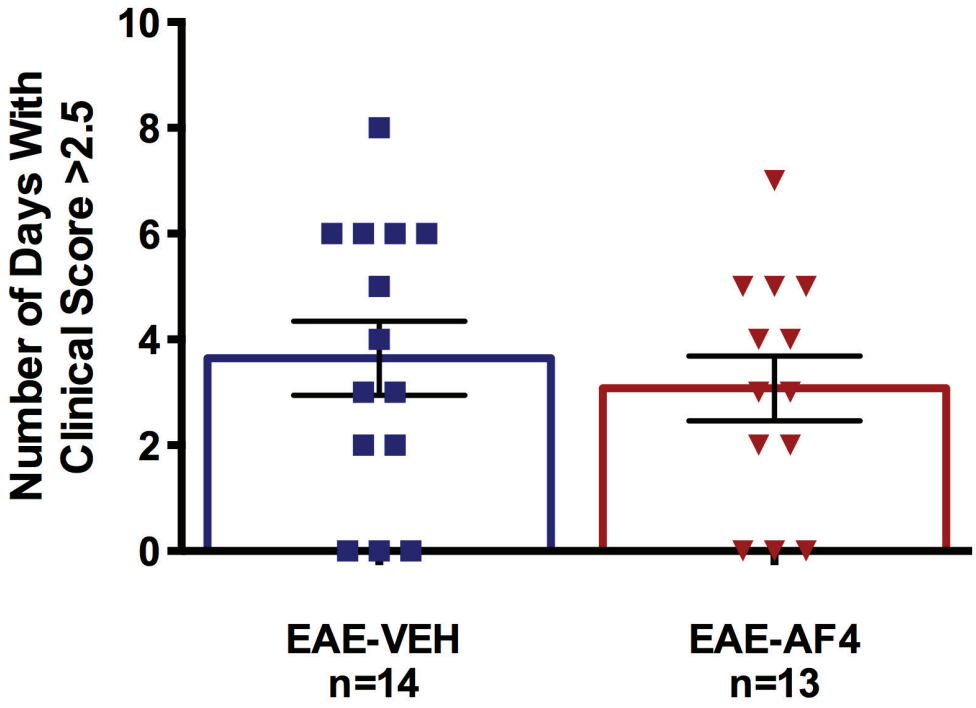

Figure 8: The total number of days each animal displayed a clinical score greater than 2.5 from days 7 to 18. No statistical differences were found between EAE-VEH and EAE-AF4 groups (two-sided Mann-Whitney U test, $p>0.05$). Data are pooled from two independent experiments and expressed as the mean ± SEM.

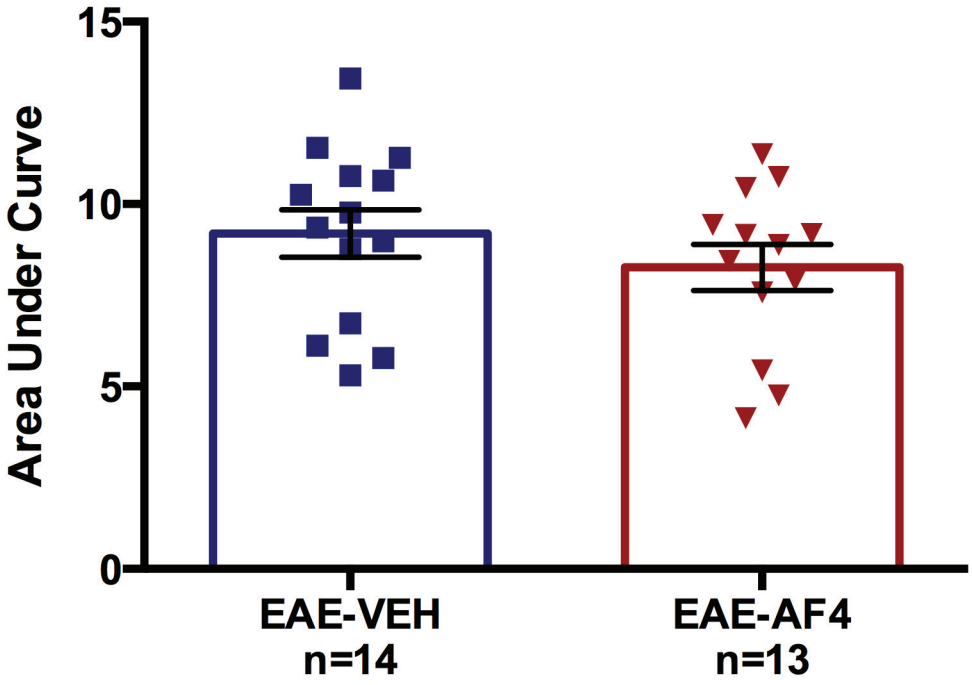

Figure 9: Oral administration of AF4 to EAE mice did not reduce the mean area under the curve for clinical scores from days 7-18 relative to the vehicle group (two-sided Mann Whitney U test, $p>0.05$). Data were pooled from two independent experiments and expressed as the mean ± SEM.

Figure 10: Oral administration of AF4 ameliorated EAE severity relative to vehicle controls from days 19-31. Mice injected with CFA + PTX alone or in combination with MOG_{35-55} received either vehicle (CFA+PTX-VEH; EAE-VEH) or AF4 (CFA+PTX-AF4; EAE-AF4) treatment. Oral administration of vehicle or AF4 began 24 hours after the first clinical signs of EAE (day 7-11; *a*) and continued until day 31, at which point tissues were harvested. **(A)** EAE-VEH (n=31) and EAE-AF4 (n=29) mice showed significant clinical improvement from days 19-31 (two-way ANOVA, $p<0.05$). **(B)** EAE-VEH and EAE-AF4 mice weighed less relative to CFA+PTX-VEH and CFA+PTX-AF4 mice from days 7-31 ($p<0.05$). No statistical differences were found between treatment conditions (Vehicle or AF4) within the EAE and CFA+PTX groups with respect to body weight from days 7-31 ($p>0.05$). Data are expressed as the mean ± SEM pooled from three independent experiments. *$p<0.05$, two-way ANOVA followed by Bonferroni post-hoc tests.

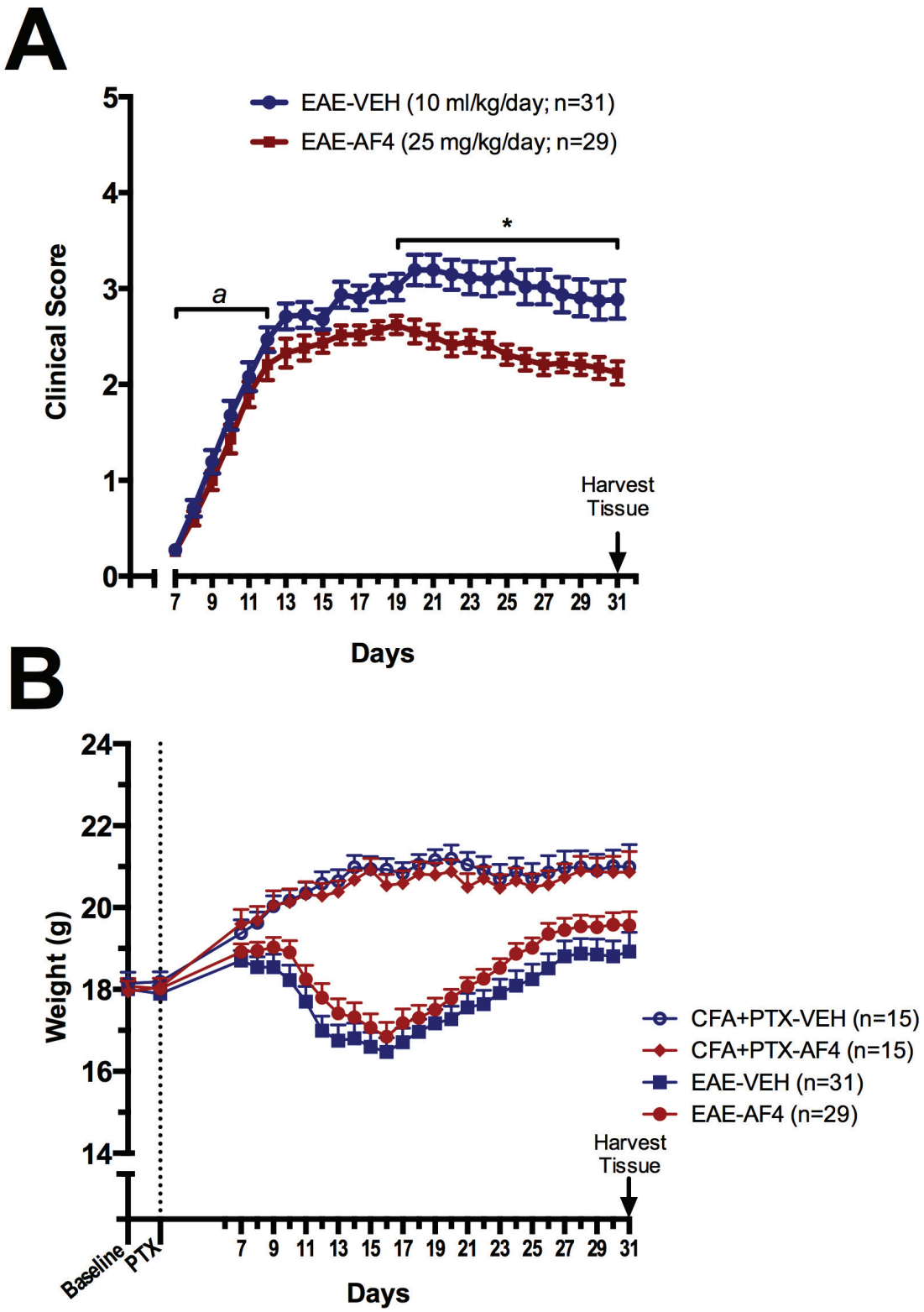
A
EAE-VEH (10 ml/kg/day; n=31)
EAE-AF4 (25 mg/kg/day; n=29)
Clinical Score
0
1
2
3
4
5
a
*
Harvest
Tissue
7 9 11 13 15 17 19 21 23 25 27 29 31
Days
B
Weight (g)
14
16
18
20
22
24
CFA+PTX-VEH (n=15)
CFA+PTX-AF4 (n=15)
EAE-VEH (n=31)
EAE-AF4 (n=29)
Harvest
Tissue
Baseline
PTX
7 9 11 13 15 17 19 21 23 25 27 29 31
Days

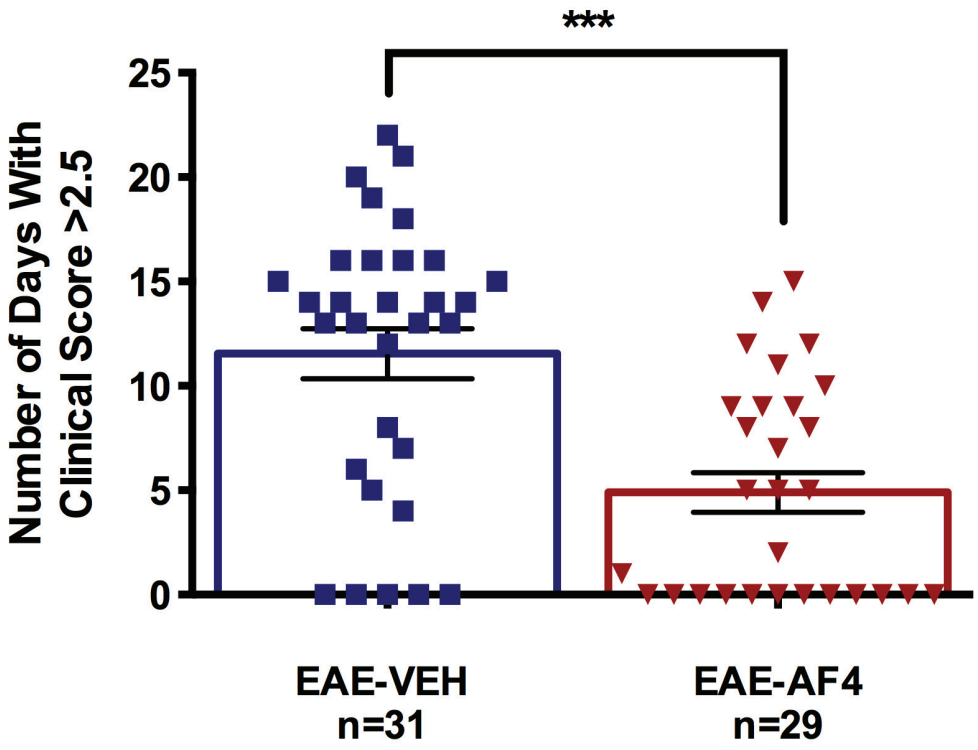

Figure 11: The number of days each animal displayed a clinical score greater than 2.5 from days 7 to 31. Relative to the EAE-VEH group, EAE-AF4 treated mice spent fewer days with a clinical score >2.5. Data were pooled from two independent experiments and expressed as the mean ± SEM. ***p<0.001, two-sided Mann-Whitney U Test.

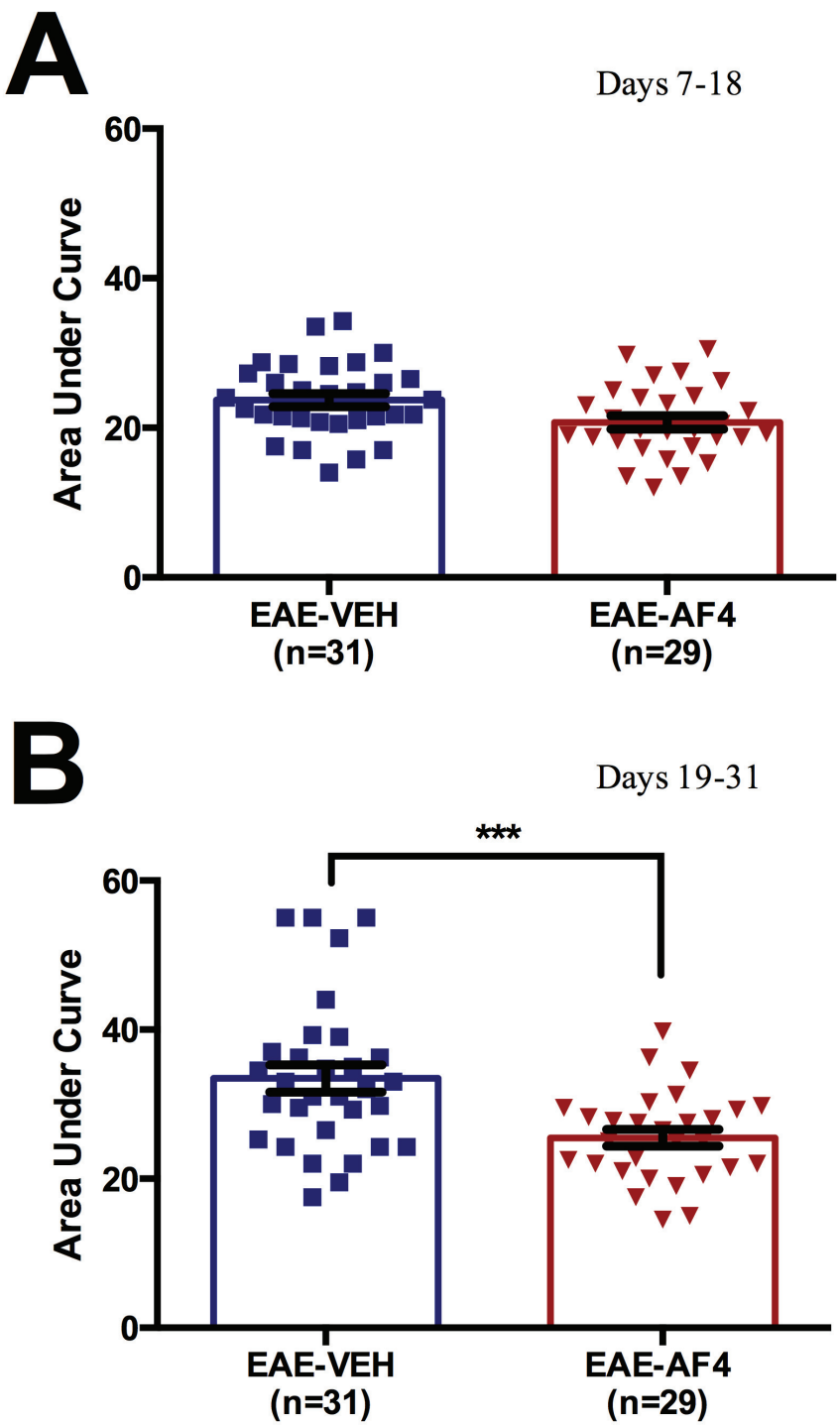

Figure 12: Area under the curve for EAE mice. **(A)** Oral administration of AF4 to EAE mice did not reduce the mean area under the curve for clinical scores from days 7-18 relative to the vehicle group. **(B)** By contrast, oral administration of AF4 to EAE mice reduced the mean area under the curve for clinical scores from days 19-31 relative to the vehicle group. Data were pooled from three independent experiments and expressed as the mean ± SEM. ***$p<0.001$, two-sided Mann-Whitney U test.

3.2 Basal and LPS-induced pro-inflammatory cytokine concentrations are reduced in whole blood from EAE mice that received AF4

The effects of AF4 administration on basal and LPS-induced concentrations of TNF-α, IL-1β and IL-6 were determined at day 18 and 31. Blood from each animal was split into two tubes, with one containing LPS, and incubated for two hours at 37 °C. Next, plasma was isolated from whole blood and protein concentrations of TNF-α, IL-1β and IL-6 were determined using a multi-plexed ELISA assay. The mean ± SEM for basal and LPS-stimulated concentrations (pg/ml) of TNF-α, IL-1β and IL-6 are shown in Tables 4A and B, respectively.

AF4 administration reduced basal cytokine levels in plasma of EAE mice

Relative to EAE-VEH treated mice, EAE-AF4 mice showed lower concentrations of TNF-α and IL-1β in plasma at days 18 and 31 (Figures 13A, B, C and D). Oral administration of AF4 did not alter IL-6 concentrations at days 18 and 31 (Table 4A; Figures 13E and F).

LPS-induced release of TNF-α and IL-1β were suppressed in whole blood from AF4 treatment

LPS-induced TNF-α release was suppressed in whole blood from EAE-AF4 relative to EAE-VEH mice at day 18 (Figure 14A). By contrast, LPS-induced release of TNF-α was the same for EAE-AF4 and EAE-VEH treated mice at day 31 (Table 4B; Figure 14B).

Table 4: The mean ± SEM protein concentrations (pg/ml) of **(A)** basal TNF-α, IL-1β and IL-6 in plasma at days 18 and 31 and **(B)** LPS-induced release of TNF-α at days 18 and 31. *p<0.05 in relation to EAE-VEH, one-sided t-test.

A

Basal Levels		EAE-VEH	EAE-AF4
TNF-α			
	Day 18	33.7 ± 9.2	3.2 ± 1.4*
	Day 31	40.4 ± 9.51	1.9 ± 1.4*
IL-1β			
	Day 18	59.8 ± 15.9	27.8 ± 3.2*
	Day 31	75.5 ± 18.9	30.9 ± 5.0*
IL-6			
	Day 18	7.9 ± 1.1	9.6 ± 1.7
	Day 31	10.6 ± 5.2	3.6 ± 1.2

B

LPS Stimulated		EAE-VEH	EAE-AF4
TNF-α			
	Day 18	413.2 ± 17.0	3.16 ± 1.5*
	Day 31	378.8 ± 180.4	670.0 ± 263.3

Figure 13: Oral administration of AF4 reduced basal protein concentrations of TNF-α and IL-1β, but not IL-6, in the plasma of EAE mice at days 18 and 31. **(A)** TNF-α concentrations were reduced in the plasma of EAE-AF4 relative to EAE-VEH animals at day 18. **(B)** TNF-α concentrations were also decreased in the plasma of EAE-AF4 relative to EAE-VEH animals at day 31. **(C)** IL-1β concentrations were reduced in the plasma of EAE-AF4 relative to EAE-VEH animals at day 18. **(D)** IL-1β protein concentrations were reduced in the plasma of EAE-AF4 relative to EAE-VEH animals at day 31. **(E)** IL-6 protein concentrations were not statistically different in the plasma of EAE-VEH and EAE-AF4 treated mice at day 18. **(F)** IL-6 concentrations were not different in the plasma of EAE-VEH and EAE-AF4 treated mice at day 31. Data are expressed as the mean ± SEM.*$p<0.05$ **$p<0.01$, one-sided student's t-test.

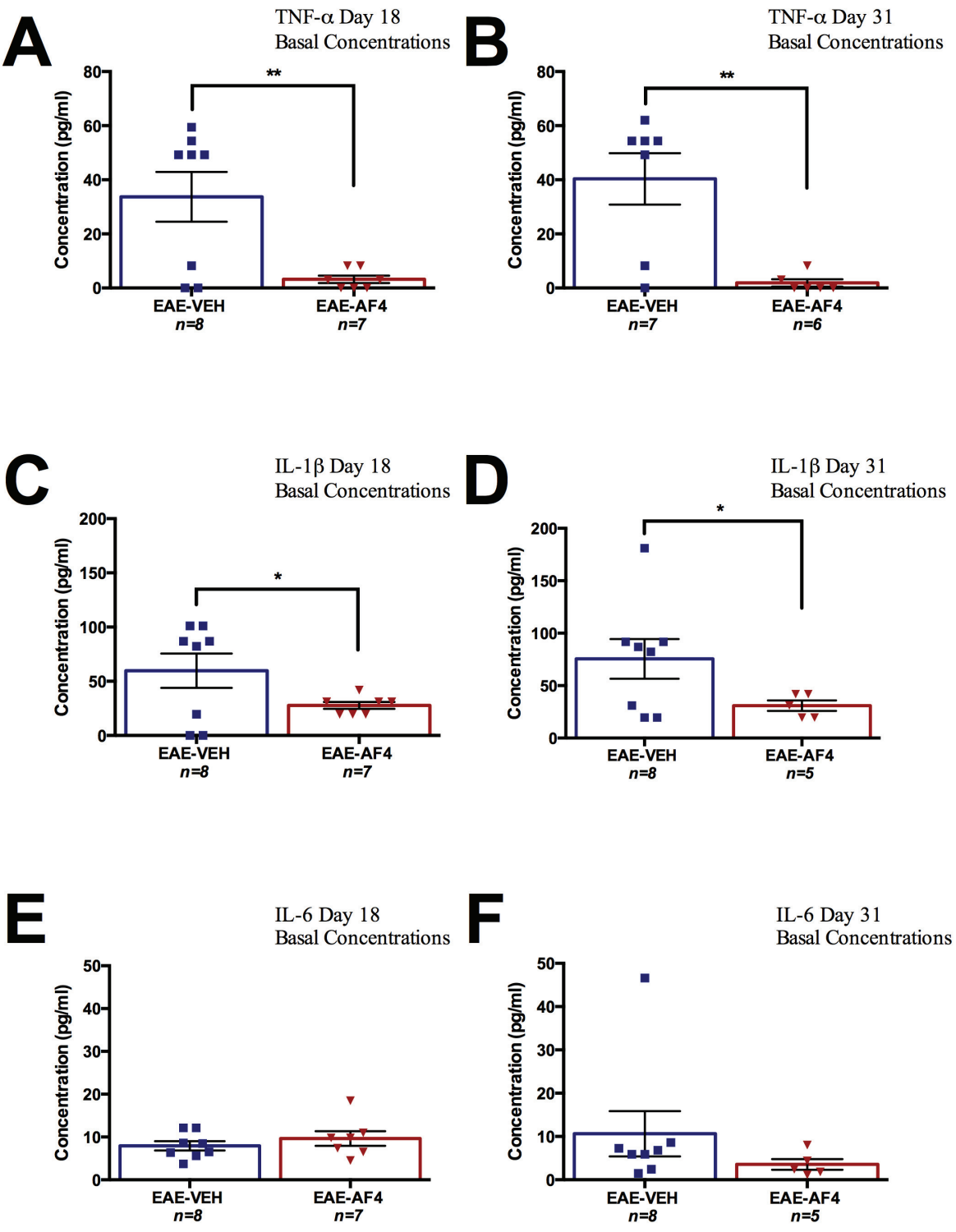
A
TNF-α Day 18
Basal Concentrations
Concentration (pg/ml)
80
60
40
20
0
**
EAE-VEH
n=8
EAE-AF4
n=7
B
TNF-α Day 31
Basal Concentrations
Concentration (pg/ml)
80
60
40
20
0
**
EAE-VEH
n=7
EAE-AF4
n=6
C
IL-1β Day 18
Basal Concentrations
Concentration (pg/ml)
200
150
100
50
0
*
EAE-VEH
n=8
EAE-AF4
n=7
D
IL-1β Day 31
Basal Concentrations
Concentration (pg/ml)
200
150
100
50
0
*
EAE-VEH
n=8
EAE-AF4
n=5
E
IL-6 Day 18
Basal Concentrations
Concentration (pg/ml)
50
40
30
20
10
0
EAE-VEH
n=8
EAE-AF4
n=7
F
IL-6 Day 31
Basal Concentrations
Concentration (pg/ml)
50
40
30
20
10
0
EAE-VEH
n=8
EAE-AF4
n=5

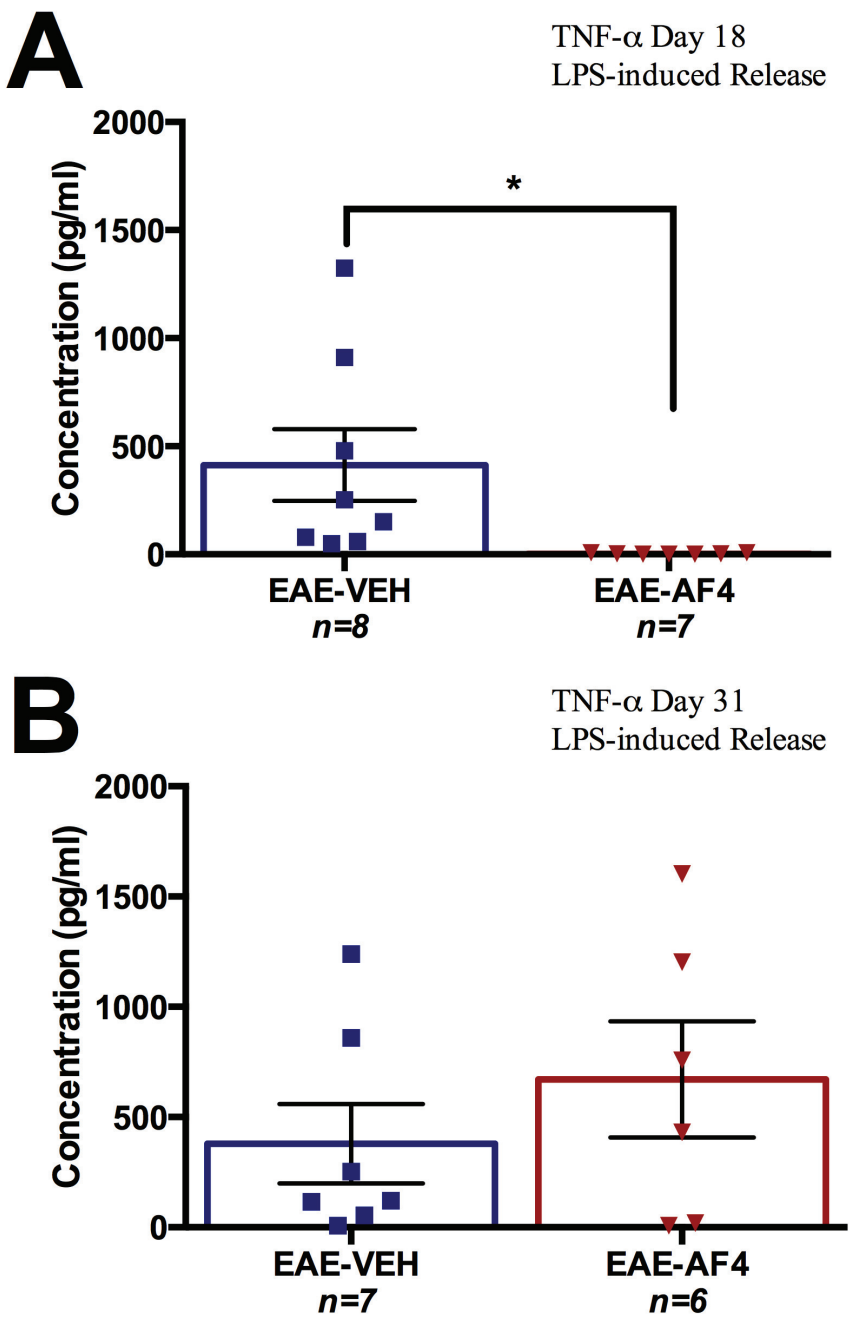

Figure 14: LPS-induced release of TNF-α was suppressed in whole blood from AF4 relative to vehicle treated EAE mice at day 18. **(A)** LPS-induced TNF-α protein concentrations were reduced in EAE-AF4 relative to EAE-VEH animals at day 18. **(B)** No difference was found between treatment groups with respect to LPS-induced TNF-α release at day 31. Data are expressed as the mean ± SEM. *$p<0.05$, one-sided student's t-test.

3.3 Effects of the oral administration of AF4 on pro-inflammatory mRNA levels in the spinal cord and cerebellum

To determine the effects of AF4 on mRNA levels for TNF-α, IL-1β and IL-6 in spinal cord CNS tissue was harvested at either day 18 or 31. TNF-α, IL-1β and IL-6 mRNA levels were quantified using qRT-PCR. The mean ± SEM for TNF-α, IL-1β and IL-6 mRNA levels are shown in Table 5.

Oral administration of AF4 reversed the elevation of TNFα mRNA in the cerebellum, but not spinal cord, of EAE animals at day 31

Relative to corresponding CFA+PTX antigen controls, EAE-VEH and EAE-AF4 mice displayed higher levels of TNF-α mRNA in the spinal cord at days 18 and 31 (Figures 15A and B). There were no differences between EAE-VEH and EAE-AF4 mice or CFA+PTX-VEH and CFA+PTX-AF4 mice at days 18 and 31 (Figures 15A and B). Similarly, EAE-VEH and EAE-AF4 mice displayed higher levels of TNF-α mRNA in cerebellum at days 18 and 31 relative to CFA+PTX antigen controls (Figures 15C and D). There were no differences between EAE-VEH and EAE-AF4 mice or CFA+PTX-VEH and CFA+PTX-AF4 mice at day 18 (Figure 15C). Administration of AF4 reduced TNF-α mRNA levels in the cerebellum of EAE-AF4 mice relative to EAE-VEH mice at day 31 (Figure 15D). TNFα mRNA levels were the highest in EAE-VEH mice whereas EAE-AF4 mice were not different from the CFA+PTX treatment groups (Figure 15D).

Oral administration of AF4 reversed the elevation of IL-1β mRNA in the spinal cord and cerebellum of EAE animals at day 31

Relative to corresponding CFA+PTX antigen controls, EAE-VEH and EAE-AF4 mice displayed increased levels of IL-1β mRNA levels in spinal cord at days 18 and 31 (Figures 16A and B). Administration of AF4 reversed this elevation in EAE mice by day 31 (Figure 16B). IL-1β mRNA levels were the highest in EAE-VEH mice whereas EAE-AF4 mice were not different from either CFA+PTX treatment group (Figure 16B). Similarly, EAE-VEH and EAE-AF4 mice displayed increased levels of IL-1β mRNA in cerebellum at day 18 relative to corresponding CFA+PTX antigen controls (Figure 16C). AF4 administration also reduced the elevation of IL-1β in EAE mice by day 31. IL-1β mRNA levels were the highest in EAE-VEH mice whereas EAE-AF4 mice were not different from either CFA+PTX treatment groups (Figure 16D).

Oral administration of AF4 reversed the elevation of IL-6 mRNA in the spinal cord and cerebellum of EAE animals at day 31

Relative to corresponding CFA+PTX antigen controls, EAE-VEH and EAE-AF4 mice displayed increased levels of IL-6 mRNA levels in spinal cord at days 18 and 31 (Figures 17A and B). Administration of AF4 reversed this elevation in EAE mice by day 31 (Figure 17B). IL-1β mRNA levels were the highest in EAE-VEH mice whereas EAE-AF4 mice were not different from either CFA+PTX treatment group (Figure 17B). Similarly, EAE-VEH and EAE-AF4 mice displayed increased levels of IL-6 mRNA in cerebellum at day 18 relative to corresponding CFA+PTX antigen controls (Figure 17C). AF4 administration also reduced the elevation of IL-6 in EAE mice by day 31 (Figure 17D).

Table 5: Mean ± SEM fold increases of TNF-α, IL-1β and IL-6 mRNA levels in spinal cord and cerebellum at days 18 and 31. *p<0.05 **p<0.01 relative to EAE-VEH, one-way ANOVA followed by SNK post-hoc tests.

Legend:

Day 18	Spinal Cord
	Cerebellum
Day 31	Spinal Cord
	Cerebellum

	CFA+PTX-VEH	CFA+PTX-AF4	EAE-VEH	EAE-AF4
TNF-α mRNA				
Day 18	1.4 ± 0.1	1.1 ± 0.2	57.0 ± 18.2	42.2 ± 9.8
	2.9 ± 0.6	***5.3 ± 0.5***	***127.1 ± 35.9***	***111.7 ± 18.6***
Day 31	1.6 ± 0.2	2.0 ± 0.3	34.8 ± 5.6	15.1 ± 4.4
	1.3 ± 0.2	***1.0 ± 0.3***	***40.2 ± 15.6***	***20.6 ± 10.8****
IL-1β mRNA				
Day 18	1.6 ± 0.4	0.9 ± 0.2	31.7 ± 8.5	25.9 ± 5.4
	2.2 ± 0.3	***2.3 ± 0.3***	***127.5 ± 44.9***	***125.4 ± 20.6***
Day 31	1.4 ± 0.1	1.7 ± 0.4	32.1 ± 9.2	12.0 ± 4.1*
	2.5 ± 0.5	***2.3 ± 0.5***	***66.2 ± 20.6***	***27.6 ± 4.5****
IL-6 mRNA				
Day 18	0.7 ± 0.08	0.7 ± 0.03	5.6 ± 1.3	4.0 ± 0.7
	0.8 ± 0.06	***0.8 ± 0.07***	***4.4 ± 1.4***	***6.2 ± 1.3***
Day 31	1.1 ± 0.03	1.0 ± 0.09	5.8 ± 1.2	2.4 ± 0.7*
	1.1 ± 0.07	***0.8 ± 0.1***	***5.9 ± 2.0***	***1.9 ± 0.3****

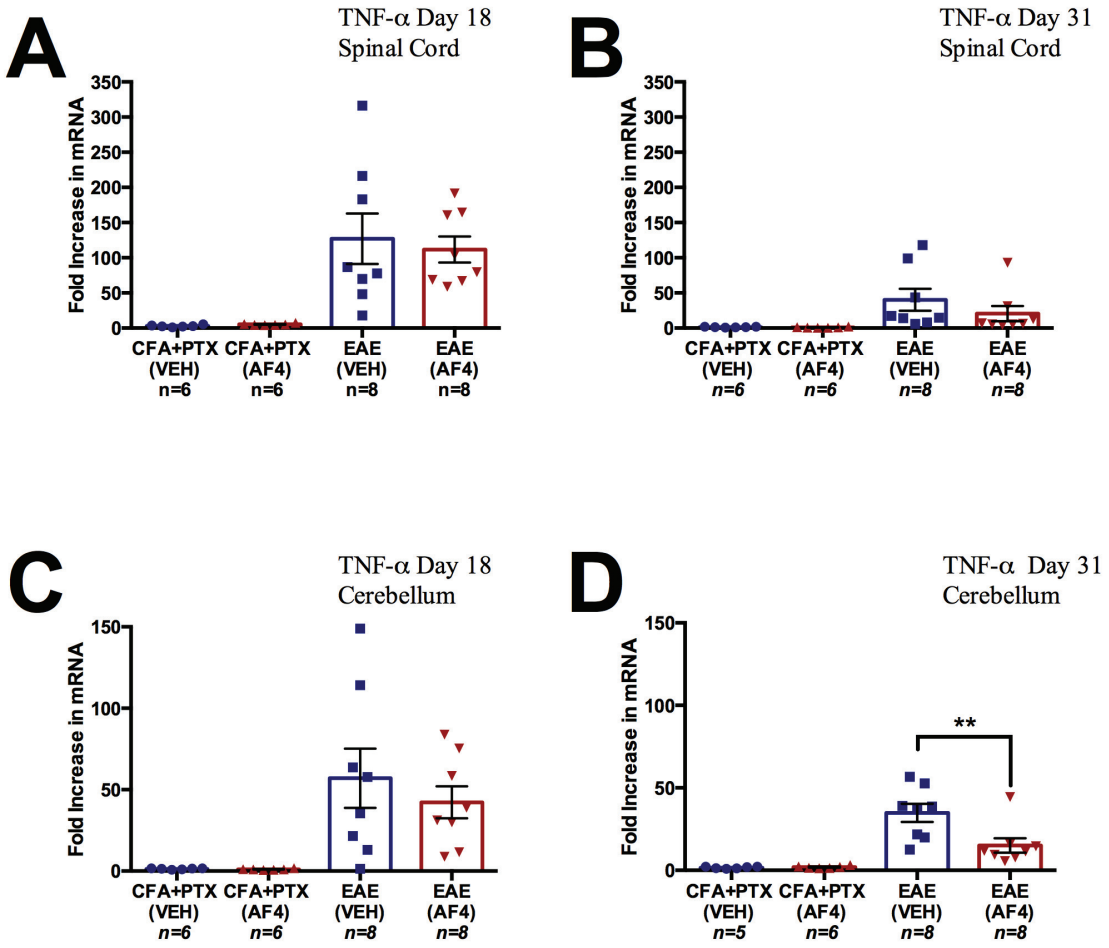

Figure 15: Oral administration of AF4 decreased TNF-α mRNA levels in the cerebellum, but not in spinal cord, of EAE animals by day 31. **(A)** EAE-VEH and EAE-AF4 treated animals displayed increased levels of TNF-α mRNA in spinal cord relative to antigen controls (CFA+PTX-VEH; CFA+PTX-AF4) at day 18. **(B)** Similarly, both EAE-VEH and EAE-AF4 mice displayed increased levels of TNF-α mRNA in the spinal cord relative to antigen controls at day 31. TNF-α mRNA levels were the same for both EAE groups. **(C)** EAE-VEH and EAE-AF4 treated mice displayed increased levels of TNF-α mRNA in cerebellum relative to antigen controls at day 18. **(D)** TNF-α mRNA levels were increased in EAE-VEH animals relative to antigen controls at day 31. By contrast, TNF-α mRNA levels in EAE-AF4 animals were the same as antigen controls. Data are expressed as the mean ± SEM. **p<0.01, one-way ANOVA followed by SNK post-hoc tests.

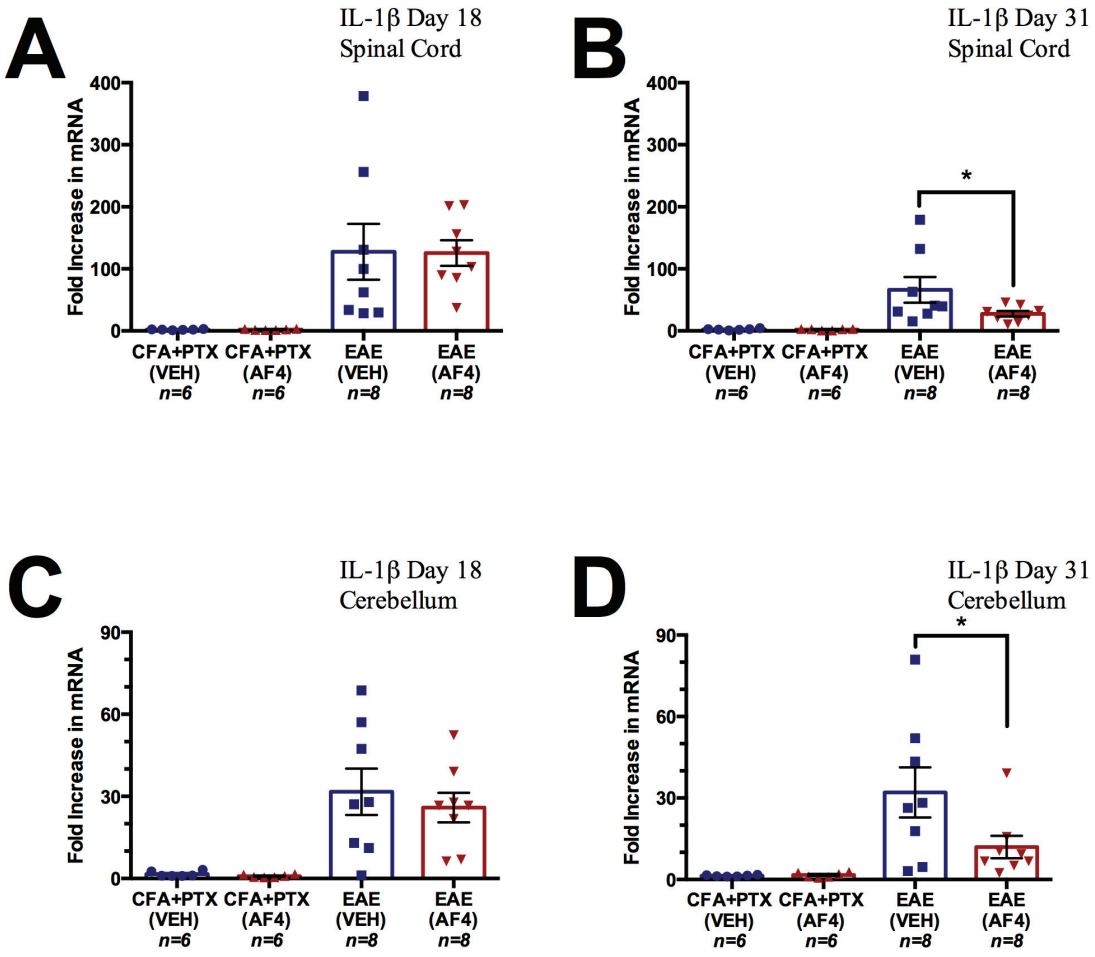

Figure 16: Oral administration of AF4 reversed the elevation of IL-1β mRNA levels in the spinal cord and cerebellum of EAE animals at day 31. **(A)** Both EAE-VEH and EAE-AF4 treated animals displayed increased levels of IL-1β mRNA in spinal cord relative to antigen controls (CFA+PTX-VEH; CFA+PTX-AF4) at day 18. IL-1β spinal cord mRNA levels were the same for both EAE groups at day 18. **(B)** EAE-AF4 animals displayed reduced levels of IL-1β mRNA levels in spinal cord relative to EAE-VEH treated animals at day 31. EAE-VEH treated mice displayed increased IL-1β mRNA levels relative to all other groups. **(C)** EAE-VEH and EAE-AF4 treated animals displayed increased levels of IL-1β mRNA in cerebellum relative to antigen controls at day 18. IL-1β mRNA levels in cerebellum were the same for both EAE groups at day 18. **(D)** IL-1β mRNA levels were increased in EAE-VEH animals relative to antigen controls at day 31. By contrast, IL-1β mRNA levels in EAE-AF4 animals were the same as antigen controls. Data are expressed as the mean ± SEM. *$p<0.05$, one-way ANOVA followed by SNK post-hoc tests.

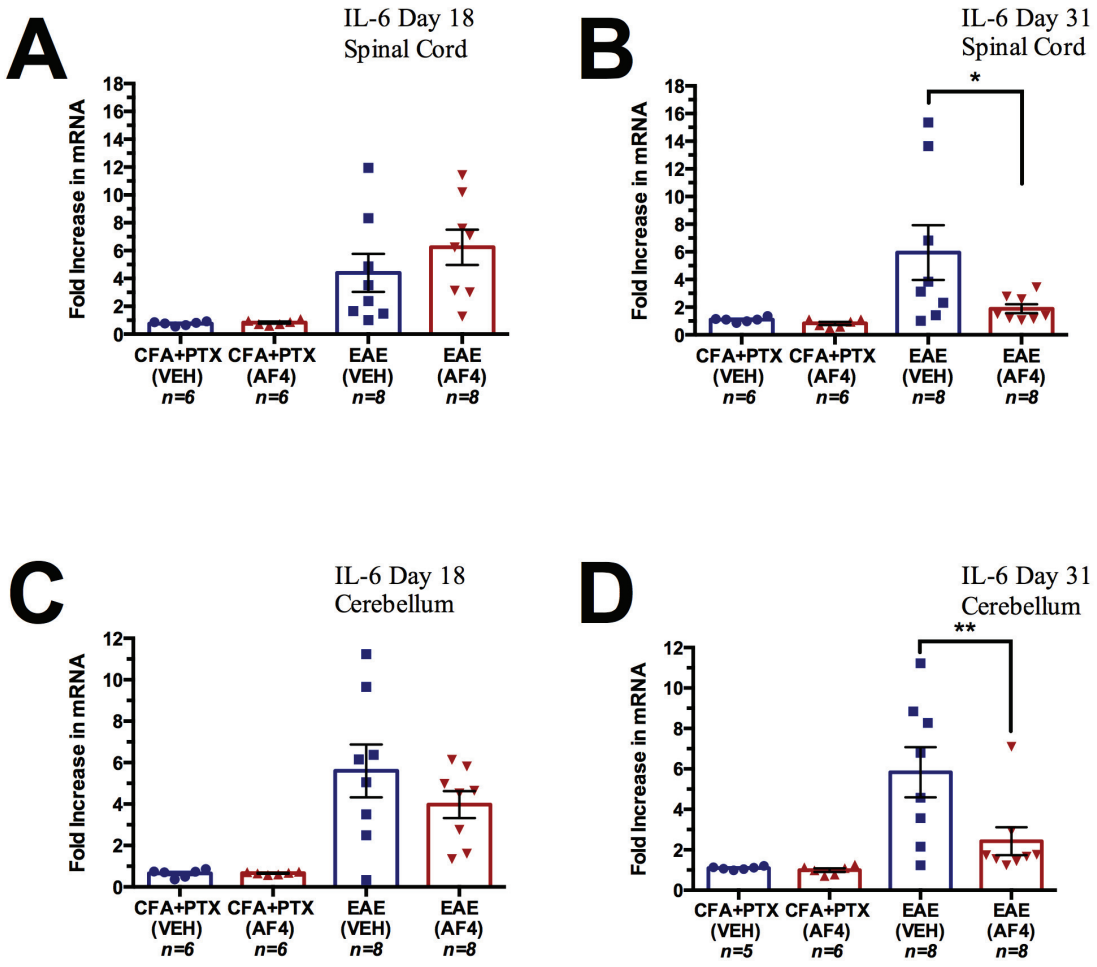

Figure 17: Oral administration of AF4 reversed the elevation of IL-6 mRNA levels in the spinal cord and cerebellum of EAE animals at day 31. **(A)** Both EAE-VEH and EAE-AF4 treated animals displayed increased levels of IL-6 mRNA in spinal cord relative to antigen controls (CFA+PTX-VEH; CFA+PTX-AF4) at day 18. IL-6 spinal cord mRNA levels were the same for both EAE groups at day 18. **(B)** EAE-AF4 animals displayed reduced IL-6 mRNA levels in spinal cord relative to EAE-VEH treated animals at day 31. Both EAE groups were different from antigen controls at day 18. **(C)** EAE-VEH and EAE-AF4 treated animals displayed increased IL-6 mRNA levels in cerebellum relative to antigen controls at day 18. IL-6 mRNA levels in cerebellum were the same for both EAE groups at day 18. **(D)** EAE-AF4 treated animals displayed reduced levels of IL-6 mRNA in cerebellum relative to EAE-VEH animals at day 31. Both EAE groups were different from antigen controls. Data are expressed as the mean ± SEM. *$p<0.05$ **$p<0.01$, one-way ANOVA followed by SNK post-hoc tests.

3.4 Oral administration of AF4 reduced the chemotaxic signaling protein MIG in the spinal cord of EAE mice

Monokine induced by gamma interferon (MIG) concentrations in the spinal cord were measured at days 18 and 31 using multi-plexed ELISA.

AF4 decreased MIG levels in spinal cord of EAE mice at day 31

Relative to CFA+PTX treatment groups, EAE-VEH and EAE-AF4 treated mice displayed increased concentrations of MIG in spinal cord at day 18 (Figure 18A). Oral administration of AF4 did not reduce MIG concentrations in the spinal cord of both EAE and CFA+PTX groups at day 18. The mean ± SEM concentrations of MIG in the spinal cord at day 18 for the four groups were as follows: CFA+PTX-VEH (159.2 ± 26.1), CFA+PTX-AF4 (132.8 ± 10.6), EAE-VEH (4132 ± 641.5), and EAE-AF4 (3644 ± 734.5).

At day 31, MIG concentrations remained elevated in the EAE-VEH mice (960.7 ± 278.9; Figure 18B). By contrast, MIG concentrations in the spinal cords of EAE-AF4 mice (446.2 ± 71.5) were reduced to the same levels observed in CFA+PTX controls (CFA+PTX-VEH, 28.2 ± 17.0; CFA+PTX-AF4, 71.7 ± 27.5).

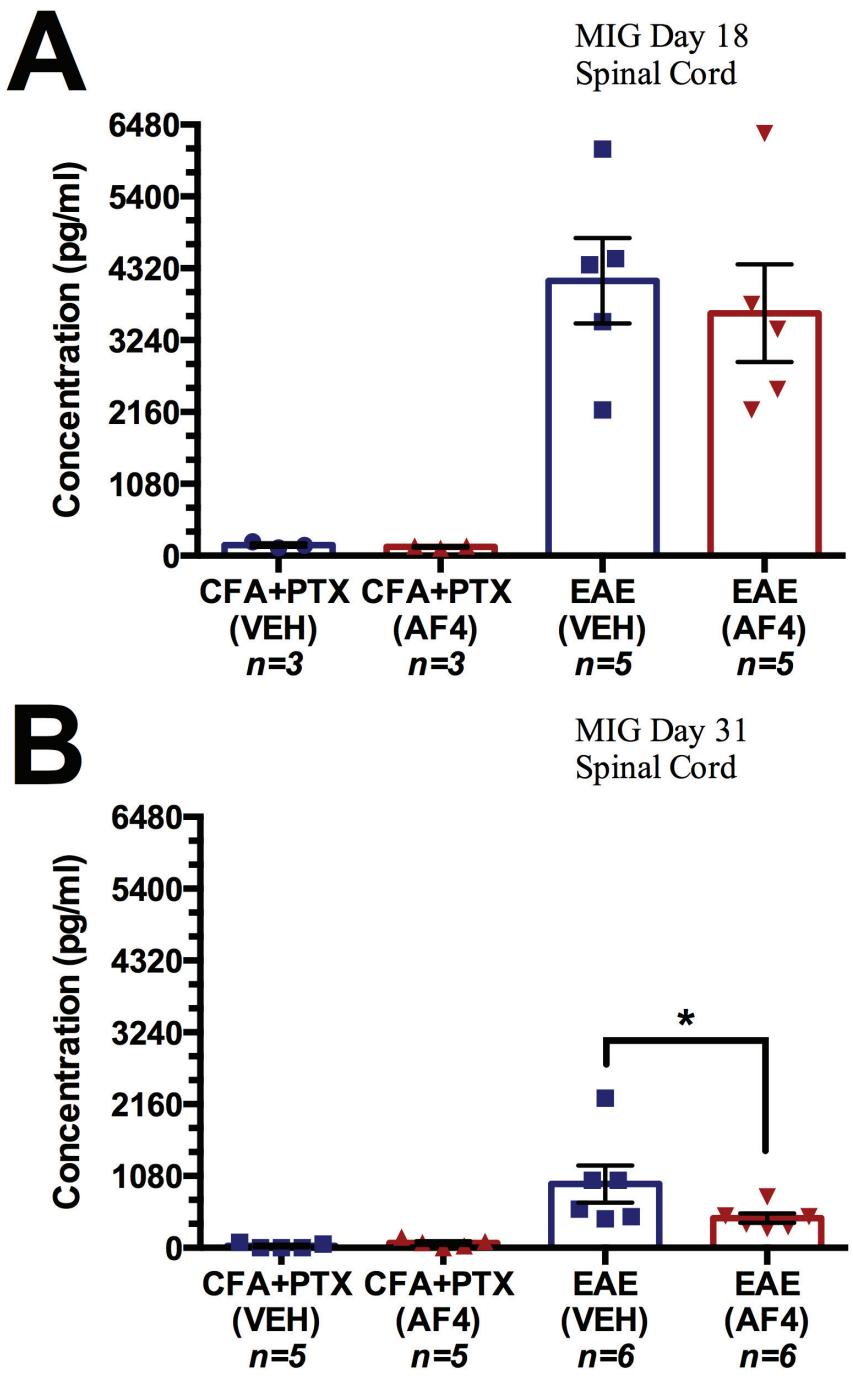

Figure 18: Oral administration of AF4 decreased monokine induced by gamma interferon (MIG) concentrations in the spinal cord of EAE animals at day 31. **(A)** EAE-VEH and EAE-AF4 animals displayed increased concentrations of MIG in spinal cord relative to antigen controls (CFA+PTX-VEH; CFA+PTX-AF4) at day 18. MIG concentrations were the same for both EAE groups. **(B)** Relative to EAE-VEH, EAE-AF4 mice displayed reduced concentrations of MIG at day 31. Both EAE groups displayed increased MIG concentrations relative to antigen controls. Data are expressed as the mean ± SEM. *$p<0.05$, one-way ANOVA followed by SNK post-hoc tests.

3.5 Oral administration of AF4 reduced inflammatory mediated pathology in the cerebellum of EAE mice

Inflammation was assessed in the cerebellum of EAE mice that received oral administration of vehicle or AF4 beginning 24 hours following the first clinical signs of EAE and continued daily until day 31, at which point 9-10 mice from each group were humanely euthanized and perfused with paraformaldehyde. Following post-fixation, the cerebellum was cut on the cryostat and the resulting tissue sections stained with either H&E or an antibody against the microglial specific marker Iba-1.

AF4 reduced perivascular cuffs and microgliosis in EAE mice at day 31

Mice dosed orally with AF4 displayed fewer perivascular cuffs surrounding blood vessels and less severe signs of microgliosis at day 31 (Figure 19A). Pathology index scores were significantly decreased in EAE-AF4 (3.17 ± 0.34) relative to EAE-VEH mice (4.00 ± 0.25; Figure 19B).

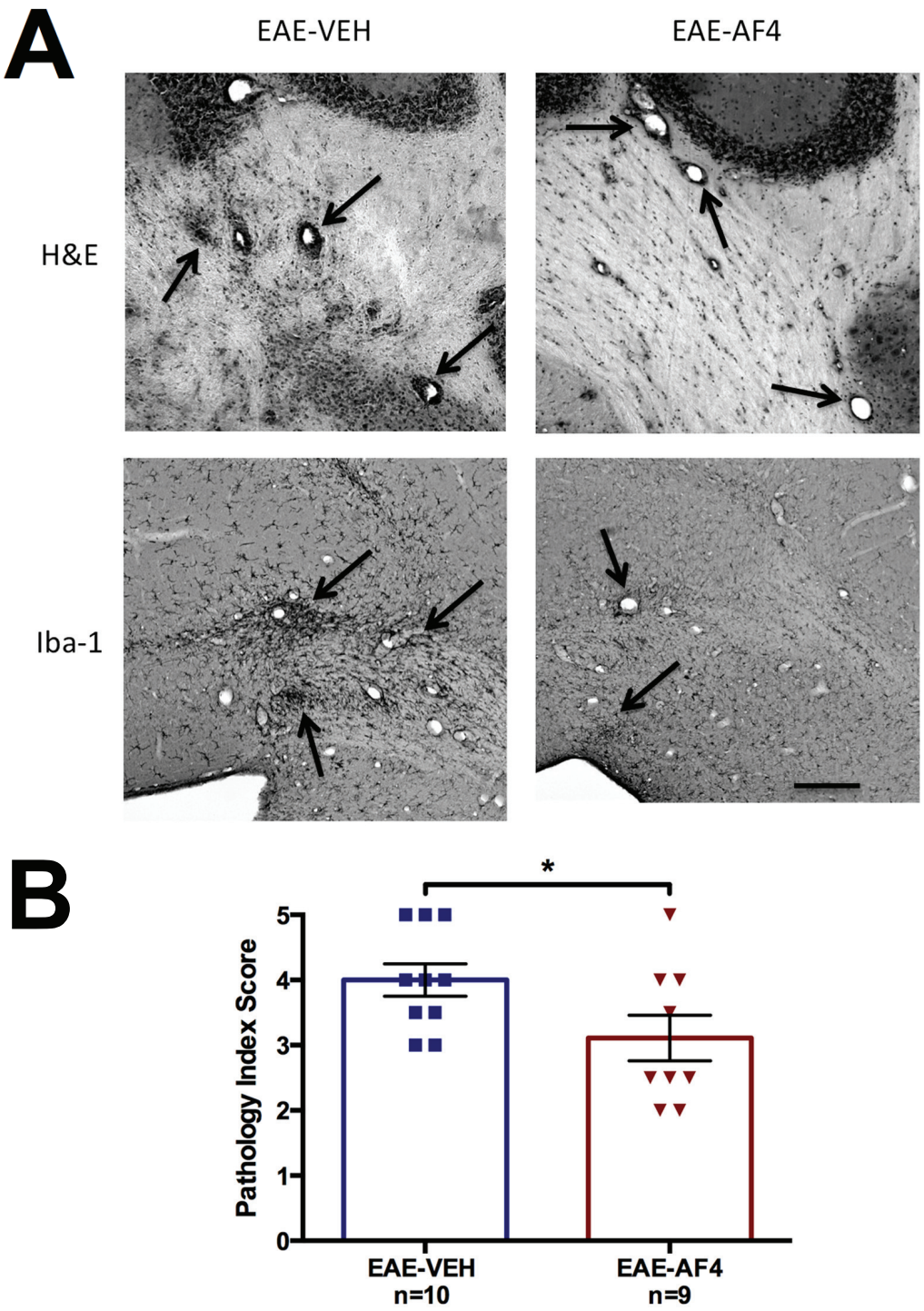

Figure 19: Oral administration of AF4 reduced inflammatory mediated pathology in the cerebellum of EAE mice. **(A)** Representative photomicrographs of the cerebellum (5.88 mm posterior to bregma) of EAE-VEH and EAE-AF4 groups processed for H&E or Iba-1 immunoreactivity. Arrows indicate areas of inflammation. The scale bar in the bottom right panel represents 100 μm. **(B)** Pathology Index Scores were significantly decreased in EAE-AF4 mice relative to EAE-VEH mice ($p<0.05$). Data are expressed as the mean ± SEM. *$p<0.05$, one-sided Mann Whitney U test.

3.6 Effects of AF4 administration on the expression of genes required for myelination in the CNS

EAE and CFA+PTX mice received either vehicle or AF4 until day 18 or day 31, at which point 6-8 animals from these four groups were humanely euthanized to provide nervous tissue (spinal cord and cerebellum) for the assessment of basal mRNA levels for myelin basic protein (MBP), peroxisome proliferator-activated receptor gamma co-activator 1-alpha (PGC-1α) and steroyl-CoA desaturase-1 (SCD1) using qRT-PCR. The mRNA levels are expressed as fold change relative to healthy, untreated 6-8 week-old female C57Bl/6 control mice. The mean ± SEM fold increases of MBP, PGC-1α, and SCD-1 are shown in Table 6.

Oral administration of AF4 increased MBP mRNA levels in the spinal cord of EAE animals at day 31

MBP mRNA levels were significantly decreased in the spinal cord of EAE mice (EAE-VEH and EAE-AF4) relative to antigen controls (CFA+PTX-VEH and CFA+PTX-AF4) at day 18 (Figure 20A). By day 31, MBP mRNA levels were still depressed in the EAE groups relative to the CFA+PTX groups (Figure 20B). However, MBP mRNA levels were increased in the spinal cords of EAE-AF4 relative to EAE-VEH mice (Figure 20B).

Oral administration of AF4 increased PGC-1α mRNA levels in the spinal cord and cerebellum of EAE animals at day 31

Relative to CFA+PTX antigen controls, EAE-VEH and EAE-AF4 treated mice displayed comparable reductions in the levels of PGC-1α mRNA in spinal cord at days 18 and 31 (Figures 21A and B). By contrast, PGC-1α mRNA levels were significantly

increased in the spinal cords of EAE-AF4 treated mice relative to EAE-VEH mice at day 31 (Figure 21B). Although less pronounced, a familiar pattern of PGC-1α expression was observed in cerebellum. At day 18, there was a trend for reduced PGC-1α mRNA levels in cerebellar tissue from EAE relative to CFA+PTX mice (Figure 21C). At day 31, PGC-1α mRNA levels were significantly decreased in the cerebellum of EAE-VEH relative to EAE-AF4 mice (Figure 21D).

Oral administration of AF4 increased SCD1 mRNA levels in the spinal cord of EAE animals at day 31

SCD1 mRNA levels were decreased in the spinal cord of EAE mice (EAE-VEH and EAE-AF4) relative to antigen controls (CFA+PTX-VEH and CFA+PTX-AF4) at day 18 (Figure 22A). By day 31, SCD1 mRNA levels were significantly increased in the spinal cords of EAE-AF4 relative to EAE-VEH mice (Figure 22B). Both EAE groups still displayed decreased SCD1 mRNA levels at day 31 relative to antigen controls.

Table 6: Mean ± SEM fold increases of MBP, PGC-1α, and SCD-1 in spinal cord and cerebellum at days 18 and 31. *p<0.05 **p<0.01 relative to EAE-VEH mice, one-way ANOVA followed by SNK post-hoc tests.

Legend:

Day 18	Spinal Cord
	Cerebellum
Day 31	Spinal Cord
	Cerebellum

	CFA+PTX-VEH	CFA+PTX-AF4	EAE-VEH	EAE-AF4
MBP mRNA				
Day 18	0.8 ± 0.02	0.9 ± 0.02	0.3 ± 0.05	0.4 ± 0.04
Day 31	**0.8 ± 0.01**	**0.8 ± 0.02**	**0.4 ± 0.05**	**0.5 ± 0.04***
PGC-1α mRNA				
Day 18	1.0 ± 0.05	0.9 ± 0.04	0.7 ± 0.05	0.8 ± 0.06
	1.1 ± 0.02	***1.1 ± 0.03***	***0.4 ± 0.07***	***0.5 ± 0.04***
Day 31	1.1 ± 0.02	1.1 ± 0.04	0.8 ± 0.03	1.0 ± 0.05*
	1.1 ± 0.05	***1.2 ± 0.04***	***0.5 ± 0.08***	***0.7 ± 0.07****
SCD1 mRNA				
Day 18	0.9 ± 0.03	0.9 ± 0.02	0.3 ± 0.03	0.4 ± 0.05
Day 31	**0.9 ± 0.02**	**0.9 ± 0.02**	**0.4 ± 0.05**	**0.6 ± 0.05****

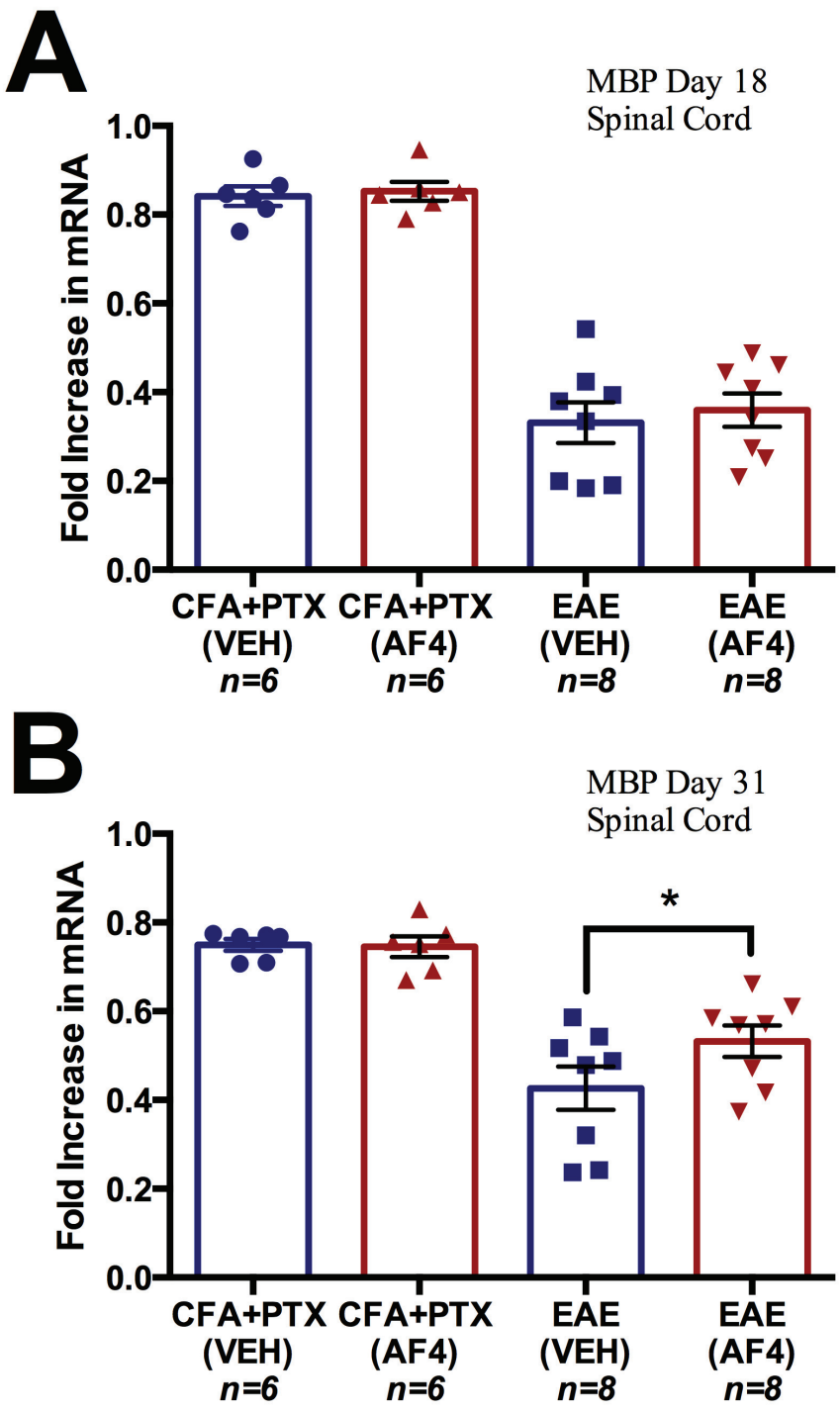

Figure 20: Oral administration of AF4 increased myelin basic protein (MBP) mRNA levels in EAE spinal cord at day 31. **(A)** MBP mRNA levels in spinal cord were reduced in both EAE groups (EAE-VEH and EAE-AF4) relative to antigen controls (CFA+PTX-VEH; CFA+PTX-AF4) at day 18. Spinal cord mRNA levels were the same for both EAE groups at day 18. **(B)** Relative to EAE-VEH mice, MBP mRNA levels were increased in EAE-AF4 treated animals at day 31. MBP mRNA levels in spinal cord were still reduced in both EAE groups relative to antigen controls at day 31. Data are expressed as the mean ± SEM. *$p<0.05$, one-way ANOVA followed by SNK post-hoc tests.

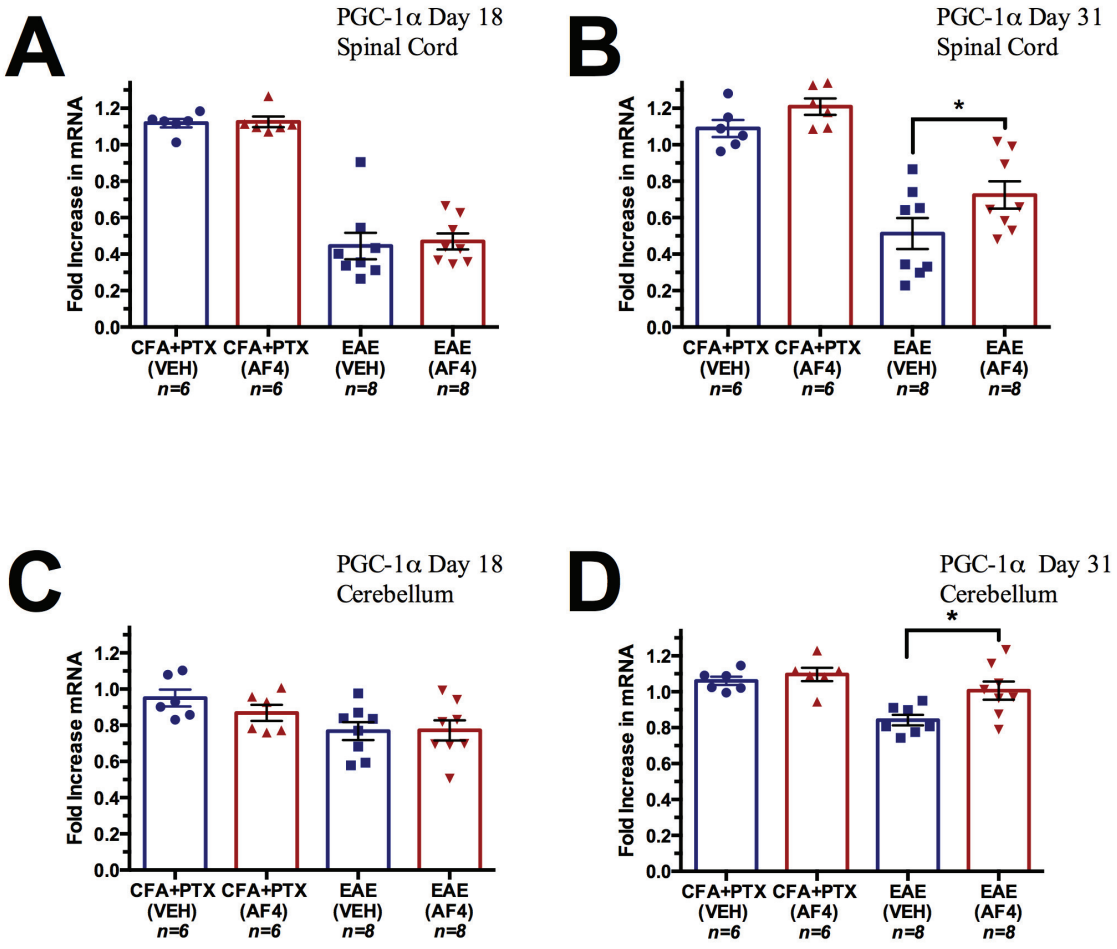

Figure 21: Oral administration of AF4 increased peroxisome proliferator-activated receptor gamma co-activator 1-alpha (PGC-1α) mRNA levels in the spinal cord and cerebellum of EAE animals at day 31. **(A)** PGC-1α mRNA levels were reduced in the spinal cord of EAE-VEH and EAE-AF4 treated animals relative to antigen controls (CFA+PTX-VEH; CFA+PTX-AF4) at day 18. PGC-1α spinal cord mRNA levels were the same for both EAE groups at day 18. **(B)** PGC-1α mRNA levels were reduced in the spinal cords of EAE-VEH animals relative to AF4-EAE animals at day 31. PGC-1α mRNA levels were reduced in both EAE groups relative to antigen controls. **(C)** There were no differences in PGC-1α mRNA levels between or within the cerebellum of EAE and antigen control groups. **(D)** PGC-1α mRNA levels were reduced in EAE-VEH animals relative to antigen controls at day 31. By contrast, PGC-1α mRNA levels in EAE-AF4 animals were the same as antigen controls. Data are expressed as the mean ± SEM. *$p<0.05$, one-way ANOVA followed by SNK post-hoc tests.

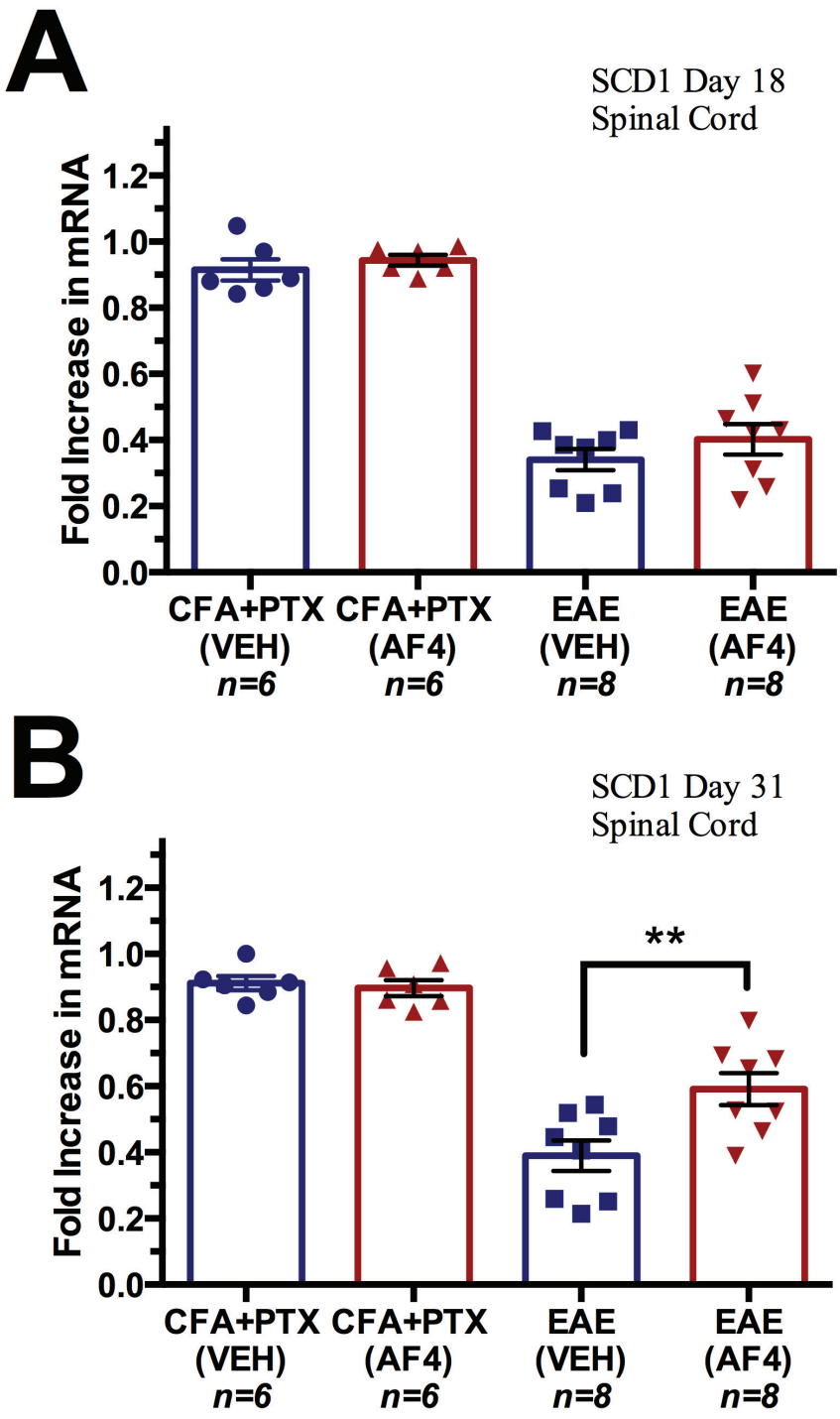

Figure 22: Oral administration of AF4 increased steroyl-CoA desaturase-1 (SCD1) mRNA levels in the spinal cord of EAE mice at day 31. **(A)** SCD1 mRNA levels were reduced in both EAE groups relative to antigen controls (CFA+PTX-VEH; CFA+PTX-AF4) at day 18. SCD1 mRNA levels in spinal cord were the same for both EAE groups at day 18. **(B)** Relative to EAE-VEH mice, SCD1 mRNA levels were increased in EAE-AF4 animals at day 31. SCD1 mRNA levels were reduced in the spinal cord of both EAE groups relative to antigen controls. Data are expressed as the mean ± SEM. **$p<0.01$, one-way ANOVA followed by SNK post-hoc tests.

3.7 Oral Administration of AF4 Reduced CXCL2 Protein Concentrations in the Spinal Cord of EAE Mice

EAE and CFA+PTX mice were treated with either vehicle or AF4 until days 18 or 31, at which point spinal cord was harvested for the assessment of Chemokine (C-X-C motif) ligand 2 (CXCL2) concentrations using multi-plexed ELISA.

AF4 decreased CXCL2 levels in spinal cord of EAE mice at day 31

Oral administration of AF4 did not reduce CXCL2 protein concentrations in the spinal cord of both EAE and CFA+PTX groups at day 18 (Figure 23A). The mean ± SEM concentrations of CXCL2 in the spinal cord at day 18 for the four groups were as follows: CFA+PTX-VEH (35.7 ± 13.9), CFA+PTX-AF4 (11.4 ± 1.1), EAE-VEH (37.6 ± 8.5), and EAE-AF4 (48.6 ± 9.5).

At day 31, CXCL2 concentrations remained elevated in the EAE-VEH mice (24.7 ± 4.0; Figure 23B). By contrast, CXCL2 concentrations in the spinal cords of EAE-AF4 mice (9.2 ± 1.2) were reduced to the same levels observed in CFA+PTX controls (CFA+PTX-VEH, 6.1 ± 1.5; CFA+PTX-AF4, 9.0 ± 2.0).

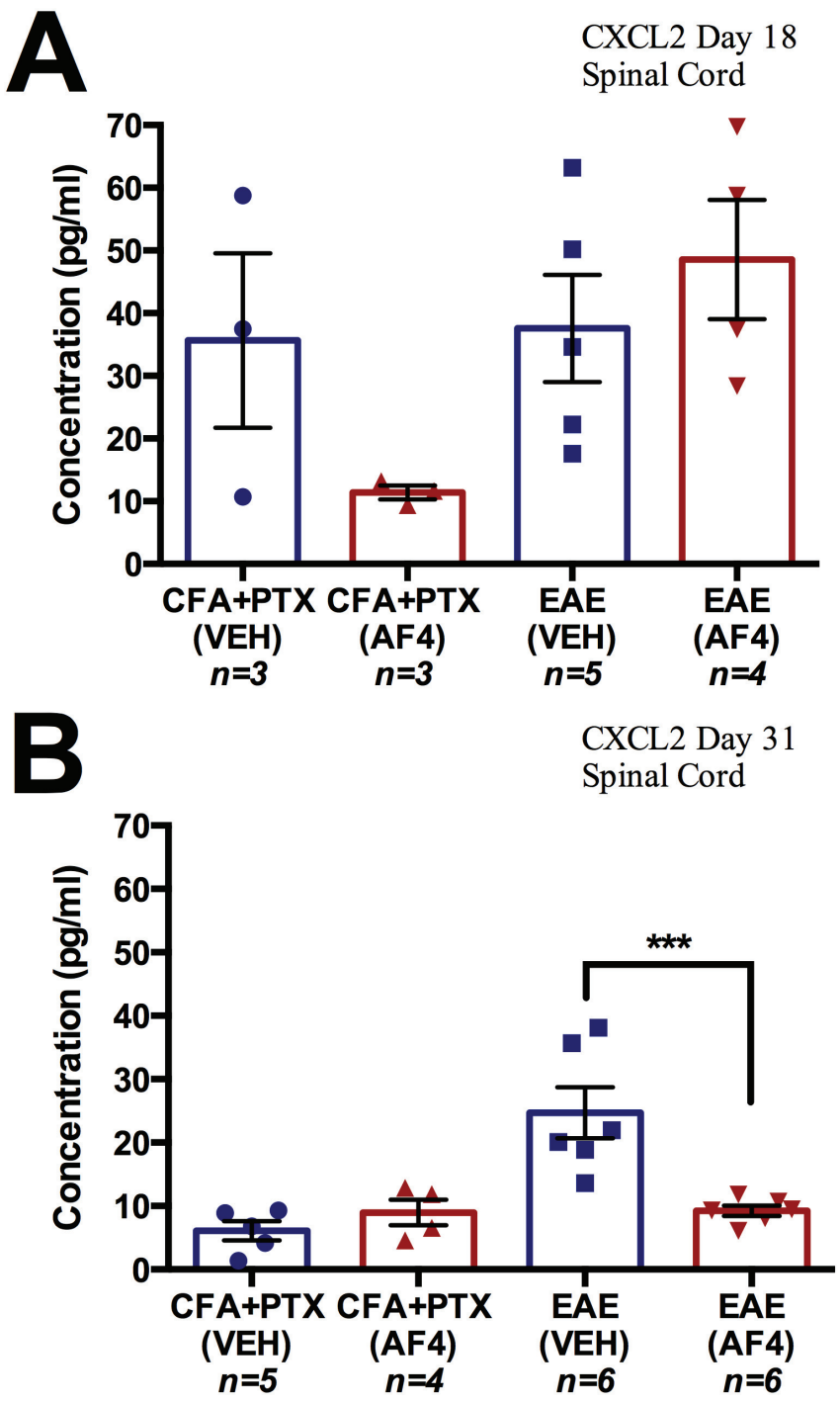

Figure 23: Oral administration of AF4 reduced Chemokine (C-X-C motif) ligand 2 (CXCL2) concentrations in EAE spinal cord at day 31. **(A)** Protein concentrations for CXCL2 were not different between EAE-VEH and EAE-AF4 animals relative to antigen controls (CFA+PTX-VEH; CFA+PTX-AF4) at day 18, $p>0.05$. **(B)** Protein levels for CXCL2 were elevated in EAE-VEH with respect to all other groups at day 31. Data are expressed as the mean ± SEM. ***$p<0.001$, one-way ANOVA followed by SNK post-hoc tests.

3.8 Effects of the oral administration of AF4 on the expression of genes associated with neuronal protection in the CNS of EAE mice

EAE and CFA+PTX mice were dosed with either vehicle or AF4 until day 18 or day 31, at which point 6-8 animals from these four groups were humanely euthanized to provide spinal cord tissue for the assessment of mRNA levels for erythropoietin (EPO) and plasma membrane Ca^{2+} ATPase-2 (PMCA2) using qRT-PCR. The mRNA levels for EPO and PMCA2 are expressed as fold change relative to healthy, untreated 6-8 week-old female C57Bl/6 mice. The mean ± SEM fold increases for EPO and PMCA2 are shown in Table 7.

AF4 elevated EPO mRNA levels in the spinal cord of EAE mice at day 31

Relative to CFA+PTX antigen controls, EAE-VEH and EAE-AF4 mice showed increased EPO mRNA levels in spinal cord at day 18 (Figure 24A). There were no statistical differences for EPO mRNA levels between EAE-VEH and EAE-AF4 mice or CFA+PTX-VEH and CFA+PTX-AF4 mice at day 18. At day 31, EPO mRNA levels were considerably reduced in all groups (Figure 24B). However, EPO mRNA levels were elevated in EAE-AF4 relative to EAE-VEH mice at this time point.

Oral administration of AF4 did not reverse the reduction of PMCA2 mRNA levels in the spinal cord of EAE mice

Relative to CFA+PTX antigen controls, EAE-VEH and EAE-AF4 treated mice displayed decreased PMCA2 mRNA levels in spinal cord at days 18 and 31 (Figure 25A and B). PMCA2 mRNA levels were the same in AF4 and vehicle treated mice at days 18 and 31.

Table 7: Mean ± SEM fold increases of EPO and PMCA2 mRNA in spinal cord at days 18 and 31.

EPO mRNA	**CFA+PTX-VEH**	**CFA+PTX-AF4**	**EAE-VEH**	**EAE-AF4**
Day 18	8.2 ± 2.1	10.5 ± 1.8	32.6 ± 2.7	29.4 ± 8.0
Day 31	0.4 ± 0.1	1.04 ± 0.4	1.4 ± 0.2	2.8 ± 0.4**
PMCA2 mRNA				
Day 18	1.05 ± 0.1	1.05 ± 0.1	0.40 ± 0.02	0.5 ± 0.04
Day 31	1.0 ± 0.04	1.0 ± 0.05	0.4 ± 0.07	0.5 ± 0.08

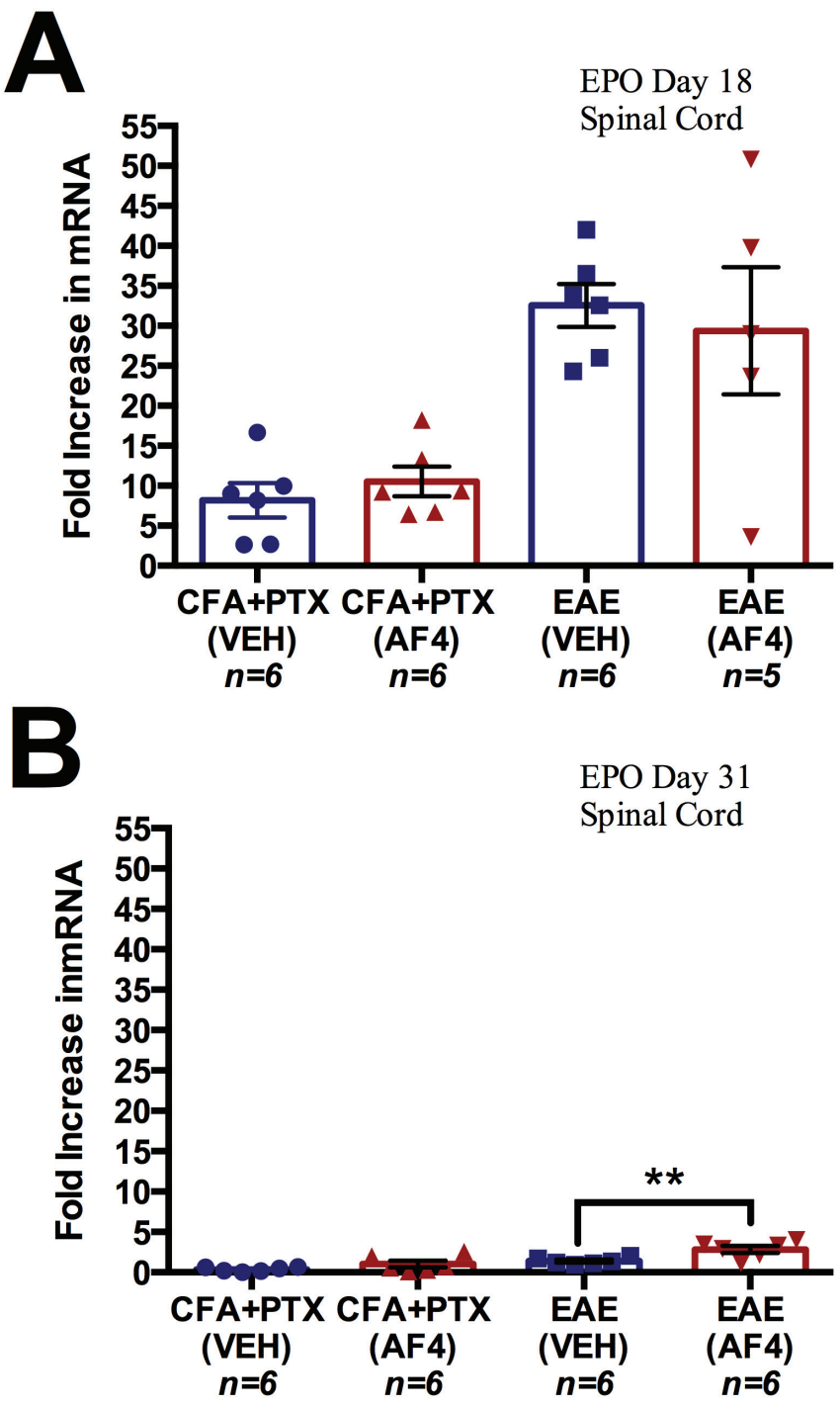

Figure 24: Oral administration of AF4 increased erythropoietin (EPO) mRNA levels in the spinal cord of EAE mice at day 31. **(A)** EPO mRNA levels were increased in both EAE groups relative to antigen controls (CFA+PTX-VEH; CFA+PTX-AF4) at day 18. EPO mRNA levels in spinal cord were the same for both EAE groups at day 18 ($p>0.05$). **(B)** Relative to EAE-VEH mice, EPO mRNA levels were increased in EAE-AF4 treated animals at day 31. The EAE-VEH treatment group was not statistically different from antigen controls at day 31. Data are expressed as the mean ± SEM. **$p<0.01$, one-way ANOVA followed by SNK post-hoc tests.

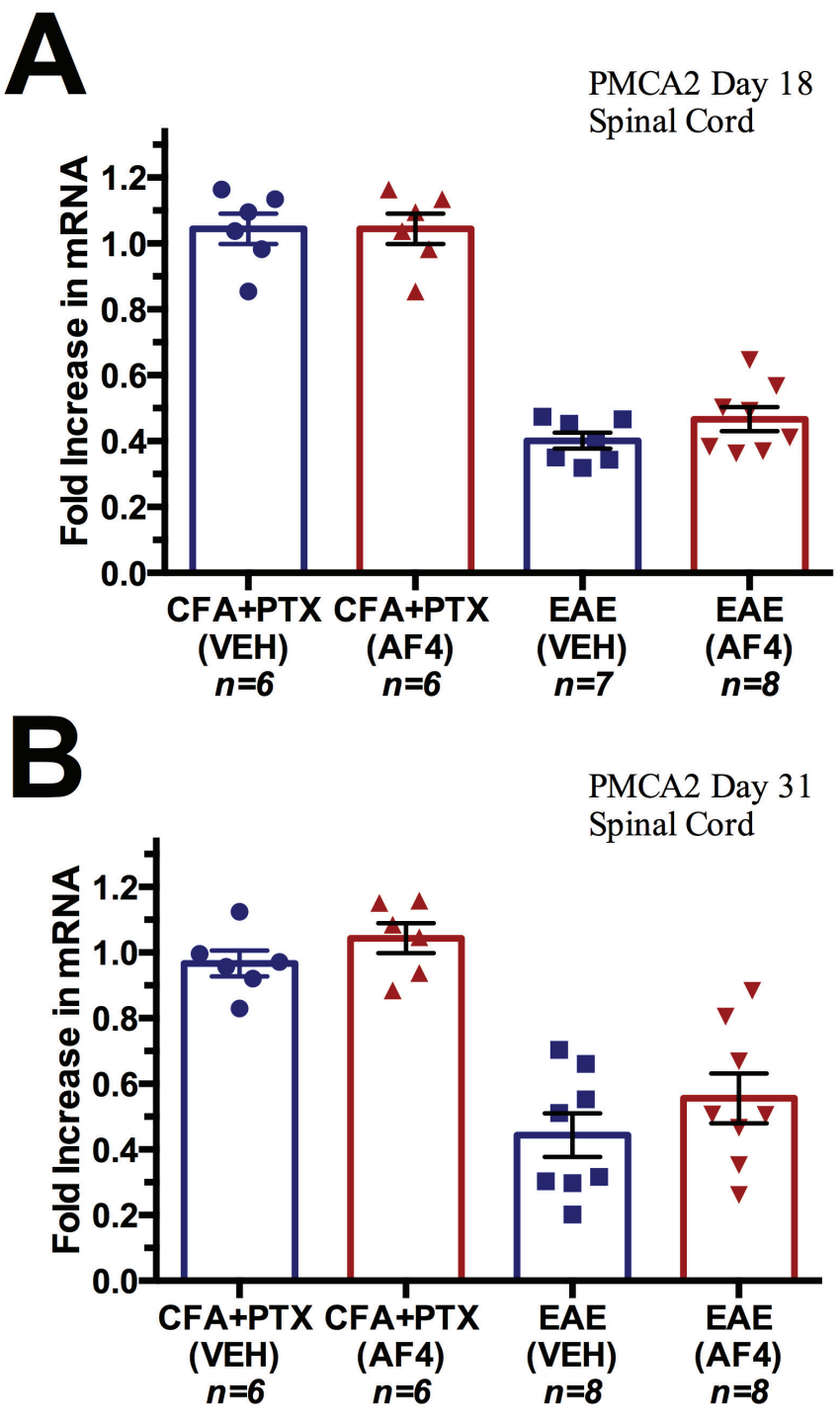

Figure 25: Oral administration of AF4 did not change plasma membrane Ca^{2+} ATPase-2 (PMCA2) mRNA levels in the spinal cord of EAE mice at days 18 and 31. **(A)** PMCA2 mRNA levels were decreased in both EAE groups relative to antigen controls (CFA+PTX-VEH; CFA+PTX-AF4) at day 18. PMCA2 mRNA levels in spinal cord were the same for both EAE groups. **(B)** PMCA2 mRNA levels were decreased in both EAE groups relative to antigen controls at day 31. PMCA2 mRNA levels in spinal cord were the same for both EAE groups. Data are expressed as the mean ± SEM and were analyzed using a one-way ANOVA followed by SNK post-hoc tests.

CHAPTER 4: DISCUSSION

4.1 AF4 reduced disease progression and inflammation in EAE mice: Sequential inhibition of pro-inflammatory signaling in peripheral blood and CNS

Relative to EAE mice that received vehicle (10 ml/kg; once daily, p.o.), EAE mice treated with AF4 (25 mg/kg; once daily) beginning 24 hours following the onset of clinical signs displayed reduced disease severity from days 19-31. Clinical improvement was first associated with a reduction in concentrations of TNF-α and IL-1β in plasma at days 18 and 31 followed by decreased mRNA levels for IL-1β and IL-6 in spinal cord and TNF-α, IL-1β, and IL-6 in cerebellum at day 31. Cytokine concentrations for LPS-induced TNF-α release were also suppressed in whole blood from EAE animals treated with AF4 relative to vehicle at day 18 but not day 31. These findings suggest that AF4 decreased disease progression in this mouse model of EAE, at least in part, by first attenuating pro-inflammatory signaling in circulating immune cells resulting in the subsequent resolution of inflammation in the CNS.

Histological examination of inflammation in the cerebellum found fewer perivascular cuffs and less microgliosis in EAE mice treated with AF4 relative to those that received vehicle at day 31. Perivascular vessels and surrounding parenchyma are the initial sites of CNS inflammation in EAE that trigger microglial activation resulting in the production of pro-inflammatory mediators which further promote immune cell infiltration (Taupin *et al.*, 1997; Frohman *et al.*, 2006). The ability of AF4 to mitigate these injurious inflammatory events that were preceded by decreased TNF-α and IL-1β levels in plasma suggests that AF4 reduced central inflammation and EAE severity by suppressing autoimmune mechanisms in the periphery. To the best of my knowledge, this is the first

evidence that polyphenolic compounds promote the sequential suppression of pro-inflammatory cytokine production in the periphery and CNS of EAE mice resulting in the amelioration of CNS pathology.

4.2 AF4 is a unique immune modulator

The suppression of LPS-induced TNF-α in whole blood from EAE-AF4 animals at day 18 but not day 31 indicates that this flavonoid-enriched fraction selectivity inhibited inflammatory signaling at the peak of EAE severity. The restoration of LPS-induced TNF-α production in whole blood from EAE-AF4 mice at day 31 suggests that AF4 does not impair immune signaling once inflammation has declined. This interpretation is supported by comparable LPS-induced TNF-α release in whole blood from normal mice pre-treated with water (10 ml/kg, once daily) or AF4 (50 mg/kg, once daily) for 3 days (Dunlop, 2011). AF4 may therefore have highly desirable immune modulatory properties enabling it to selectively suppress pro-inflammatory signaling in circulating immune cells that would otherwise exacerbate CNS injury without impairing the normal immune response once brain inflammation subsides.

The ability of AF4 to reduce concentrations of the chemokines MIG and CXCL2 in spinal cord by day 31 signifies an inhibition of chemotactic signaling. The production of chemotactic cytokines by infiltrating inflammatory cells promotes further immune cell infiltration which correlates positively with clinical severity (Karpus & Ransohoff, 1998). Peak MIG concentrations in the CNS occur during the later chronic stages of the EAE disease course and reflect the presence of inflammatory infiltrates in the parenchyma (Berard *et al.*, 2010). In an elegant series of experiments, Glabinski et al. (1995)

demonstrated that central chemokine production was dependent on the presence of inflammatory infiltrates in the CNS of EAE mice. This work resulted in the hypothesis that autoreactive T cells migrate to perivascular areas of the CNS and secrete chemokines that recruit subsequent waves of inflammatory cell infiltration. Blockade of CXCL2 receptors with the small molecule antagonist FC 131 reduced cellular infiltration and damage in the spinal cord of EAE mice that was associated with improved EAE clinical scores (Kerstetter *et al.*, 2009). In this study, dosing with FC 131 began following the initial presentation of clinical signs, allowing sufficient time for the initial wave of autoreactive T cells to reach perivascular sites. Hence, FC 131 reduced EAE severity by blocking immune events mediated by CXCL2 receptor activation subsequent to T cell infiltration. Assessment of CXCL2 concentrations in the spinal cords of EAE mice revealed that AF4 reduced levels of this pro-inflammatory cytokine. It is therefore tempting to speculate that AF4 may also have reduced EAE severity from days 19-31 by blocking the pro-inflammatory effects of CXCL2 during late disease course.

LPS-induced TNF-α release from the monocytic MonoMac6 cell line is diminished in the presence of apple-derived procyanidins (Huemmer *et al.*, 2008; Jung *et al.*, 2009). Furthermore, oral administration of an apple polyphenolic extract enriched with tannins (Apple Poly®) attenuated inflammation in a mouse model of dextran sodium sulphate induced colitis, in part, by dampening the recruitment of lymphocytes to the colon (Skyberg *et al.*, 2011). The most notable finding of this study was the necessity of T cells for the apple polyphenolic fraction to initiate anti-inflammatory signaling cascades. This suggests that AF4 may have also reduced EAE severity by promoting the production of anti-inflammatory cytokines such as IL-10 from T cells. It will therefore be

important to compare IL-10 levels in the spinal cords of EAE-AF4 and EAE-VEH mice in future studies to determine whether AF4 also elevates the production of this anti-inflammatory cytokine.

4.3 AF4 promotes the expression of genes in the CNS of EAE animals required for remyelination

Quantitative RT-PCR measurements showed that the reduction in disease progression produced by AF4 in EAE animals was associated with elevated mRNA levels for MBP (spinal cord), PGC-1α (spinal cord and cerebellum), and SCD1 (spinal cord). In spinal cord tissue from EAE animals that received either vehicle or AF4, PGC-1α, and SCD1 mRNA levels were reduced at day 18 relative to non-immunized controls (CFA+PTX-VEH, CFA+PTX-AF4). At day 31, when clinical scores for EAE-AF4 animals were lower relative to EAE-VEH animals, mRNA levels for MBP, PGC-1α and SCD1 in spinal cord tissue from EAE-AF4 mice were elevated relative to EAE-VEH animals. Since MBP is a constituent of myelin, produced exclusively by oligodendrocytes (Franklin *et al.*, 2012), these findings suggest that AF4 may have increased the number and/or the transcriptional activity of these myelin-producing cells in the spinal cord of EAE animals.

The production of myelin is a very costly energetic event requiring mitochondrial biogenesis to provide the necessary ATP for myelin synthesis (Nave, 2010). Inhibition of mitochondrial respiration in oligodendrocyte precursor cells (OPC) with rotenone, a complex I inhibitor, substantially reduced MBP and 2', 3'-cyclic-nucleotide 3'-phosphodiesterase (CNPase) mRNA levels at a concentration of 1 nM, which blocks ATP synthesis but does not reduce OPC viability. This dose therefore prevented the

differentiation of these cells into functional oligodendrocytes (Schoenfeld *et al.*, 2010). Differentiation of OPCs into myelin producing oligodendrocytes is therefore exquisitely sensitive to complex I inhibition and highly dependent on mitochondrial activity. Recently, it was convincingly shown that mitochondrial dysfunction is a critical component of autoimmune mediated axonal degeneration in EAE mice (Nikić *et al.*, 2011). The authors demonstrated for the first time that energy failure resulting from impaired mitochondrial function contributes to demyelination and axonal injury.

Nikić *et al*. (2011) reported that neuronal loss in brain tissue from MS patients is inversely correlated with PGC-1α levels, a transcriptional regulating factor essential for mitochondrial biogenesis and respiration (St-Pierre *et al.*, 2006; Witte *et al.*, 2012). MS patients with progressive forms of the disease displayed profound decreases in PGC-1α levels in layers 4-6 of the cingulate cortex and forebrain relative to healthy neurological controls (Witte *et al*., 2012). Consistent with this finding, PGC-1α also serves as a co-activator for the liver X receptor (LXR), a key regulator of cellular cholesterol synthesis necessary for myelin production (Oberkofler *et al.*, 2003). Furthermore, PGC-1α null mice display marked dysmyelination, increased ROS levels, and sequential reductions in myelin and cholesterol-synthesis associated genes in experimental models of Huntington's and Parkinson's disease (St-Pierre *et al.*, 2006; Weydt *et al.*, 2006; Pacelli *et al.*, 2011; Xiang *et al.*, 2011).

SCD-1 catalyzes a rate-limiting step in the synthesis of cholesterol (palmitic acid → oleic acid), a major component of myelin (Polo-Hernández *et al.*, 2010). During development, production of oleic acid promotes axonal and dendritic growth and accounts for approximately 30% of the fatty acids in myelin (DeWille & Farmer, 1992;

Polo-Hernández *et al.*, 2010). Swiss et al. (2011) used cDNA microarrays to map the transcriptome of differentiating oligodendrocytes. Using cluster analysis, many genes associated with lipid metabolism were upregulated during OPC differentiation, including SCD-1. Transcriptional levels for these lipid synthesis genes returned to basal levels following the completion of differentiation. This finding indicates that SCD-1 plays a central role in the formation of functional oligodendrocytes (Swiss *et al.*, 2011).

Taken together, these findings suggest that the elevation of PGC-1α and SCD-1 mRNA levels by AF4 may have promoted recovery from EAE by enhancing the expression of genes which provide the necessary energy (mitochondria) and lipid (cholesterol) required for remyelination (MBP; Saher & Simons, 2010). In further support of this hypothesis, the neuroprotective effects of quercetin-3-*O*-glucoside, a major flavonoid component of AF4, are also mediated by the induction of genes that improve cholesterol synthesis and are associated with enhanced mitochondrial bioenergetics (Soundararajan *et al.*, 2008).

4.4 Administration of AF4 reduces CXCL2 levels: the link to remyelination

Chemokines act through G-protein-coupled receptors to regulate cell migration, activation, and proliferation (Charo & Ransohoff, 2006). As previously described, the CXC families of cytokines, including the ligand CXCL2, serve as a homing beacon for immune cell recruitment during neuroinflammation. The cognate receptor for CXCL2 is CXCR2, which is preferentially expressed on a variety of inflammatory cells, such as macrophages, in addition to OPCs (Fernandez & Lolis, 2002). Blocking CXCR2 receptors in spinal cord cultures increases the numbers of mature OPCs that strongly express MBP, enabling efficient myelination (Liu *et al.*, 2010). Kertetter *et al.* (2009)

have extended these findings to a mouse model of EAE by demonstrating that elevated production of CXCL2 impairs remyelination, which is preventable upon the administration of a CXCR2 antagonist. Lastly, treatments that suppress CXCL2 induction following lysolecithin or cuprizone-induced demyelination have been reported to improve remyelination (Kerstetter *et al.*, 2009; Liu *et al.*, 2010). Therefore, the reversal of elevated CXCL2 levels in the spinal cord of EAE animals at day 31 by AF4 administration suggests another mechanism whereby this flavonoid-enriched fraction may improve remyelination.

4.5 Neuroprotective properties of AF4

Erythropoietin (EPO): A potent neuroprotective cytokine

EPO, a cytokine produced by the kidney, was originally recognized for its role in promoting the survival of hematopoietic progenitor cells destined to become red blood cells thus stimulating erythropoiesis (Alnaeeli *et al.*, 2012). EPO and receptors for this cytokine are also expressed by neurons and astrocytes in the CNS (Chong et al., 2003; Genc et al., 2004). Administration of recombinant EPO provides neuroprotection in several different rodent models of CNS injury including stroke (Wen et al., 2002; Aydin et al., 2003), blunt head trauma (Brines et al., 2000), and MS (Sattler et al., 2004). EPO also reduces clinical progression and neuropathology in the MOG_{35-55} model of EAE (Li *et al.*, 2004). The underlying immune mechanism is thought to involve expansion of T_{reg} cells that suppress the production of pro-inflammatory Th17 cells within lymphoid tissue and the CNS (Yuan *et al.*, 2008). The expansion of T_{reg} cells by EPO may therefore reduce levels of pro-inflammatory mediators, decreasing EAE severity (Agnello *et al.*, 2002). BBB by the matrix metalloprotease (MMP) release from activated immune cells is

an early event in EAE that enables the infiltration of autoreactive immune cells resulting in CNS injury (Minagar & Alexander, 2003). The reduction of MMP levels by EPO in astrocytes and endothelial cells that comprise the BBB may therefore also contribute to the alleviation of EAE severity by this cytokine (Thorne *et al.*, 2009). Lastly, EPO may promote recovery from EAE by stimulating the production of oligodendrocytes necessary for remyelination (Sugawa *et al.*, 2002).

In the present study, EPO mRNA levels were elevated in both EAE treatment groups at day 18 relative to antigen controls. Kang et al. (2009) reported similar findings in a rat model of EAE demonstrating that maximal EPO induction coincides with peak disease severity, followed by a gradual decline as clinical scores improved. In agreement with this work, both EAE groups showed significant decreases in EPO mRNA levels in the spinal cord by day 31. However, EPO mRNA levels in EAE-AF4 mice remained elevated in the spinal cord relative to EAE-VEH mice. This is in keeping with evidence that EPO offers neuroprotection in EAE by promoting neuronal survival in the spinal cord (Yuan *et al.*, 2008).

Plasma membrane calcium ATPase-2 (PMCA2): A marker for neuronal stress

PMCA2 is an essential calcium ion pump that is expressed exclusively in the cell body of motor neurons found within the grey matter of the spinal cord and cerebellum (Fakira & Elkabes, 2010). Recent observations have reported a weak correlation between myelin loss and clinical severity in MS and EAE, indicating that demyelination is not the sole determinant in clinical outcome (Filippi *et al.*, 1995). This evidence points to dysfunctional motor neurons as a potential basis for clinical disability. The pro-inflammatory cytokines TNF-α and IL-1β potently enhance the excitotoxic effects of

glutamate on neurons in the spinal cord. These pro-inflammatory cytokines enhance glutamate-mediated excitotoxcitiy by increasing the number of AMPA receptors on the surface of spinal cord neurons (Leonoudakis *et al.*, 2004; Bernardino *et al.*, 2005; Lai *et al.*, 2006). Enhanced calcium influx through AMPA receptors triggers the activation of calcium dependent proteases such as calpain, resulting in neuronal injury (Trump & Berezesky, 1995).

Plasma membrane calcium ATPases (PMCAs) are expressed in the brain and spinal cord where they play an important role by maintaining calcium homeostasis (Fakira & Elkabes, 2010). PMCA2 is essential for the clearance of elevated intracellular calcium after stimulation or depolarization of spinal cord neurons (Kurnellas *et al.*, 2005). Knockdown of PMCA2 with small interfering RNA (siRNA) causes the death of cultured spinal cord neurons (Kurnellas *et al.*, 2005) while mice heterozygously null for PMCA2 suffer a delayed loss of spinal cord motor neurons (Souayah *et al.*, 2008).

PMCA2 mRNA and protein levels are reduced at the onset of clinical signs in acute EAE, remain depressed during peak clinical severity, and increase immediately prior to the improvement of clinical scores (Nicot *et al.*, 2005). In a chronic mouse model of EAE (MOG_{35-55}), PMCA2 levels remained depressed throughout the disease course and did not recover (Nicot *et al.*, 2005). Taken together, these findings indicate that reduced PMCA2 activity is closely correlated with disease severity and is a marker for the recovery of motor neuron function in two rodent models of EAE.

A decrease in PMCA2 mRNA levels in the spinal cords of EAE mice was observed at days 18 and 31, with modest recovery occurring in both groups at day 31. There was a statistical trend for increased PMCA2 in the EAE-AF4 group ($p=0.14$),

suggesting that AF4 may have improved motor neuron function at day 31. Further studies will be required to determine if this trend reaches statistical significance and to provide spinal cord tissue for the measurement of PMCA2 protein levels.

4.6 Mechanistic possibilities and future directions

AF4 is novel apple peel fraction comprised primarily of quercetin glycosides (approximately 70%) with epicatcehin, cyanidin-3-*O*-galactoside, cholorogenic acid, cafeic acid, and phlorizidin accounting for the remaining 30% of the total phenolic content. Many of these flavonoids have shown efficacy in pre-clinical models of stroke, MS, Parkinson's, and Alzheimer's disease (Muthian & Bright, 2004b; Ahmad *et al.*, 2011; Dragicevic *et al.*, 2011; Min *et al.*, 2011; Lv *et al.*, 2012). The combination of flavonoids, each with distinct mechanisms of action, is thought to result in co-operative effects that may synergistically reduce inflammation, oxidative stress, and neuronal cell death (Liu, 2003). Moreover, combining flavonoids with different mechanisms of action reduces the concentration required for each phenolic component, producing a safer therapeutic profile (Jones *et al.*, 2012). It will therefore be important to perform a component analysis to determine the relative contributions of the various phenolic acids that comprise AF4 to these biological activities.

Immunomodulation by regulation of phosphodiesterase activity

Phosphodiesterases (PDEs) are responsible for the degradation of cyclic adenosine monophosphate (cAMP), a second messenger that drives many pro-survival pathways such as the downstream transcription of PGC-1α. PDEs are inhibited by several major flavonoid subtypes represented by quercetin (flavonols), luteolin

(flavones), catechin (flavan-3-ols), hesperetin (flavanones), and genistein (isoflavones) with IC_{50} values (1-10 μM) superior to that of the classical inhibitor 3-isobutyl-2-methylxanthine (IC_{50} = 30 μM; Kuppusamy & Das, 1992; Ko et al., 2004). Moreover, this activity is preserved in the quercetin metabolite isorhamnetin (3-*O*-methylquercetin), which reaches micromolar concentrations in blood sufficient to inhibit PDE activity (Ko *et al.*, 2004). PDE4 is the most important isozyme of this large family for the function of neurons, airway smooth muscle, and almost all immune cells (Francis *et al.*, 2011). Flavonoids belonging to the same chemical class of quercetin, such as hesperetin, potently reduce the expansion of macrophages, lymphocytes, neutrophils, and eosinophils and the release of pro-inflammatory cytokines from these cells in a mouse model of asthma by blocking PDE4 (Shih *et al.*, 2012).

The induction of β-glucuronidase in activated immune cells provides an important mechanism by which deconjugated flavonoids may reach the concentrations necessary to inhibit PDE4 in these cells (Shimoi & Nakayama, 2005). Following ingestion quercetin glycosides are converted to glucoronide conjugates that have greater PDE4 inhibitory activity that the quercetin aglycone (Chan *et al.*, 2008). The increased β-glucuronidase levels in activated immune cells at the peak of disease (day 18) enables quercetin to reach concentrations necessary to inhibit PDE4 activity. β-glucuronidase activity is markedly elevated in LPS stimulated macrophages and inflamed endothelial cells of the vasculature and is therefore preferentially increased at sites of inflammation (Shimoi & Nakayama, 2005). The peak inflammatory response occurs at day 18 in our MOG_{35-55} model of EAE, which may coincide with maximal β-glucuronidase activity in infiltrating immune cells and endothelial cells of the BBB. By contrast, pro-inflammatory cytokine mRNA levels

in spinal cord were reduced at day 31 in EAE mice. This suggests that the high level of β-glucuronidase activity at day 18 and the corresponding reduction at day 31 may have been responsible for the relative inhibition of LPS-induced activity by AF4 at day 18 but not day 31. This mechanism may account for the ability of AF4 to selectively suppress immune activity at the peak of disease severity. If this hypothesis is correct, inhibition of β-glucuronidase activity by administration of saccharolactone should block the suppression of LPS-induced TNF-α release in AF4 treated EAE mice at day 18.

To test this hypothesis, it will first be necessary to determine if β-glucuronidase activity is elevated in circulating and infiltrating immune cells of EAE mice. I predict that peak elevations of β-glucuronidase will occur at day 18 following immunization with MOG_{35-55}. I therefore expect this peak of β-glucuronidase activity will be correlated with a reduction in PDE4 activity in peripheral blood immune cells from EAE-AF4 relative to EAE-VEH mice. By contrast, at day 31, I predict that β-glucuronidase and PDE4 activities will be the same in peripheral blood immune cells from EAE-AF4 and EAE-VEH mice. This result would suggest that β-glucuronidase mediated deconjugation was responsible for the generation of quercetin, which subsequently blocked PDE4 activity in peripheral blood immune cells. If this is the case, administration of saccharolactone to EAE-AF4 mice will prevent the inhibition of basal PDE4 activity and LPS-induced TNF-α release whole blood from these animals at day 18 but not day 31. Similarly, circulating levels of quercetin are expected to be reduced by saccharolactone at day 18 but not day 31 in EAE-AF4 mice.

Reduced cellular infiltration: Inhibition of chemotaxis

The reduction of MIG and CXCL2 in AF4 treated EAE mice suggest that the observed anti-inflammatory properties may be mediated, in part, by inhibiting chemotactic signaling. To test this hypothesis, I propose using multi-plexed ELISAs to quantify the concentrations other chemotactic cytokines such as KC, MCP-1, MIP-1α and MIP-1β in the spinal cords of EAE mice that receive vehicle (water; 10 ml/kg/day, p.o.) or AF4 (25 mg/kg/day; p.o.). Spinal cord tissue from these mice will also enable the confirmation of the gene expression data presented for TNF-α, IL-1β, and IL-6 by measuring protein concentrations for these pro-inflammatory cytokines as well as the concentration of the anti-inflammatory cytokine IL-10.

Remyelination

A limitation of the present study is a lack of direct evidence for remyelinated axons in EAE-AF4 relative to EAE-VEH mice. While there is substantial evidence to support demyelination in MOG_{35-55} induced EAE, remyelination is not a synchronized event in this model (Buckley *et al.*, 2008). The stochastic nature of remyelination in the MOG_{35-55} model makes it difficult to discern whether AF4 promotes remyelination. I therefore propose to use the cuprizone model of demyelination to assess the ability of AF4 to promote remyelination. Female C57Bl/6 mice will be fed a diet of mouse chow containing 0.2% (w/w) cuprizone (Sigma-Aldrich) *ad libitum* for a period of 6 weeks to induce CNS demyelination. Oral administration of either vehicle (water; 10 ml/kg/day, p.o.) or AF4 (25 mg/kg/day; p.o.) would be begin on the last day of cuprizone exposure and continue for 3, 5, 7, or 10 days, at which points mice will be euthanized for histological examination of myelin in the corpus callosum. Quantification of

remyelination in vehicle and AF4 mice will be done using the histochemical stain Black-Gold and quantifying the total area of the corpus callosum using ImageJ software (Liu *et al.*, 2010).

4.7 Conclusions

The present study investigated the anti-inflammatory, neuroprotective, and restorative potential of a novel flavonoid enriched fraction called AF4 isolated from the peel of local Northern Spy apples in an animal model of MS that features chronic inflammation and demyelination. Oral administration of AF4 beginning 24 hours after the first onset of symptoms reduced disease progression in EAE mice that was associated with decreased pro-inflammatory cytokine levels (TNF-α and IL-1β) in plasma (days 18 and 31) as well as mRNA levels for IL-1β and IL-6 in spinal cord and TNF-α, IL-1β, and IL-6 in cerebellum at day 31. Histological examination of the cerebellum confirmed that these measures were associated with a reduction in neuroinflammation. A further mechanism for the anti-inflammatory properties of AF4 may be its ability to reduce the chemokines MIG and CXCL2, both known to promote cellular infiltration and enhance EAE severity.

LPS-induced release of TNF-α from whole blood revealed that AF4 selectively suppressed pro-inflammatory signaling during peak disease severity (day 18 but not day 31). This is strong evidence that AF4 is an immune-modulator rather than a general immunosuppressant, reducing the potential for systemic side effects following the resolution of inflammation in healthy individuals.

Another important finding of this study was that AF4 increased the expression of genes required for remyelination in EAE animals. Quantitative RT-PCR measurements showed that the reduction in disease progression produced by AF4 in EAE animals was closely associated with elevated mRNA levels for MBP (spinal cord), PGC-1α (spinal cord and cerebellum), and SCD1 (spinal cord). The ability of AF4 to reduce CXCL2 concentrations that otherwise depress the proliferation of OPCs may have also contributed to the ability of AF4 to increase the expression of genes associated with remyelination.

Lastly, AF4 promoted the expression of EPO mRNA in EAE mice during the chronic stage of the clinical disease course, possibly preventing the peripheral immune system from initializing subsequent waves of inflammation, protecting spinal cord neurons and oligodendrocytes, and promoting the proliferation of OPCs necessary for remyelination.

Taken together, these findings suggest that AF4 exacts anti-inflammatory, immuno-modulatory, restorative, and neuroprotective effects through a variety of distinct mechanisms that converge to produce additive benefit in an EAE model. Given the excellent projected safety profile of this extract and the high bioavailability of its flavonoids components, AF4 is a promising therapeutic candidate for the treatment of MS.

REFERENCE LIST

Ader, P., Wessmann, A., & Wolffram, S. (2000) Bioavailability and metabolism of the flavonol quercetin in the pig. *Free Radical Biology & Medicine*, **28**, 1056–1067.

Agnello, D., Bigini, P., Villa, P., Mennini, T., Cerami, A., Brines, M.L., & Ghezzi, P. (2002) Erythropoietin exerts an anti-inflammatory effect on the CNS in a model of experimental autoimmune encephalomyelitis. *Brain research*, **952**, 128–134.

Ahmad, A., Khan, M.M., Hoda, M.N., Raza, S.S., Khan, M.B., Javed, H., Ishrat, T., Ashafaq, M., Ahmad, M.E., Safhi, M.M., & Islam, F. (2011) Quercetin protects against oxidative stress associated damages in a rat model of transient focal cerebral ischemia and reperfusion. *Neurochemical Research*, **36**, 1360–1371.

Alcázar, a, Regidor, I., Masjuan, J., Salinas, M., & Alvarez-Cermeño, J.C. (2000) Axonal damage induced by cerebrospinal fluid from patients with relapsing-remitting multiple sclerosis. *Annual Review of Immunology*, **104**, 58–67.

Alnaeeli, M., Wang, L., Piknova, B., Rogers, H., Li, X., & Noguchi, C.T. (2012) Erythropoietin in brain development and beyond. *Anatomy Research International*, **2012**, 953264.

Arnett, H.A., Mason, J., Marino, M., Suzuki, K., Matsushima, G.K., & Ting, J.P. (2001) TNF alpha promotes proliferation of oligodendrocyte progenitors and remyelination. *Nature Neuroscience*, **4**, 1116–1122.

Arora, A., Nair, M.G., & Strasburg, G.M. (1998) Structure-activity relationships for antioxidant activities of a series of flavonoids in a liposomal system. *Free Radical Biology & Medicine*, **24**, 1355–1363.

Ascherio, A., Munger, K.L., Lennette, E.T., Spiegelman, D., Hernán, M.A., Olek, M.J., Hankinson, S.E., & Hunter, D.J. (2001) Epstein-Barr virus antibodies and risk of multiple sclerosis: a prospective study. *JAMA*, **286**, 3083–3088.

Baker, D. & Amor, S. (2012) Publication guidelines for refereeing and reporting on animal use in experimental autoimmune encephalomyelitis. *Journal of Neuroimmunology*, **242**, 78–83.

Baxter, A.G. (2007) The origin and application of experimental autoimmune encephalomyelitis. *Nature Reviews Immunology*, **7**, 904–912.

Beck, C.A., Metz, L.M., Svenson, L.W., & Patten, S.B. (2005) Regional variation of multiple sclerosis prevalence in Canada. *Multiple Sclerosis*, **11**, 516–519.

Berard, J.L., Wolak, K., Fournier, S., & David, S. (2010) Characterization of relapsing-remitting and chronic forms of experimental autoimmune encephalomyelitis in C57BL/6 mice. *Glia*, **58**, 434–445.

Bernardino, L., Xapelli, S., Silva, A.P., Jakobsen, B., Poulsen, F.R., Oliveira, C.R., Vezzani, A., Malva, J.O., & Zimmer, J. (2005) Modulator effects of interleukin-1beta and tumor necrosis factor-alpha on AMPA-induced excitotoxicity in mouse organotypic hippocampal slice cultures. *The Journal of Neuroscience*, **25**, 6734–6744.

Bollen, E. & Prickaerts, J. (2012) Phosphodiesterases in neurodegenerative disorders. *IUBMB Life*,.

Bongioanni, P., Mosti, S., Romano, M.R., Lombardo, F., Moscato, G., & Meucci, G. (2000) Increased T-lymphocyte interleukin-6 binding in patients with multiple sclerosis. *European Journal of Neurology*, **7**, 291–297.

Buckley, C.E., Goldsmith, P., & Franklin, R.J.M. (2008) Zebrafish myelination: a transparent model for remyelination? *Disease Models & Mechanisms*, **1**, 221–228.

Charcot, J.M. (1868) Histologie de la sclerose en plaques. *Gazette des Hopitaux*, Paris, **41**, 554-558

Carrasco-Pozo, C., Gotteland, M., & Speisky, H. (2011) Apple peel polyphenol extract protects against indomethacin-induced damage in Caco-2 cells by preventing mitochondrial complex I inhibition. *Journal of agricultural and food chemistry*, **59**, 11501–11508.

Centonze, D., Muzio, L., Rossi, S., Furlan, R., Bernardi, G., & Martino, G. (2010) The link between inflammation, synaptic transmission and neurodegeneration in multiple sclerosis. *Cell death and differentiation*, **17**, 1083–1091.

Chan, A.L.-F., Huang, H.-L., Chien, H.-C., Chen, C.-M., Lin, C.-N., & Ko, W.-C. (2008) Inhibitory effects of quercetin derivatives on phosphodiesterase isozymes and high-affinity [(3) H]-rolipram binding in guinea pig tissues. *Investigational New Drugs*, **26**, 417–424.

Charo, I.F. & Ransohoff, R.M. (2006) The many roles of chemokines and chemokine receptors in inflammation. *The New England Journal of Medicine*, **354**, 610–621.

Chirumbolo, S. (2010) The role of quercetin, flavonols and flavones in modulating inflammatory cell function. *Inflammation & Allergy Drug Targets*, **9**, 263–285.

Compston, A. & Coles, A. (2008) Multiple sclerosis. *Lancet*, **372**, 1502–1517.

Day, A.J., Bao, Y., Morgan, M.R., & Williamson, G. (2000) Conjugation position of quercetin glucuronides and effect on biological activity. *Free Radical Biology & Medicine*, **29**, 1234–1243.

Day, A.J., DuPont, M.S., Ridley, S., Rhodes, M., Rhodes, M.J., Morgan, M.R., & Williamson, G. (1998) Deglycosylation of flavonoid and isoflavonoid glycosides by human small intestine and liver beta-glucosidase activity. *FEBS Letters*, **436**, 71–75.

Dedrick, R.L. & Conlon, P.J. (1995) Prolonged expression of lipopolysaccharide (LPS)-induced inflammatory genes in whole blood requires continual exposure to LPS. *Infection and Immunity*, **63**, 1362–1368.

Denic, A., Johnson, A.J., Bieber, A.J., Warrington, A.E., Rodriguez, M., & Pirko, I. (2011) The relevance of animal models in multiple sclerosis research. *Pathophysiology*, **18**, 21–29.

DeWille, J.W. & Farmer, S.J. (1992) Postnatal dietary fat influences mRNAS involved in myelination. *Developmental Neuroscience*, **14**, 61–68.

Dragicevic, N., Smith, A., Lin, X., Yuan, F., Copes, N., Delic, V., Tan, J., Cao, C., Shytle, R.D., & Bradshaw, P.C. (2011) Green tea epigallocatechin-3-gallate (EGCG) and other flavonoids reduce Alzheimer's amyloid-induced mitochondrial dysfunction. *Journal of Alzheimer's Disease*, **26**, 507–521.

Dunliop, K. (2011) Neuroprotective effects of a novel apple peel extract AF4 in a mouse model of hypoxic-ischemic brain injury. *Thesis, Dalhousie University*

Duprez, L., Wirawan, E., Vanden Berghe, T., & Vandenabeele, P. (2009) Major cell death pathways at a glance. *Microbes and infection / Institut Pasteur*, **11**, 1050–1062.

Fakira, A.K. & Elkabes, S. (2010) Role of plasma membrane calcium ATPase 2 in spinal cord pathology. *Neuron Glia Biology*, **1**, 103–108.

Fernandez, E.J. & Lolis, E. (2002) Structure, function, and inhibition of chemokines. *Annual Review of Pharmacology and Toxicology*, **42**, 469–499.

Fernández, M., Montalban, X., & Comabella, M. (2010) Orchestrating innate immune responses in multiple sclerosis: Molecular players. *Journal of Neuroimmunology*, **225**, 5–12.

Filippi, M., Paty, D.W., Kappos, L., Barkhof, F., Compston, D.A., Thompson, A.J., Zhao, G.J., Wiles, C.M., McDonald, W.I., & Miller, D.H. (1995) Correlations between changes in disability and T2-weighted brain MRI activity in multiple sclerosis: a follow-up study. *Neurology*, **45**, 255–260.

Fiorani, M., Guidarelli, A., Blasa, M., Azzolini, C., Candiracci, M., Piatti, E., & Cantoni, O. (2010) Mitochondria accumulate large amounts of quercetin: prevention of mitochondrial damage and release upon oxidation of the extramitochondrial fraction of the flavonoid. *The Journal of Nutritional Biochemistry*, **21**, 397–404.

Francis, S.H., Houslay, M.D., & Conti, M. (2011) Phosphodiesterase inhibitors: factors that influence potency, selectivity, and action. *Handbook of Experimental Pharmacology*, 47–84.

Franklin, R.J.M. & Ffrench-Constant, C. (2008) Remyelination in the CNS: from biology to therapy. *Nature Reviews Neuroscience*, **9**, 839–855.

Franklin, R.J.M., Ffrench-Constant, C., Edgar, J.M., & Smith, K.J. (2012) Neuroprotection and repair in multiple sclerosis. *Nature Reviews Neurology*, 1–11.

Frohman, E.M., Racke, M.K., & Raine, C.S. (2006) Multiple sclerosis--the plaque and its pathogenesis. *The New England Journal of Medicine*, **354**, 942–955.

Fulton, D., Paez, P.M., & Campagnoni, A.T. (2010) The multiple roles of myelin protein genes during the development of the oligodendrocyte. *ASN Neuroscience*, **2**, e00027.

Gao, H.-M., Zhou, H., & Hong, J.-S. (2012) NADPH oxidases: novel therapeutic targets for neurodegenerative diseases. *Trends in Pharmacological Sciences*, **33**, 295–303.

Gao, Y., Deng, K., Hou, J., Bryson, J.B., Barco, A., Nikulina, E., Spencer, T., Mellado, W., Kandel, E.R., & Filbin, M.T. (2004) Activated CREB is sufficient to overcome inhibitors in myelin and promote spinal axon regeneration in vivo. *Neuron*, **44**, 609–621.

Glabinski, A.R., Tani, M., Tuohy, V.K., Tuthill, R.J., & Ransohoff, R.M. (1995) Central nervous system chemokine mRNA accumulation follows initial leukocyte entry at the onset of acute murine experimental autoimmune encephalomyelitis. *Brain, Behavior, and Immunity*, **9**, 315–330.

Griffiths, I., Klugmann, M., Anderson, T., Yool, D., Thomson, C., Schwab, M.H., Schneider, A., Zimmermann, F., McCulloch, M., Nadon, N., & Nave, K.A. (1998) Axonal swellings and degeneration in mice lacking the major proteolipid of myelin. *Science*, **280**, 1610–1613.

Hartung, H.-P., Gonsette, R., König, N., Kwiecinski, H., Guseo, A., Morrissey, S.P., Krapf, H., & Zwingers, T. (2002) Mitoxantrone in progressive multiple sclerosis: a placebo-controlled, double-blind, randomised, multicentre trial. *Lancet*, **360**, 2018–2025.

Hauser, S.L., Doolittle, T.H., Lincoln, R., Brown, R.H., & Dinarello, C.A. (1990) Cytokine accumulations in CSF of multiple sclerosis patients: frequent detection of interleukin-1 and tumor necrosis factor but not interleukin-6. *Neurology*, **40**, 1735–1739.

Heinrich, P.C., Behrmann, I., Haan, S., Hermanns, H.M., Müller-Newen, G., & Schaper, F. (2003) Principles of interleukin (IL)-6-type cytokine signalling and its regulation. *The Biochemical Journal*, **374**, 1–20.

Hendriks, J.J. a. (2004) Flavonoids Influence Monocytic GTPase Activity and Are Protective in Experimental Allergic Encephalitis. *Journal of Experimental Medicine*, **200**, 1667–1672.

Hertog, M.G., Kromhout, D., Aravanis, C., Blackburn, H., Buzina, R., Fidanza, F., Giampaoli, S., Jansen, A., Menotti, A., & Nedeljkovic, S. (1995) Flavonoid intake and long-term risk of coronary heart disease and cancer in the seven countries study. *Archives of Internal Medicine*, **155**, 381–386.

Hodson, L. & Fielding, B. a (2012) Stearoyl-CoA desaturase: rogue or innocent bystander? *Progress in lipid research*, **52**, 15–42.

Hollman, P.C., de Vries, J.H., van Leeuwen, S.D., Mengelers, M.J., & Katan, M.B. (1995) Absorption of dietary quercetin glycosides and quercetin in healthy ileostomy volunteers. *The American Journal of Clinical Nutrition*, **62**, 1276–1282.

Huber, G.M. & Rupasinghe, H.P. V (2009) Phenolic profiles and antioxidant properties of apple skin extracts. *Journal of food science*, **74**, C693–700.

Huemmer, W., Dietrich, H., Will, F., Schreier, P., & Richling, E. (2008) Content and mean polymerization degree of procyanidins in extracts obtained from clear and cloudy apple juices. *Biotechnology Journal*, **3**, 234–243.

Imitola, J., Chitnis, T., & Khoury, S.J. (2005) Cytokines in multiple sclerosis: from bench to bedside. *Pharmacology & Therapeutics*, **106**, 163–177.

Jones, Q.R.D., Warford, J., Rupasinghe, H.P.V., & Robertson, G.S. (2012) Target-based selection of flavonoids for neurodegenerative disorders. *Trends in Pharmacological Sciences*, **33**, 602–610.

Jones, M. V, Nguyen, T.T., Deboy, C.A., Griffin, J.W., Whartenby, K.A., Kerr, D.A., & Calabresi, P.A. (2008) Behavioral and pathological outcomes in MOG 35-55 experimental autoimmune encephalomyelitis. *Journal of Neuroimmunology*, **199**, 83–93.

Jung, M., Triebel, S., Anke, T., Richling, E., & Erkel, G. (2009) Influence of apple polyphenols on inflammatory gene expression. *Molecular Nutrition & Food Research*, **53**, 1263–1280.

Jurevics, H. & Morell, P. (1995) Cholesterol for synthesis of myelin is made locally, not imported into brain. *Journal of neurochemistry*, **64**, 895–901.

Kang, S.-Y., Kang, J.-H., Choi, J.C., Lee, J.S., Lee, C.S., & Shin, T. (2009) Expression of erythropoietin in the spinal cord of lewis rats with experimental autoimmune encephalomyelitis. *Journal of Clinical Neurology*, **5**, 39–45.

Karpus, W.J. & Ransohoff, R.M. (1998) Chemokine regulation of experimental autoimmune encephalomyelitis: temporal and spatial expression patterns govern disease pathogenesis. *Journal of Immunology*, **161**, 2667–2671.

Keough, M.B. & Yong, V.W. (2012) Remyelination Therapy for Multiple Sclerosis. *Neurotherapeutics*.

Keddy, P.G., Dunlop, K., **Warford, J.**, Samson, M.L., Jones, Q.R.D., Rupasinghe, V.H.P., Robertson, G.S. (2012) Neuroprotective and anti-inflammatory effects of the flavonoid-enriched fraction AF4 in a mouse model of hypoxic-ischemia brain injury. *PLoS ONE*, in press.

Kerstetter, a E., Padovani-Claudio, D. a, Bai, L., & Miller, R.H. (2009) Inhibition of CXCR2 signaling promotes recovery in models of multiple sclerosis. *Experimental Neurology*, **220**, 44–56.

Kijima, K., Numakura, C., Izumino, H., Umetsu, K., Nezu, A., Shiiki, T., Ogawa, M., Ishizaki, Y., Kitamura, T., Shozawa, Y., & Hayasaka, K. (2005) Mitochondrial GTPase mitofusin 2 mutation in Charcot-Marie-Tooth neuropathy type 2A. *Human Genetics*, **116**, 23–27.

Ko, W.-C., Shih, C.-M., Lai, Y.-H., Chen, J.-H., & Huang, H.-L. (2004) Inhibitory effects of flavonoids on phosphodiesterase isozymes from guinea pig and their structure-activity relationships. *Biochemical Pharmacology*, **68**, 2087–2094.

Korn, T. (2008) Pathophysiology of multiple sclerosis. *Journal of Neurology*, **255 Suppl**, 2–6.

Kroon, P.A., Clifford, M.N., Crozier, A., Day, A.J., Donovan, J.L., Manach, C., & Williamson, G. (2004) How should we assess the effects of exposure to dietary polyphenols in vitro? *The American Journal of Clinical Nutrition*, **80**, 15–21.

Kuppusamy, U.R. & Das, N.P. (1992) Effects of flavonoids on cyclic AMP phosphodiesterase and lipid mobilization in rat adipocytes. *Biochemical Pharmacology*, **44**, 1307–1315.

Kurnellas, M.P., Nicot, A., Shull, G.E., & Elkabes, S. (2005) Plasma membrane calcium ATPase deficiency causes neuronal pathology in the spinal cord: a potential mechanism for neurodegeneration in multiple sclerosis and spinal cord injury. *Cell Death and Differentiation*, **19**, 298–300.

Kuroda, Y. & Shimamoto, Y. (1991) Human tumor necrosis factor-alpha augments experimental allergic encephalomyelitis in rats. *Journal of Neuroimmunology*, **34**, 159–164.

Lagoa, R., Graziani, I., Lopez-Sanchez, C., Garcia-Martinez, V., & Gutierrez-Merino, C. (2011) Complex I and cytochrome c are molecular targets of flavonoids that inhibit hydrogen peroxide production by mitochondria. *Biochimica et Biophysica Acta*, **1807**, 1562–1572.

Lai, A.Y., Swayze, R.D., El-Husseini, A., & Song, C. (2006) Interleukin-1 beta modulates AMPA receptor expression and phosphorylation in hippocampal neurons. *Journal of Neuroimmunology*, **175**, 97–106.

Langer-Gould, A., Garren, H., Slansky, A., Ruiz, P.J., & Steinman, L. (2002) Late pregnancy suppresses relapses in experimental autoimmune encephalomyelitis: evidence for a suppressive pregnancy-related serum factor. *Journal of Immunology*, **169**, 1084–1091.

Lemberger, T., Parkitna, J.R., Chai, M., Schütz, G., & Engblom, D. (2008) CREB has a context-dependent role in activity-regulated transcription and maintains neuronal cholesterol homeostasis. *FASEB*, **22**, 2872–2879.

Leonoudakis, D., Braithwaite, S.P., Beattie, M.S., & Beattie, E.C. (2004) TNFalpha-induced AMPA-receptor trafficking in CNS neurons; relevance to excitotoxicity? *Neuron Glia Biology*, **1**, 263–273.

Li, W., Maeda, Y., Yuan, R.R., Elkabes, S., Cook, S., & Dowling, P. (2004) Beneficial effect of erythropoietin on experimental allergic encephalomyelitis. *Annals of Neurology*, **56**, 767–777.

Libbey, J.E., McCoy, L.L., & Fujinami, R.S. (2007) Molecular mimicry in multiple sclerosis. *International Review of Neurobiology*, **79**, 127–147.

Liu, L., Darnall, L., Hu, T., Choi, K., Lane, T.E., & Ransohoff, R.M. (2010) Myelin repair is accelerated by inactivating CXCR2 on nonhematopoietic cells. *The Journal of Neuroscience*, **30**, 9074–9083.

Liu, R.H. (2003) Health benefits of fruit and vegetables are from additive and synergistic combinations of phytochemicals. *The American Journal of Clinical Nutrition*, **78**, 517S–520S.

Livak, K.J. & Schmittgen, T.D. (2001) Analysis of relative gene expression data using real-time quantitative PCR and the 2(-Delta Delta C(T)) Method. *Methods*, **25**, 402–408.

Lu, F., Selak, M., O'Connor, J., Croul, S., Lorenzana, C., Butunoi, C., & Kalman, B. (2000) Oxidative damage to mitochondrial DNA and activity of mitochondrial enzymes in chronic active lesions of multiple sclerosis. *Journal of Neurological Sciences*, **177**, 95–103.

Ludwin, S.K. (2006) The pathogenesis of multiple sclerosis: relating human pathology to experimental studies. *Journal of Neuropathology and Experimental Neurology*, **65**, 305–318.

Lv, C., Hong, T., Yang, Z., Zhang, Y., Wang, L., Dong, M., Zhao, J., Mu, J., & Meng, Y. (2012) Effect of Quercetin in the 1-Methyl-4-phenyl-1, 2, 3, 6-tetrahydropyridine-Induced Mouse Model of Parkinson's Disease. *Evidence-Based Complementary and Alternative Medicine*, **2012**, 928643.

Magnano, M.D., Robinson, W.H., & Genovese, M.C. (2004) Demyelination and inhibition of tumor necrosis factor (TNF). *Clinical and Experimental Rheumatology*, **22**, S134–40.

Mahad, D., Ziabreva, I., Lassmann, H., & Turnbull, D. (2008) Mitochondrial defects in acute multiple sclerosis lesions. *Brain*, **131**, 1722–1735.

Makino, T., Shimizu, R., Kanemaru, M., Suzuki, Y., Moriwaki, M., & Mizukami, H. (2009) Enzymatically modified isoquercitrin, alpha-oligoglucosyl quercetin 3-O-glucoside, is absorbed more easily than other quercetin glycosides or aglycone after oral administration in rats. *Biological & Pharmaceutical Bulletin*, **32**, 2034–2040.

Markovic-Plese, S. (2009) Degenerate T-cell receptor recognition, autoreactive cells, and the autoimmune response in multiple sclerosis. *The Neuroscientist*, **15**, 225–231.

Markovic-Plese, S., Pinilla, C., & Martin, R. (2004) The initiation of the autoimmune response in multiple sclerosis. *Clinical Neurology and Neurosurgery*, **106**, 218–222.

Marta, M., Meier, U.C., & Lobell, A. (2009) Regulation of autoimmune encephalomyelitis by toll-like receptors. *Autoimmunity Reviews*, **8**, 506–509.

Matsuki, T., Nakae, S., Sudo, K., Horai, R., & Iwakura, Y. (2006) Abnormal T cell activation caused by the imbalance of the IL-1/IL-1R antagonist system is responsible for the development of experimental autoimmune encephalomyelitis. *International Immunology*, **18**, 399–407.

McCarthy, D.P., Richards, M.H., & Miller, S.D. (2012) Mouse models of multiple sclerosis: experimental autoimmune encephalomyelitis and Theiler's virus-induced demyelinating disease. *Methods in Molecular Biology*, **900**, 381–401.

Min, J., Yu, S.-W., Baek, S.-H., Nair, K.M., Bae, O.-N., Bhatt, A., Kassab, M., Nair, M.G., & Majid, A. (2011) Neuroprotective effect of cyanidin-3-O-glucoside anthocyanin in mice with focal cerebral ischemia. *Neuroscience Letters*, **500**, 157–161.

Minagar, A. & Alexander, J.S. (2003) Blood-brain barrier disruption in multiple sclerosis. *Multiple Sclerosis*, **9**, 540–549.

Mix, E., Meyer-Rienecker, H., Hartung, H.-P., & Zettl, U.K. (2010) Animal models of multiple sclerosis--potentials and limitations. *Progress in Neurobiology*, **92**, 386–404.

Mizrachi, K., Aricha, R., Feferman, T., Kela-Madar, N., Mandel, I., Paperna, T., Miller, A., Ben-Nun, A., Berrih-Aknin, S., Souroujon, M.C., & Fuchs, S. (2010) Involvement of phosphodiesterases in autoimmune diseases. *Journal of Neuroimmunology*, **220**, 43–51.

Moore, C.S., Earl, N., Frenette, R., Styhler, A., Mancini, J.A., Nicholson, D.W., Hebb, A.L.O., Owens, T., & Robertson, G.S. (2006) Peripheral phosphodiesterase 4 inhibition produced by 4-[2-(3,4-Bis-difluoromethoxyphenyl)-2-[4-(1,1,1,3,3,3-hexafluoro-2-hydroxypropan-2-yl)-phenyl]-ethyl]-3-methylpyridine-1-oxide (L-826,141) prevents experimental autoimmune encephalomyelitis. *The Journal of Pharmacology and Experimental Therapeutics*, **319**, 63–72.

Mullen, W., Edwards, C.A., & Crozier, A. (2006) Absorption, excretion and metabolite profiling of methyl-, glucuronyl-, glucosyl- and sulpho-conjugates of quercetin in human plasma and urine after ingestion of onions. *The British Journal of Nutrition*, **96**, 107–116.

Murota, K. & Terao, J. (2003) Antioxidative flavonoid quercetin: implication of its intestinal absorption and metabolism. *Archives of Biochemistry and Biophysics*, **417**, 12–17.

Muthian, G. & Bright, J.J. (2004a) Quercetin, a flavonoid phytoestrogen, ameliorates experimental allergic encephalomyelitis by blocking IL-12 signaling through JAK-STAT pathway in T lymphocyte. *Journal of Clinical Immunology*, **24**, 542–552.

Muthian, G. & Bright, J.J. (2004b) Quercetin, a flavonoid phytoestrogen, ameliorates experimental allergic encephalomyelitis by blocking IL-12 signaling through JAK-STAT pathway in T lymphocyte. *Journal of Clinical Immunology*, **24**, 542–552.

Nave, K.-A. (2010) Myelination and the trophic support of long axons. *Nature Reviews Neuroscience*, **11**, 275–283.

Nicot, A., Kurnellas, M., & Elkabes, S. (2005) Temporal pattern of plasma membrane calcium ATPase 2 expression in the spinal cord correlates with the course of clinical symptoms in two rodent models of autoimmune encephalomyelitis. *The European Journal of Neuroscience*, **21**, 2660–2670.

Nikić, I., Merkler, D., Sorbara, C., Brinkoetter, M., Kreutzfeldt, M., Bareyre, F.M., Brück, W., Bishop, D., Misgeld, T., & Kerschensteiner, M. (2011) A reversible form of axon damage in experimental autoimmune encephalomyelitis and multiple sclerosis. *Nature Medicine*, **17**, 495–499.

Oberkofler, H., Schraml, E., Krempler, F., & Patsch, W. (2003) Potentiation of liver X receptor transcriptional activity by peroxisome-proliferator-activated receptor gamma co-activator 1 alpha. *The Biochemical Journal*, **371**, 89–96.

Okuda, Y., Sakoda, S., Fujimura, H., Saeki, Y., Kishimoto, T., & Yanagihara, T. (1999) IL-6 plays a crucial role in the induction phase of myelin oligodendrocyte glucoprotein 35-55 induced experimental autoimmune encephalomyelitis. *Journal of Neuroimmunology*, **101**, 188–196.

Pacelli, C., De Rasmo, D., Signorile, A., Grattagliano, I., di Tullio, G., D'Orazio, A., Nico, B., Comi, G. Pietro, Ronchi, D., Ferranini, E., Pirolo, D., Seibel, P., Schubert, S., Gaballo, A., Villani, G., & Cocco, T. (2011) Mitochondrial defect and PGC-1α dysfunction in parkin-associated familial Parkinson's disease. *Biochimica et Biophysica Acta*, **1812**, 1041–1053.

Pan, B., Fromholt, S.E., Hess, E.J., Crawford, T.O., Griffin, J.W., Sheikh, K.A., & Schnaar, R.L. (2005) Myelin-associated glycoprotein and complementary axonal ligands, gangliosides, mediate axon stability in the CNS and PNS: neuropathology and behavioral deficits in single- and double-null mice. *Experimental Neurology*, **195**, 208–217.

Patani, R., Balaratnam, M., Vora, A., & Reynolds, R. (2007) Remyelination can be extensive in multiple sclerosis despite a long disease course. *Neuropathology and Applied Neurobiology*, **33**, 277–287.

Patrikios, P., Stadelmann, C., Kutzelnigg, A., Rauschka, H., Schmidbauer, M., Laursen, H., Sorensen, P.S., Brück, W., Lucchinetti, C., & Lassmann, H. (2006) Remyelination is extensive in a subset of multiple sclerosis patients. *Brain*, **129**, 3165–3172.

Peluso, M.R. (2006) Flavonoids attenuate cardiovascular disease, inhibit phosphodiesterase, and modulate lipid homeostasis in adipose tissue and liver. *Experimental Biology and Medicine*, **231**, 1287–1299.

Perez-Vizcaino, F., Duarte, J., & Santos-Buelga, C. (2012) The flavonoid paradox: conjugation and deconjugation as key steps for the biological activity of flavonoids. *Journal of the Science of Food and Agriculture*, **92**, 1822–1825.

Polo-Hernández, E., De Castro, F., García-García, A.G., Tabernero, A., & Medina, J.M. (2010) Oleic acid synthesized in the periventricular zone promotes axonogenesis in the striatum during brain development. *Progress in Lipid Research*, **114**, 1756–1766.

Prayoonwiwat, N. & Rodriguez, M. (1993) The potential for oligodendrocyte proliferation during demyelinating disease. *Journal of Neuropathology and Experimental Neurology*, **52**, 55–63.

Probert, L., Akassoglou, K., Pasparakis, M., Kontogeorgos, G., & Kollias, G. (1995) Spontaneous inflammatory demyelinating disease in transgenic mice showing central nervous system-specific expression of tumor necrosis factor alpha. *PNAS*, **92**, 11294–11298.

Racke, M.K., Burnett, D., Pak, S.H., Albert, P.S., Cannella, B., Raine, C.S., McFarlin, D.E., & Scott, D.E. (1995) Retinoid treatment of experimental allergic encephalomyelitis. IL-4 production correlates with improved disease course. *Journal of Immunology*, **154**, 450–458.

Reinboth, M., Wolffram, S., Abraham, G., Ungemach, F.R., & Cermak, R. (2010) Oral bioavailability of quercetin from different quercetin glycosides in dogs. *The British Journal of Nutrition*, **104**, 198–203.

Reynolds, J.M., Martinez, G.J., Chung, Y., & Dong, C. (2012) Toll-like receptor 4 signaling in T cells promotes autoimmune inflammation. *PNAS*, **109**, 13064–13069.

Robbins, D.S., Shirazi, Y., Drysdale, B.E., Lieberman, A., Shin, H.S., & Shin, M.L. (1987) Production of cytotoxic factor for oligodendrocytes by stimulated astrocytes. *Journal of Immunology*, **139**, 2593–2597.

Saher, G., Brügger, B., Lappe-Siefke, C., Möbius, W., Tozawa, R., Wehr, M.C., Wieland, F., Ishibashi, S., & Nave, K.-A. (2005) High cholesterol level is essential for myelin membrane growth. *Nature Neuroscience*, **8**, 468–475.

Saher, G., Quintes, S., & Nave, K.-A. (2011) Cholesterol: a novel regulatory role in myelin formation. *The Neuroscientist*, **17**, 79–93.

Saher, G. & Simons, M. (2010) Cholesterol and myelin biogenesis. *Sub-Cellular Biochemistry*, **51**, 489–508.

Saidha, S., Eckstein, C., & Calabresi, P.A. (2012) New and emerging disease modifying therapies for multiple sclerosis. *Annals of the New York Academy of Sciences*, **1247**, 117–137.

Scapagnini, G., Vasto, S., Sonya, V., Abraham, N.G., Nader, A.G., Caruso, C., Calogero, C., Zella, D., & Fabio, G. (2011) Modulation of Nrf2/ARE pathway by food polyphenols: a nutritional neuroprotective strategy for cognitive and neurodegenerative disorders. *Molecular Neurobiology*, **44**, 192–201.

Schoenfeld, R., Wong, A., Silva, J., Li, M., Itoh, A., Horiuchi, M., Itoh, T., Pleasure, D., & Cortopassi, G. (2010) Oligodendroglial differentiation induces mitochondrial genes and inhibition of mitochondrial function represses oligodendroglial differentiation. *Mitochondrion*, **10**, 143–150.

Scholz, C., Patton, K.T., Anderson, D.E., Freeman, G.J., & Hafler, D.A. (1998) Expansion of autoreactive T cells in multiple sclerosis is independent of exogenous B7 costimulation. *Journal of Immunology*, **160**, 1532–1538.

Schroeder, E.K., Kelsey, N.A., Doyle, J., Breed, E., Bouchard, R.J., Loucks, F.A., Harbison, R.A., & Linseman, D.A. (2009) Green tea epigallocatechin 3-gallate accumulates in mitochondria and displays a selective antiapoptotic effect against inducers of mitochondrial oxidative stress in neurons. *Antioxidants & Redox Signaling*, **11**, 469–480.

Selin, L.K., Cornberg, M., Brehm, M.A., Kim, S.-K., Calcagno, C., Ghersi, D., Puzone, R., Celada, F., & Welsh, R.M. (2004) CD8 memory T cells: cross-reactivity and heterologous immunity. *Seminars in Immunology*, **16**, 335–347.

Shih, C.-H., Lin, L.-H., Hsu, H.-T., Wang, K.-H., Lai, C.-Y., Chen, C.-M., & Ko, W.-C. (2012) Hesperetin, a Selective Phosphodiesterase 4 Inhibitor, Effectively Suppresses Ovalbumin-Induced Airway Hyperresponsiveness without Influencing Xylazine/Ketamine-Induced Anesthesia. *Evidence-based Complementary and Alternative Medicine*, **2012**, 472897.

Shimoi, K. & Nakayama, T. (2005) Glucuronidase deconjugation in inflammation. *Methods in Enzymology*, **400**, 263–272.

Shrikant, P., Chung, I.Y., Ballestas, M.E., & Benveniste, E.N. (1994) Regulation of intercellular adhesion molecule-1 gene expression by tumor necrosis factor-alpha, interleukin-1 beta, and interferon-gamma in astrocytes. *Journal of Neuroimmunology*, **51**, 209–220.

Simi, A., Lerouet, D., Pinteaux, E., & Brough, D. (2007) Mechanisms of regulation for interleukin-1beta in neurodegenerative disease. *Neuropharmacology*, **52**, 1563–1569.

Skyberg, J. a, Robison, A., Golden, S., Rollins, M.F., Callis, G., Huarte, E., Kochetkova, I., Jutila, M. a, & Pascual, D.W. (2011) Apple polyphenols require T cells to ameliorate dextran sulfate sodium-induced colitis and dampen proinflammatory cytokine expression. *Journal of Leukocyte Biology*, **90**, 1043–1054.

Souayah, N., Sharovetskaya, A., Kurnellas, M.P., Myerson, M., Deitch, J.S., & Elkabes, S. (2008) Reductions in motor unit number estimates (MUNE) precede motor neuron loss in the plasma membrane calcium ATPase 2 (PMCA2)-heterozygous mice. *Experimental Neurology*, **214**, 341–346.

Soundararajan, R., Wishart, A.D., Rupasinghe, H.P.V., Arcellana-Panlilio, M., Nelson, C.M., Mayne, M., & Robertson, G.S. (2008) Quercetin 3-glucoside protects neuroblastoma (SH-SY5Y) cells in vitro against oxidative damage by inducing sterol regulatory element-binding protein-2-mediated cholesterol biosynthesis. *The Journal of Biological Chemistry*, **283**, 2231–2245.

St-Pierre, J., Drori, S., Uldry, M., Silvaggi, J.M., Rhee, J., Jäger, S., Handschin, C., Zheng, K., Lin, J., Yang, W., Simon, D.K., Bachoo, R., & Spiegelman, B.M. (2006) Suppression of reactive oxygen species and neurodegeneration by the PGC-1 transcriptional coactivators. *Cell*, **127**, 397–408.

Stadelmann, C., Wegner, C., & Brück, W. (2011) Inflammation, demyelination, and degeneration - recent insights from MS pathology. *Biochimica et Biophysica Acta*, **1812**, 275–282.

Steinman, L. & Zamvil, S.S. (2005) Virtues and pitfalls of EAE for the development of therapies for multiple sclerosis. *Trends in Immunology*, **26**, 565–571.

Stoeckle, C. & Tolosa, E. (2010) Antigen processing and presentation in multiple sclerosis. *Results and Problems in Cell Differentiation*, **51**, 149–172.

Sugawa, M., Sakurai, Y., Ishikawa-Ieda, Y., Suzuki, H., & Asou, H. (2002) Effects of erythropoietin on glial cell development; oligodendrocyte maturation and astrocyte proliferation. *Neuroscience Research*, **44**, 391–403.

Sun, J., Chu, Y.-F., Wu, X., & Liu, R.H. (2002) Antioxidant and antiproliferative activities of common fruits. *Journal of Agricultural and Food Chemistry*, **50**, 7449–7454.

Suri, S., Liu, X.H., Rayment, S., Hughes, D.A., Kroon, P.A., Needs, P.W., Taylor, M.A., Tribolo, S., & Wilson, V.G. (2010) Quercetin and its major metabolites selectively modulate cyclic GMP-dependent relaxations and associated tolerance in pig isolated coronary artery. *British Journal of Pharmacology*, **159**, 566–575.

Swiss, V.A., Nguyen, T., Dugas, J., Ibrahim, A., Barres, B., Androulakis, I.P., & Casaccia, P. (2011) Identification of a gene regulatory network necessary for the initiation of oligodendrocyte differentiation. *PloS one*, **6**, e18088.

Takeda, K. & Akira, S. (2005) Toll-like receptors in innate immunity. *International Immunology*, **17**, 1–14.

Taupin, V., Renno, T., Bourbonnière, L., Peterson, A.C., Rodriguez, M., & Owens, T. (1997) Increased severity of experimental autoimmune encephalomyelitis, chronic macrophage/microglial reactivity, and demyelination in transgenic mice producing tumor necrosis factor-alpha in the central nervous system. *European Journal of Immunology*, **27**, 905–913.

Taveggia, C., Feltri, M.L., & Wrabetz, L. (2010) Signals to promote myelin formation and repair. *Nature Reviews Neurology*, **6**, 276–287.

Terao, J., Murota, K., & Kawai, Y. (2011) Conjugated quercetin glucuronides as bioactive metabolites and precursors of aglycone in vivo. *Food & Function*, **2**, 11–17.

Thorne, M., Moore, C.S., & Robertson, G.S. (2009) Lack of TIMP-1 increases severity of experimental autoimmune encephalomyelitis: Effects of darbepoetin alfa on TIMP-1 null and wild-type mice. *Journal of Neuroimmunology*, **211**, 92–100.

Trapp, B.D., Peterson, J., Ransohoff, R.M., Rudick, R., Mörk, S., & Bö, L. (1998) Axonal transection in the lesions of multiple sclerosis. *The New England Journal of Medicine*, **338**, 278–285.

Trump, B.F. & Berezesky, I.K. (1995) Calcium-mediated cell injury and cell death. *FASEB Journal*, **9**, 219–228.

Tsai, H.-H., Frost, E., To, V., Robinson, S., Ffrench-Constant, C., Geertman, R., Ransohoff, R.M., & Miller, R.H. (2002) The chemokine receptor CXCR2 controls positioning of oligodendrocyte precursors in developing spinal cord by arresting their migration. *Cell*, **110**, 373–383.

Van Kampen, J., Robertson, H., Hagg, T., & Drobitch, R. (2003) Neuroprotective actions of the ginseng extract G115 in two rodent models of Parkinson's disease. *Experimental Neurology*, **184**, 521–529.

Wang, L. & Morris, M.E. (2005) Liquid chromatography-tandem mass spectroscopy assay for quercetin and conjugated quercetin metabolites in human plasma and urine. *Journal of Chromatography*, **821**, 194–201.

Wang, Y., Piao, J.-H., Larsen, E.C., Kondo, Y., & Duncan, I.D. (2011) Migration and remyelination by oligodendrocyte progenitor cells transplanted adjacent to focal areas of spinal cord inflammation. *Journal of Neuroscience Research*, **89**, 1737–1746.

Weinberg, A.D. & Montler, R. (2005) Modulation of TNF receptor family members to inhibit autoimmune disease. *Current Drug Targets Inflammation and Allergy*, **4**, 195–203.

Wen, A.Y., Sakamoto, K.M., & Miller, L.S. (2010) The role of the transcription factor CREB in immune function. *Journal of Immunology*, **185**, 6413–6419.

Weydt, P., Pineda, V. V, Torrence, A.E., Libby, R.T., Satterfield, T.F., Lazarowski, E.R., Gilbert, M.L., Morton, G.J., Bammler, T.K., Strand, A.D., Cui, L., Beyer, R.P., Easley, C.N., Smith, A.C., Krainc, D., Luquet, S., Sweet, I.R., Schwartz, M.W., & La Spada, A.R. (2006) Thermoregulatory and metabolic defects in Huntington's disease transgenic mice implicate PGC-1alpha in Huntington's disease neurodegeneration. *Cell Metabolism*, **4**, 349–362.

Williamson, G. & Manach, C. (2005) Bioavailability and bioefficacy of polyphenols in humans. II. Review of 93 intervention studies. *The American Journal of Clinical Nutrition*, **81**, 243S–255S.

Witte, M.E., Nijland, P.G., Drexhage, J.A.R., Gerritsen, W., Geerts, D., van Het Hof, B., Reijerkerk, A., de Vries, H.E., van der Valk, P., & van Horssen, J. (2012) Reduced expression of PGC-1α partly underlies mitochondrial changes and correlates with neuronal loss in multiple sclerosis cortex. *Acta neuropathologica*,.

Wu, D., Wang, J., Pae, M., & Meydani, S.N. (2012) Green tea EGCG, T cells, and T cell-mediated autoimmune diseases. *Molecular Aspects of Medicine*, **33**, 107–118.

Xiang, Z., Valenza, M., Cui, L., Leoni, V., Jeong, H.-K., Brilli, E., Zhang, J., Peng, Q., Duan, W., Reeves, S. a, Cattaneo, E., & Krainc, D. (2011) Peroxisome-proliferator-activated receptor gamma coactivator 1 α contributes to dysmyelination in experimental models of Huntington's disease. *The Journal of Neuroscience*, **31**, 9544–9553.

Yin, L.-L., Lin, L.-L., Zhang, L., & Li, L. (2012) Epimedium flavonoids ameliorate experimental autoimmune encephalomyelitis in rats by modulating neuroinflammatory and neurotrophic responses. *Neuropharmacology*, **63**, 851–862.

Youdim, K.A., Shukitt-Hale, B., & Joseph, J.A. (2004) Flavonoids and the brain: interactions at the blood-brain barrier and their physiological effects on the central nervous system. *Free Radical Biology & Medicine*, **37**, 1683–1693.

Yuan, R., Maeda, Y., Li, W., Lu, W., Cook, S., & Dowling, P. (2008) Erythropoietin: a potent inducer of peripheral immuno/inflammatory modulation in autoimmune EAE. *PloS One*, **3**, e1924.

Zeng, Y., Song, C., Ding, X., Ji, X., Yi, L., & Zhu, K. (2007) Baicalin reduces the severity of experimental autoimmune encephalomyelitis. *Brazilian Journal of Medical and Biological Research*, **40**, 1003–1010.

APPENDIX - PERMISSION TO REPRINT

ELSEVIER LICENSE
TERMS AND CONDITIONS

Dec 06, 2012

This is a License Agreement between Jordan R Warford ("You") and Elsevier ("Elsevier") provided by Copyright Clearance Center ("CCC"). The license consists of your order details, the terms and conditions provided by Elsevier, and the payment terms and conditions.

All payments must be made in full to CCC. For payment instructions, please see information listed at the bottom of this form.

Supplier	Elsevier Limited The Boulevard,Langford Lane Kidlington,Oxford,OX5 1GB,UK
Registered Company Number	1982084
Customer name	Jordan R Warford
Customer address	6492 Quinpool Rd Halifax, NS B3L 1B3
License number	3043420643448
License date	Dec 06, 2012
Licensed content publisher	Elsevier
Licensed content publication	Trends in Pharmacological Sciences
Licensed content title	Target-based selection of flavonoids for neurodegenerative disorders
Licensed content author	Quinton R.D. Jones,Jordan Warford,H.P. Vasantha Rupasinghe,George S. Robertson
Licensed content date	November 2012
Licensed content volume number	33
Licensed content issue number	11
Number of pages	9
Start Page	602
End Page	610
Type of Use	reuse in a thesis/dissertation
Portion	excerpt
Number of excerpts	3
Format	both print and electronic

Are you the author of this Elsevier article?	Yes
Will you be translating?	No
Order reference number	
Title of your thesis/dissertation	Modulation of Immune Function and Promotion of Restorative Gene Expression by AF4 in a Mouse Model of Experimental Autoimmune Encephalomyelitis
Expected completion date	Dec 2012
Estimated size (number of pages)	131
Elsevier VAT number	GB 494 6272 12
Permissions price	0.00 USD
VAT/Local Sales Tax	0.0 USD / 0.0 GBP
Total	0.00 USD
Terms and Conditions	

INTRODUCTION

1. The publisher for this copyrighted material is Elsevier. By clicking "accept" in connection with completing this licensing transaction, you agree that the following terms and conditions apply to this transaction (along with the Billing and Payment terms and conditions established by Copyright Clearance Center, Inc. ("CCC"), at the time that you opened your Rightslink account and that are available at any time at http://myaccount.copyright.com).

GENERAL TERMS

2. Elsevier hereby grants you permission to reproduce the aforementioned material subject to the terms and conditions indicated.

3. Acknowledgement: If any part of the material to be used (for example, figures) has appeared in our publication with credit or acknowledgement to another source, permission must also be sought from that source. If such permission is not obtained then that material may not be included in your publication/copies. Suitable acknowledgement to the source must be made, either as a footnote or in a reference list at the end of your publication, as follows:

"Reprinted from Publication title, Vol /edition number, Author(s), Title of article / title of chapter, Pages No., Copyright (Year), with permission from Elsevier [OR APPLICABLE SOCIETY COPYRIGHT OWNER]." Also Lancet special credit - "Reprinted from The Lancet, Vol. number, Author(s), Title of article, Pages No., Copyright (Year), with permission from Elsevier."

4. Reproduction of this material is confined to the purpose and/or media for which permission is hereby given.

5. Altering/Modifying Material: Not Permitted. However figures and illustrations may be altered/adapted minimally to serve your work. Any other abbreviations, additions, deletions and/or any other alterations shall be made only with prior written authorization of Elsevier Ltd. (Please contact Elsevier at permissions@elsevier.com)

6. If the permission fee for the requested use of our material is waived in this instance, please be advised that your future requests for Elsevier materials may attract a fee.

7. Reservation of Rights: Publisher reserves all rights not specifically granted in the combination of (i) the license details provided by you and accepted in the course of this licensing transaction, (ii) these terms and conditions and (iii) CCC's Billing and Payment terms and conditions.

8. License Contingent Upon Payment: While you may exercise the rights licensed immediately upon issuance of the license at the end of the licensing process for the transaction, provided that you have disclosed complete and accurate details of your proposed use, no license is finally effective unless and until full payment is received from you (either by publisher or by CCC) as provided in CCC's Billing and Payment terms and conditions. If full payment is not received on a timely basis, then any license preliminarily granted shall be deemed automatically revoked and shall be void as if never granted. Further, in the event that you breach any of these terms and conditions or any of CCC's Billing and Payment terms and conditions, the license is automatically revoked and shall be void as if never granted. Use of materials as described in a revoked license, as well as any use of the materials beyond the scope of an unrevoked license, may constitute copyright infringement and publisher reserves the right to take any and all action to protect its copyright in the materials.

9. Warranties: Publisher makes no representations or warranties with respect to the licensed material.

10. Indemnity: You hereby indemnify and agree to hold harmless publisher and CCC, and their respective officers, directors, employees and agents, from and against any and all claims arising out of your use of the licensed material other than as specifically authorized pursuant to this license.

11. No Transfer of License: This license is personal to you and may not be sublicensed, assigned, or transferred by you to any other person without publisher's written permission.

12. No Amendment Except in Writing: This license may not be amended except in a writing signed by both parties (or, in the case of publisher, by CCC on publisher's behalf).

13. Objection to Contrary Terms: Publisher hereby objects to any terms contained in any purchase order, acknowledgment, check endorsement or other writing prepared by you, which terms are inconsistent with these terms and conditions or CCC's Billing and Payment terms and conditions. These terms and conditions, together with CCC's Billing and Payment terms and conditions (which are incorporated herein), comprise the entire agreement between you and publisher (and CCC) concerning this licensing transaction. In the event of any conflict between your obligations established by these terms and conditions and those

established by CCC's Billing and Payment terms and conditions, these terms and conditions shall control.

14. Revocation: Elsevier or Copyright Clearance Center may deny the permissions described in this License at their sole discretion, for any reason or no reason, with a full refund payable to you. Notice of such denial will be made using the contact information provided by you. Failure to receive such notice will not alter or invalidate the denial. In no event will Elsevier or Copyright Clearance Center be responsible or liable for any costs, expenses or damage incurred by you as a result of a denial of your permission request, other than a refund of the amount(s) paid by you to Elsevier and/or Copyright Clearance Center for denied permissions.

LIMITED LICENSE

The following terms and conditions apply only to specific license types:

15. **Translation**: This permission is granted for non-exclusive world **English** rights only unless your license was granted for translation rights. If you licensed translation rights you may only translate this content into the languages you requested. A professional translator must perform all translations and reproduce the content word for word preserving the integrity of the article. If this license is to re-use 1 or 2 figures then permission is granted for non-exclusive world rights in all languages.

16. **Website**: The following terms and conditions apply to electronic reserve and author websites:
Electronic reserve: If licensed material is to be posted to website, the web site is to be password-protected and made available only to bona fide students registered on a relevant course if:
This license was made in connection with a course,
This permission is granted for 1 year only. You may obtain a license for future website posting,
All content posted to the web site must maintain the copyright information line on the bottom of each image,
A hyper-text must be included to the Homepage of the journal from which you are licensing at http://www.sciencedirect.com/science/journal/xxxxx or the Elsevier homepage for books at http://www.elsevier.com , and
Central Storage: This license does not include permission for a scanned version of the material to be stored in a central repository such as that provided by Heron/XanEdu.

17. **Author website** for journals with the following additional clauses:

All content posted to the web site must maintain the copyright information line on the bottom of each image, and the permission granted is limited to the personal version of your paper. You are not allowed to download and post the published electronic version of your article (whether PDF or HTML, proof or final version), nor may you scan the printed edition to create an electronic version. A hyper-text must be included to the Homepage of the journal from which you are licensing at http://www.sciencedirect.com/science/journal/xxxxx . As part of our normal production process, you will receive an e-mail notice when your

article appears on Elsevier's online service ScienceDirect (www.sciencedirect.com). That e-mail will include the article's Digital Object Identifier (DOI). This number provides the electronic link to the published article and should be included in the posting of your personal version. We ask that you wait until you receive this e-mail and have the DOI to do any posting.

Central Storage: This license does not include permission for a scanned version of the material to be stored in a central repository such as that provided by Heron/XanEdu.

18. **Author website** for books with the following additional clauses:
Authors are permitted to place a brief summary of their work online only.
A hyper-text must be included to the Elsevier homepage at http://www.elsevier.com . All content posted to the web site must maintain the copyright information line on the bottom of each image. You are not allowed to download and post the published electronic version of your chapter, nor may you scan the printed edition to create an electronic version.

Central Storage: This license does not include permission for a scanned version of the material to be stored in a central repository such as that provided by Heron/XanEdu.

19. **Website** (regular and for author): A hyper-text must be included to the Homepage of the journal from which you are licensing at http://www.sciencedirect.com/science/journal/xxxxx. or for books to the Elsevier homepage at http://www.elsevier.com

20. **Thesis/Dissertation**: If your license is for use in a thesis/dissertation your thesis may be submitted to your institution in either print or electronic form. Should your thesis be published commercially, please reapply for permission. These requirements include permission for the Library and Archives of Canada to supply single copies, on demand, of the complete thesis and include permission for UMI to supply single copies, on demand, of the complete thesis. Should your thesis be published commercially, please reapply for permission.

21. **Other Conditions**:

v1.6

If you would like to pay for this license now, please remit this license along with your payment made payable to "COPYRIGHT CLEARANCE CENTER" otherwise you will be invoiced within 48 hours of the license date. Payment should be in the form of a check or money order referencing your account number and this invoice number RLNK500912743.
Once you receive your invoice for this order, you may pay your invoice by credit card. Please follow instructions provided at that time.

Make Payment To:
Copyright Clearance Center
Dept 001
P.O. Box 843006
Boston, MA 02284-3006

For suggestions or comments regarding this order, contact RightsLink Customer Support: customercare@copyright.com or +1-877-622-5543 (toll free in the US) or +1-978-646-2777.

Gratis licenses (referencing $0 in the Total field) are free. Please retain this printable license for your reference. No payment is required.